GENERAL ATOMIC

GA-A13593
UC-77

THORIUM UTILIZATION PROGRAM

QUARTERLY PROGRESS REPORT FOR THE PERIOD ENDING AUGUST 31, 1975

Prepared under
Contract E(04-3)-167
Project Agreement No. 53
for the San Francisco Operations Office
U.S. Energy Research and Development Administration

GENERAL ATOMIC PROJECT 3225 DATE PUBLISHED: SEPTEMBER 30, 1975

DISCLAIMER

QUARTERLY REPORT SERIES*

GA-A13178 - June 1974 through August 1974

GA-A13255 - September 1974 through November 1974

GA-A13366 - December 1974 through February 1975

GA-A13510 - March 1975 through June 1975

*Prior to GA-A13178, the Thorium Utilization Program was reported in the Base Program Quarterly Progress Report.

ABSTRACT

This publication continues the quarterly series presenting results of work performed under the National HTGR Fuel Recycle Program (also known as the Thorium Utilization Program) at General Atomic Company. Results of work on this program prior to June 1974 were included in a quarterly series on the HTGR Base Program.

The work reported includes the development of unit processes and equipment for reprocessing of High-Temperature Gas-Cooled Reactor (HTGR) fuel and the design and development of an integrated line to demonstrate the head end of HTGR reprocessing using unirradiated fuel materials. Work is also described on the evaluation of alternate techniques for fuel reprocessing to surmount possible operating problems with the reference flow sheet and the development of the conceptual design of a target recycle facility to identify the requirements of large-scale recycle of HTGR fuels.

INTRODUCTION

This report covers the work performed by General Atomic Company under U.S. Energy Research and Development Administration Contract AT(04-3)-167, Project Agreement No. 53. The work done under this project agreement is part of the program for development of recycle technology for High-Temperature Gas-Cooled Reactor (HTGR) fuels described in the "National HTGR Fuel Recycle Development Program" (ORNL 4702).

The objective of the program is to provide the necessary technology, development, engineering, and demonstration of the steps required in the economic recycle of HTGR fuels utilizing thorium as a fertile material. Work at General Atomic Company is concentrating on the development of reprocessing methods (subtask 110 of the National Program), engineering and economic studies (subtask 310), and the application of recycle technology to the conceptual design of a large-scale recycle facility (subtask 320).

The objectives of subtask 110, Reprocessing Development, are to develop the necessary technology for the construction and operation of a prototype reprocessing facility which will process irradiated fuel materials and to provide the capability for commercial recycle of HTGR fuels. The output of this subtask includes (1) definition of process flow sheets, (2) development of equipment components, and (3) definition of operating data.

The objectives of subtask 310 are to guide the development program from the viewpoint of overall recycle needs and to obtain an economical HTGR fuel recycle method for early recovery and use of bred U-233. Alternate methods and options for reprocessing and refabrication are evaluated, and recommendations are made for possible further experimental development.

The objectives of subtask 320 are to develop a conceptual design of a target-size recycle plant for the reprocessing and refabrication of HTGR fuels and to use the results developed in the preparation of this design to guide the development work. The output of this task is in the form of design criteria, reference process flow sheets, and equipment sizing for a target recycle facility.

TABLE OF CONTENTS

FIGURES

FIGURES (Continued)

FIGURES (Continued)

TABLES

TABLES (Continued)

1. SUMMARY

The development program for HTGR fuel reprocessing continues to emphasize the design and construction of a prototype head-end line. Design and procurement of the multistage crushing system, the primary and secondary fluidized bed burners, and pneumatic transport systems connecting these unit operations are continuing. Design is complete or nearing completion on most systems and procurements have been placed.

Experimental studies are continuing on the transport of solid materials in pneumatic systems and the measurement of properties of these materials pertinent to the design of handling systems.

Test runs on the 20-cm-diameter primary fluidized-bed burner have provided design verification of the gas distributor design and fines recycle entry point for the prototype. A series of runs with dense-phase recycle of graphite fines has demonstrated the most successful operation and burning of fines of all systems tested to date and permits the finalization of the design for the prototype burner.

Design recommendations for the induction heating system and automatic controls have been completed for the prototype secondary burner. An experimental run was performed on the 10-cm-diameter secondary burner to confirm design values of heat transfer coefficients during the operating cycle.

Eleven leaching runs were performed during the quarter on burned-back ThC_2 particles. Rapid dissolution was observed in all cases and initial experiments have not detected significant rate variations for different air sparging rates.

It has been experimentally shown that a carbon content as high as 4.5% will not increase the time required for dissolution of thoria. However,

potential difficulties in the solvent extraction and waste processing flowsheets may still be encountered with high carbon contents due to formation of organic acids.

Steam jet transfer for removal of slurries from the leacher continues to be investigated. Temperature limits have now been defined, but further work is still required to prevent occasional suction leg plugging.

A fluid-bed dryer is being tested for drying the insols from leacher runs. Data to date indicate this approach is feasible for drying insols separated by continuous centrifugation. Temperature balances and gas distribution design are presently under study. Preliminary operating tests with a batch centrifuge for separating insolubles have been completed.

Five solvent extraction runs were completed during the quarter covering first cycle extraction and scrub and the second uranium cycle of the Acid-Thorex flowsheet. Addition of up to 0.005M fluoride to the thorium partition solution has been shown to be beneficial in reducing or preventing thorium carryover into the uranium stripping column, even when dibutyl phosphate is added to the system to simulate solvent irradiation damage.

Design of fixtures to demonstrate remote maintenance and handling concepts on the prototype line is under way. Assembly drawings have been prepared for several systems.

2. FUEL ELEMENT CRUSHING

Design, procurement, and documentation are continuing on the fuel element size reduction system (UNIFRAME) to be installed as part of the prototype cold reprocessing line at General Atomic Company.

The design of the special structure that replaces the standard machine frames has been completed and requests for quote for construction have been issued.

Designs of the primary crusher pitman and stationary jaw assemblies have been completed. Bids on their construction were reviewed and purchase orders have been issued. The secondary crusher pitman and stationary jaw assemblies have been designed and detailing of these designs is under way. Double-roll crusher components, toggle/pin joint materials, and the oversize crusher have been received. The final design of the screener has been established and construction will begin in the near future.

2.1. UNIFRAME PROTOTYPE FUEL ELEMENT SIZE REDUCTION SYSTEM

2.1.1. Introduction

A size reduction system, designated UNIFRAME (Fig. 2-1), has been proposed for reducing spent HTGR fuel and control rod elements to a suitable feed for fluidized-bed burning to separate the fuel and graphite for subsequent fissile material recovery. The design and procurement of a full-scale prototype of this system is under way.

The UNIFRAME system comprises five major equipment items, arranged in an array that utilizes gravity flow, eliminates the need for intra-equipment material transport devices, and provides a continuous size reduction process without recycle.

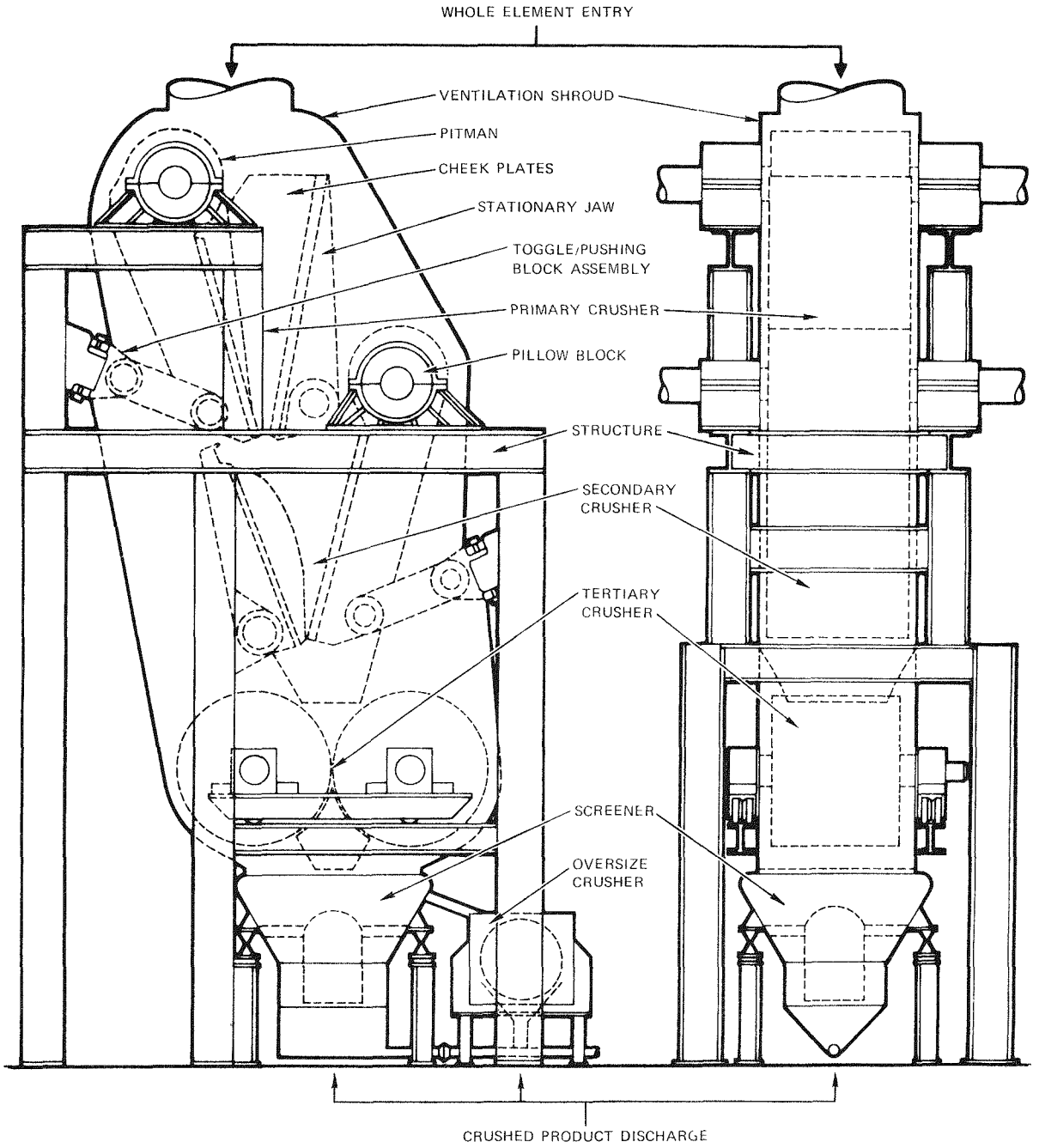

Fig. 2-1. UNIFRAME size reduction system

The major equipment items are:

1. Primary crusher: an overhead eccentric jaw crusher for reducing the elements to ≤6-in. ring-sized fragments.

2. Secondary crusher: an overhead eccentric jaw crusher for further reduction of the fragments to ≤2-in. ring-sized fragments.

3. Tertiary crusher: a double-roll crusher for final reduction of the fragments to ≤3/16-in. ring-sized product.

4. Screener: a vibratory screener-separator for separating the acceptable product from any oversized fragments.

5. Oversize crusher: an eccentrically mounted single-roll crusher for reduction of oversize fragments to acceptable product size.

The components of the UNIFRAME system have been categorized into five subsystems to provide a logical plan for the design efforts. These subsystems are:

1. Structural: the special framework replacing standard machine frames to enable an efficient array of the equipment.

2. Ventilation: the enclosure that provides containment and collection of radioactive materials and dusts while minimizing the surfaces exposed.

3. Lubrication: the standard and special lubrication and bearings for equipment that make it more reliable and compatible with the radioactive environment and the remote operation requirements.

4. Drive: the standard and special drive components required to make the UNIFRAME system compatible with remote operation requirements and the radioactive environment.

5. Mechanical: the standard and special components required to make the major equipment items compatible with the structural, ventilation, and remote operation requirements.

2.1.2. Documentation

As the design of the UNIFRAME progresses, continuing formal documentation will be provided as an information exchange for Title I and Title II design phases of the proposed reprocessing demonstration facility.

To date, the following design documents have been issued:

Document No.	Title
DC-521002, Issue A	Equipment Design Criteria - Fuel Element Size Reduction System
SD-521001, Issue A	System Description - Fuel Element Size Reduction System

2.1.3. Current Status

2.1.3.1. Structural Analysis and Design

Previously reported (Ref. 2-1) structural analyses have been refined using the SAP IV computer code (Ref. 2-2). The present configuration is shown by the spatial diagram of Fig. 2-2. Also shown in Fig. 2-2 is an end-elevation view of the frame, which was modeled according to the SAP IV code and is a portion of the computer model. Table 2-1 identifies the respective components of the UNIFRAME, their model element type, and the number of such elements used in the entire model.

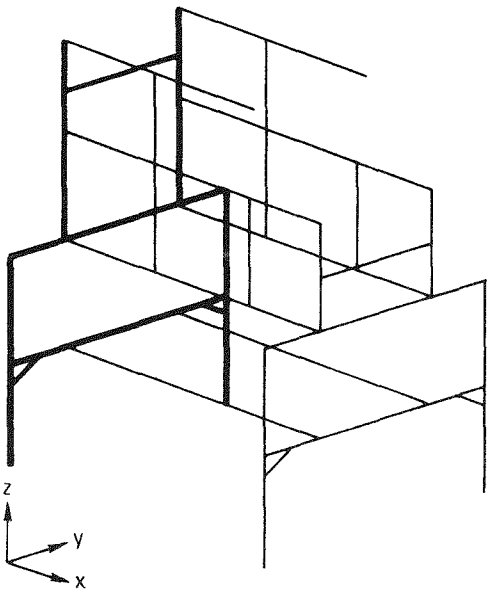

XX ≡ NODE POINT
YY ≡ ELEMENT NUMBER

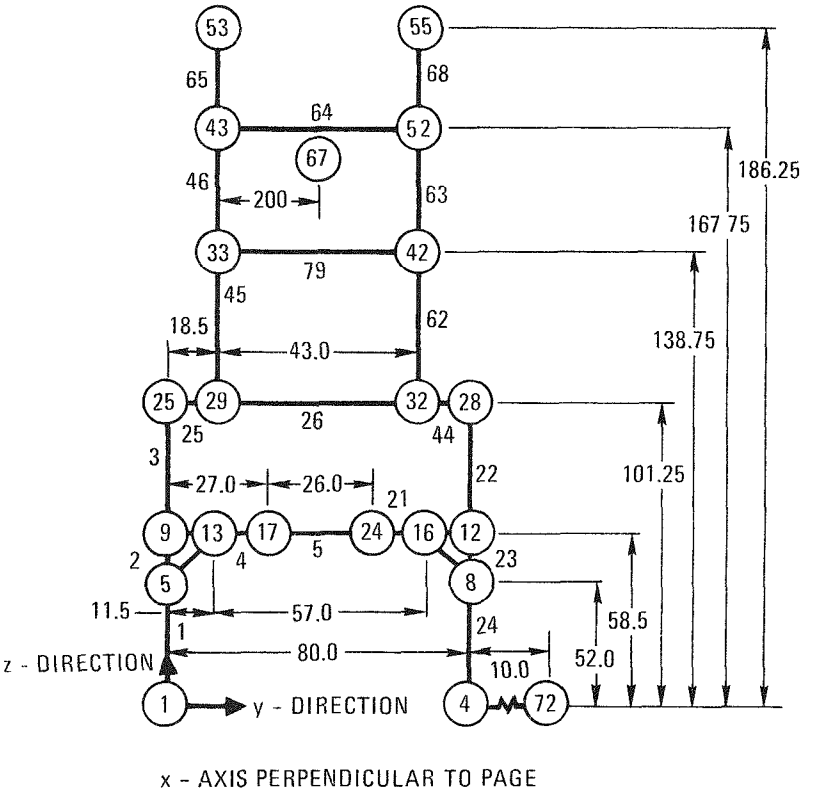

x - AXIS PERPENDICULAR TO PAGE

Fig. 2-2. Spatial configuration of UNIFRAME and end-view model

TABLE 2-1
COMPONENTS OF UNIFRAME SYSTEM

Component Designation	Element Type	Quantity
Cross-bracing	Truss	15
Beams	Beam	80
Gussets	Triangular plate	8
Cheek plates	Quadrilateral plate	4
Pitmans	Quadrilateral plate	2
Base pads	Boundary elements	12
Eccentric shaft	Tangent pipe	2
Double-roll	Tangent pipe	2

Having modeled the UNIFRAME as described, node point displacements were calculated for each of six degrees of freedom (three translational and three rotational) for two types of loading conditions: (1) fixed end forces on the beams, and (2) application of static loads to specific node points.

The first loading condition describes loads that are not applied directly to a node but are transferred from the point of application to the nearest fixed-end node of that particular element (beam, truss, etc.). The data obtained for the first loading condition are applicable to "start-under-load" conditions; this design requirement and associated data are presently under consideration.

Mode shape and frequency analyses using the model (partially described in Fig. 2-2) established that the y-direction natural frequency is more difficult to "stiffen" than the x-direction. In these analyses an eigen-value problem is created and a solution is sought for the lowest possible eigenvalues and corresponding eigenvectors. With this solution the lowest

natural frequencies are determined and the node displacements/rotations are established for each eigenvector. The mode shape can subsequently be determined for each eigenvector by the relative magnitudes and directions of the node displacement/rotations.

The highest forcing frequency in the UNIFRAME system is the secondary crusher operating at 300 rpm or 5 Hertz. The lowest natural frequency (x- or y-direction) of the structure is 10.0 Hertz.

2.1.3.2. Screener Design and Analysis

A final design for the screener has been established. The design incorporates two major subassemblies, a static subassembly and a dynamic subassembly. The static subassembly includes a spring support and an oversize material outflow pipe [items (2) and (5), respectively, of Fig. 2-3] and the circular housing to which both items are attached. The dynamic subassembly includes the support structure, screen, and motion generator enclosure [items (1), (3), and (4), respectively, of Fig. 2-3].

Two types of dynamic subassemblies have been designed for use in a common static subassembly. The first type closely resembles the design presented in the Design Status Report (Ref. 2-3). This design is shown in Fig. 2-3. The second type of dynamic subassembly has the following two features that differ from the design shown in Fig. 2-3:

1. Radially oriented tubes are used in place of the vertical plates [see item (1) of Fig. 2-3].

2. The motion generator and the electrical motor drive have forced air cooling.

The tube design was chosen to improve stress conditions at the ends of the supports and to admit external motor cooling. Whether or not the electrical motor needs to be cooled will be determined during initial operation of

the screener when operating temperature data will be collected and analyzed to determine the impact of cooling on the overall screener reliability.

2.1.3.3. Procurement - Current Status

A crack was discovered in one of the pitman castings received last quarter. An approved method of repair has been selected with rigorous inspection requirements. Repair is currently under way and is scheduled to be complete by October 1, 1975.

Design of the primary crusher pitman assembly and stationary jaw plate has been completed and fabrication has begun.

A request for quotation has been issued for fabrication and machining of the main frame.

Double-roll crusher components and the oversize pulverizer have been received.

REFERENCES

2-1. "Thorium Utilization Program Quarterly Progress Report for the Period Ending February 28, 1975," ERDA Report GA-A13366, General Atomic Company, May 30, 1975.

2-2. Bathe, K., E. L. Wilson, and F. E. Peterson, "SAP IV - A Structural Analysis Program for Static and Dynamic Response of Linear Systems," University of California Report EERC 73-11, Earthquake Engineering Research Center, College of Engineering, University of California at Berkeley, June 1973.

2-3. Baxter, B. J., et al., "Conceptual Design for a Prototype Fuel Element Size Reduction System Designated UNIFRAME," ERDA Report GA-A13275, General Atomic Company, July 1, 1975.

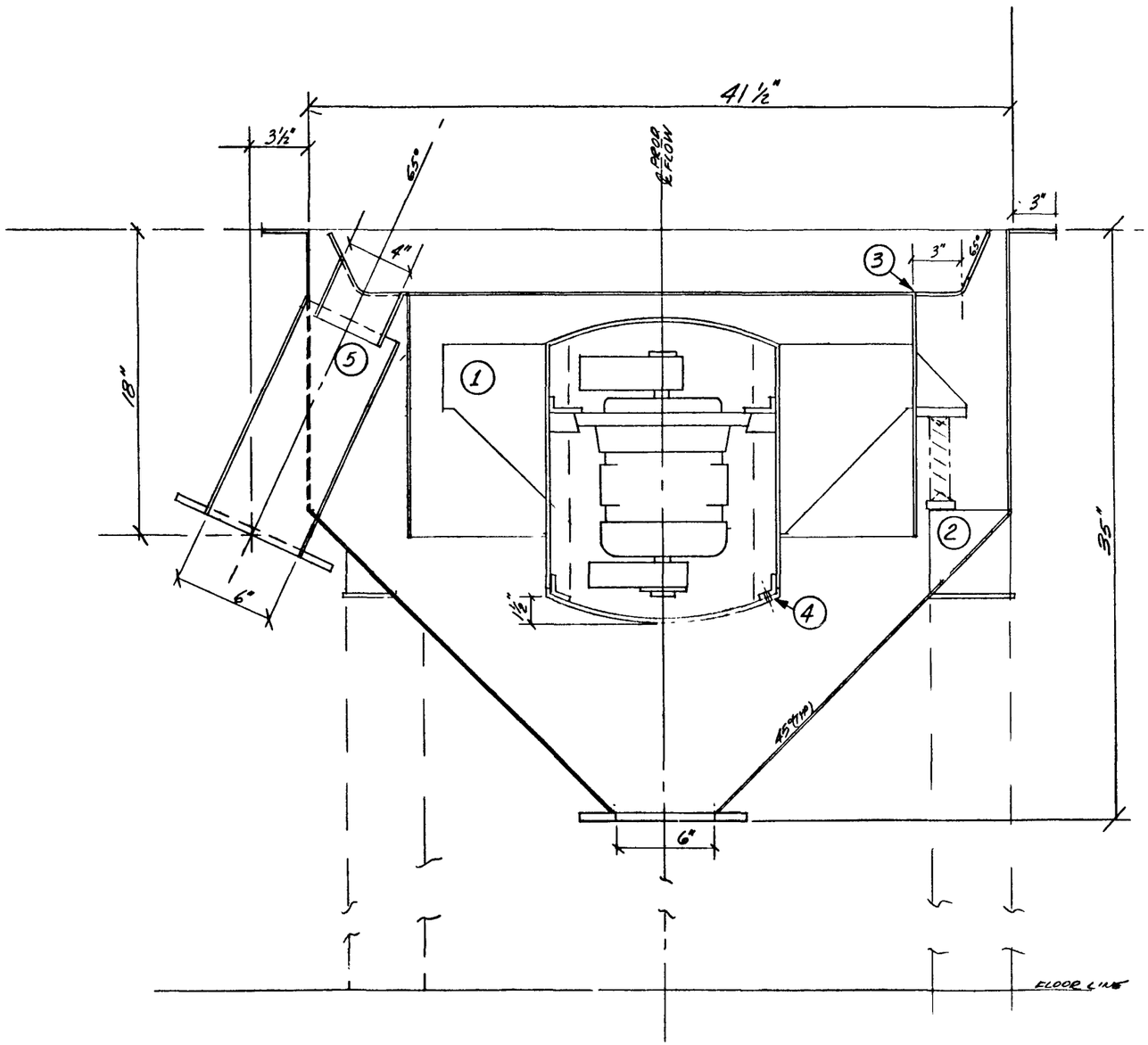

SECTION VIEW A-A

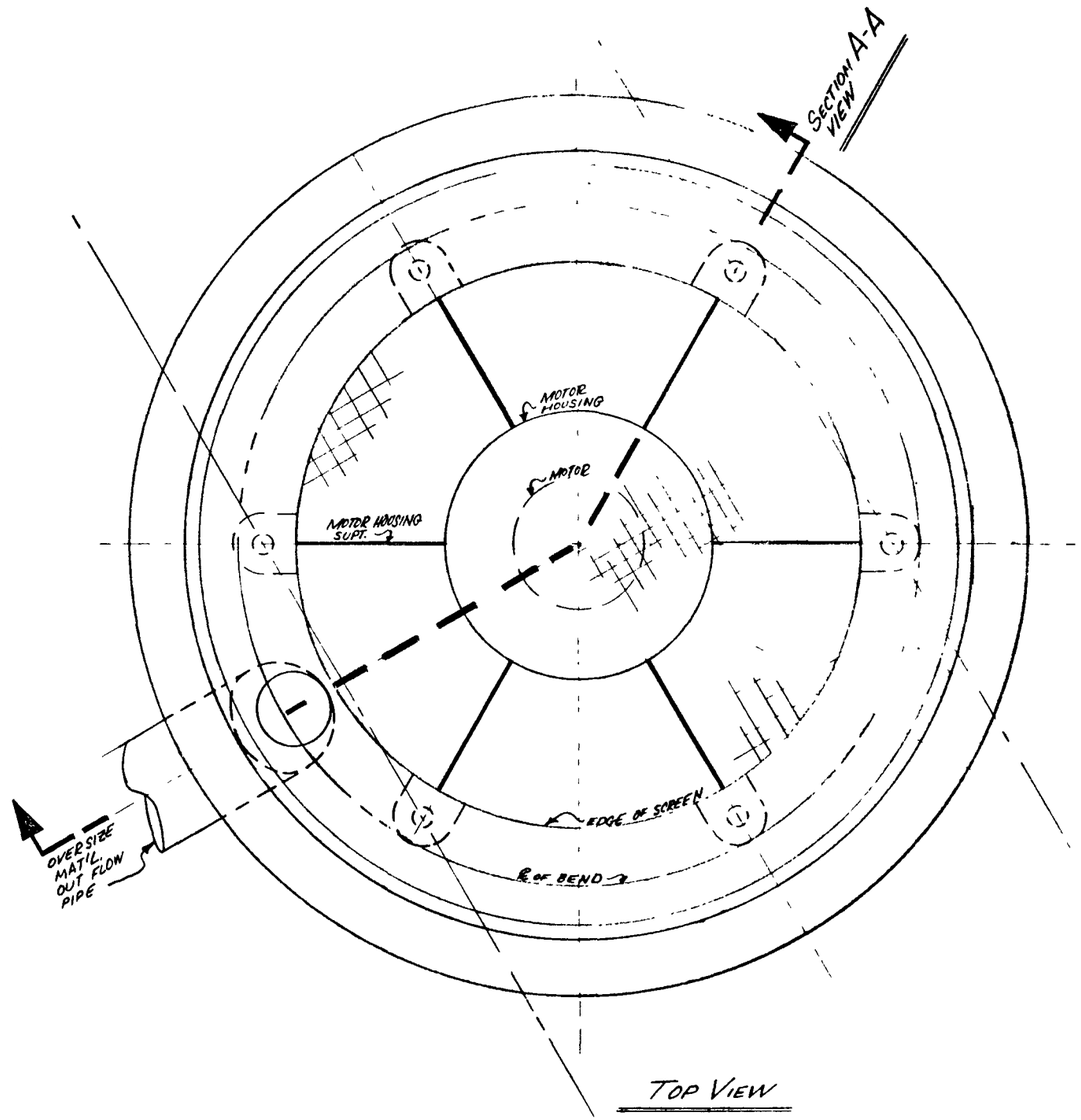

TOP VIEW

ITEM NO.	DESCRIPTION
1	SUPPORT RIBS
2	SPRING SUPPORT
3	SCREEN CLOTH
4	MOTION GENERATOR ENCLOSURE
5	OUTFLOW PIPE

Fig. 2-3. Screener assembly

3. SOLIDS HANDLING

Tests using the experimental pneumatic transport system continued, centering on pressure drop measurements during flow of crushed graphite.

Final design of the weighing system for the feed bunker for the primary burner is complete. Design of the remaining transport systems is under way. The main column for the pneumatic classifier for the prototype line has been designed, fabricated, and delivered on site.

Construction of experimental equipment and testing continues on solids flow properties to obtain additional information for design and prediction of solids behavior for solids handling systems.

3.1. PNEUMATIC TRANSPORT

Transfer of material between unit operations in the head-end reprocessing system will be by pneumatic transport. Investigation of vacuum pneumatic transport systems began in 1973 for the purpose of evaluating the conveyance of product streams. Vacuum transport was determined to be the best conveyance method for radioactive materials. Any leakage in the piping loop will be toward the negative pressure side and thus internal. This eliminates the potential hazard posed by pressure pneumatic systems in the event of a leak.

Three separate pilot plant systems were operated to demonstrate the utility of vacuum pneumatic transport and to obtain design information:

1. System A: crusher to primary burner.
2. System B: primary burner to air classifier.
3. System C: secondary burner to leachers.

Each of the above systems includes a positive displacement pump, stainless steel transfer lines, a suitable material pickup device, and a product hopper as supplied by VAC-U-MAX.

Although installation of the piping systems provided experience with actual process material, the length of time for material transfer was not sufficient to obtain parametric data for use in subsequent designs. Information needed for design of the prototype system is therefore being obtained with a separate experimental pneumatic transport test unit. Solids to be studied in the experimental schedule include (1) crushed graphite (-3/16-in. ring size), (2) primary burner fines, (3) secondary burner product, (4) fuel particles, and (5) fresh feed.

3.1.1. Pilot Plant Systems

The pilot plant systems are operable and capable of being used in routine operations of the 20-cm primary burner and 10-cm secondary burner experiments (see Section 4, Fluidized-Bed Combustion).

3.1.2. Pneumatic Transport Test System

An experimental pneumatic transport system, separate from the equipment associated with the pilot plant facility, has been assembled to obtain information on equipment operation and the effects of process variables. The system as shown in Fig. 3-1 is capable of testing a variety of equipment and modes of operation. The experimental system consists of six basic subsystems:

1. Material feed vessel
2. Material feeder
3. Transport piping
4. Filter vessel
5. Material receiver
6. Positive displacement blower

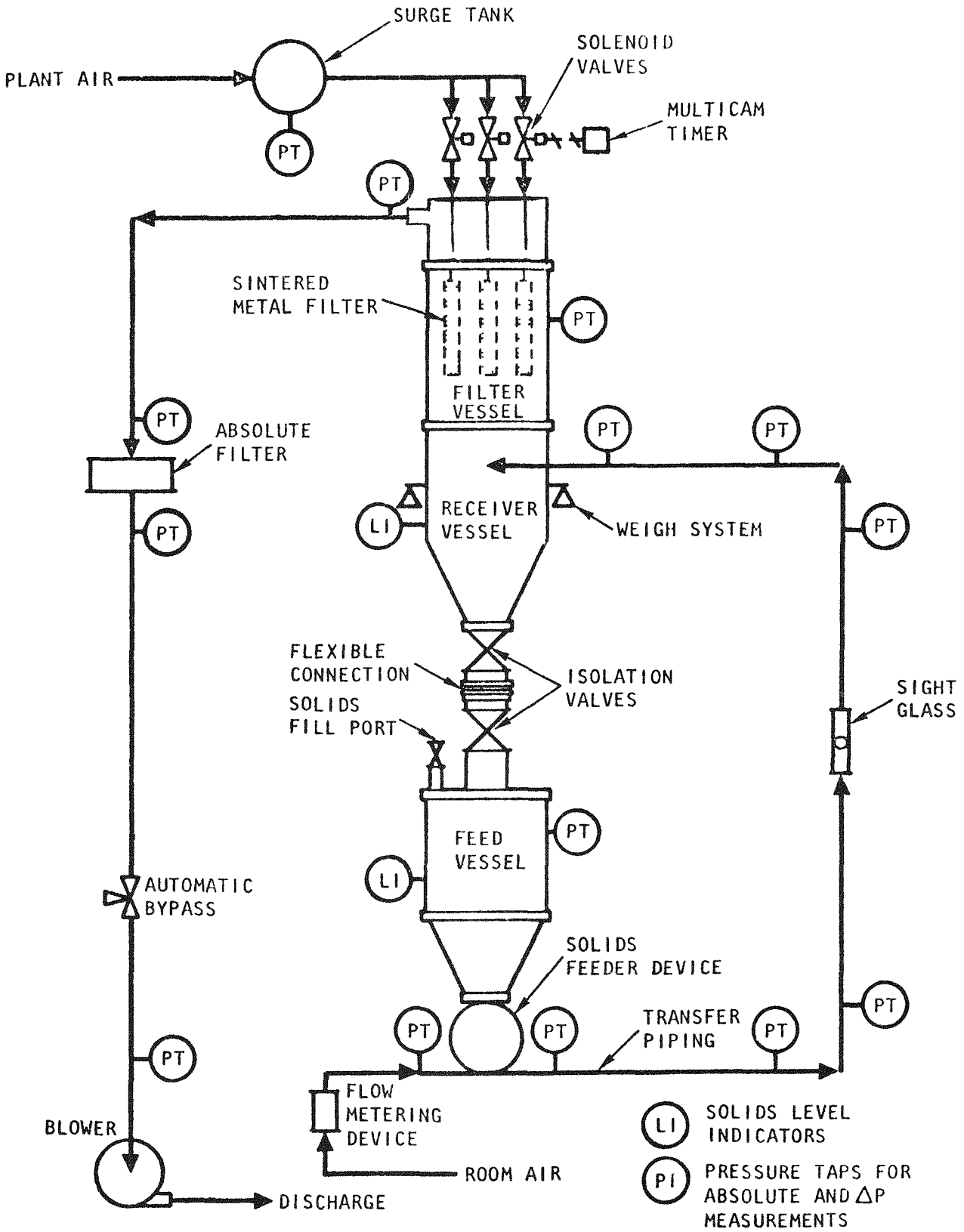

Fig. 3-1. Pneumatic transport system

Pressure drop data were obtained during transport of an air/crushed-graphite system. The data showed considerable scatter (See Fig. 3-2). The degree of scatter was found to be the result of gas flow instabilities, as measured by the rotometer, and extreme particle attrition. Fluctuations in the flow of gas that arose from the rotometer were eliminated upon substitution of a calibrated orifice.

Additional runs are planned for next quarter to establish saltation and choking velocity criteria for the air/crushed-graphite system.

3.1.3. Prototype Pneumatic Transport Systems

Material weighing devices for prototype head-end transport systems are typically as shown in Fig. 3-3. A final design of a weighing system has been completed for the prototype primary burner. An assembly drawing for this sytem is shown in Fig. 3-4. In this figure the stay rods, load cells, and swing-away mechanisms are not shown; however, their size has been determined and the expected gross weight of the bunker and its contents are known.

The remaining transport systems for the prototype line are presently being designed. A procurement package for all prototype line transport systems is expected to be issued in September 1975.

3.2. PNEUMATIC CLASSIFICATION

The economics of reprocessing HTGR and LHTGR fuel are affected by the ability to separate the fissile and the fertile fuel. This separation allows isolation of the bred U-233 in the fertile stream from the neutron poison U-236, which is contained in the fissile particles. Presently, the flowsheets for the TRISO/TRISO and the TRISO/BISO fuels are identical

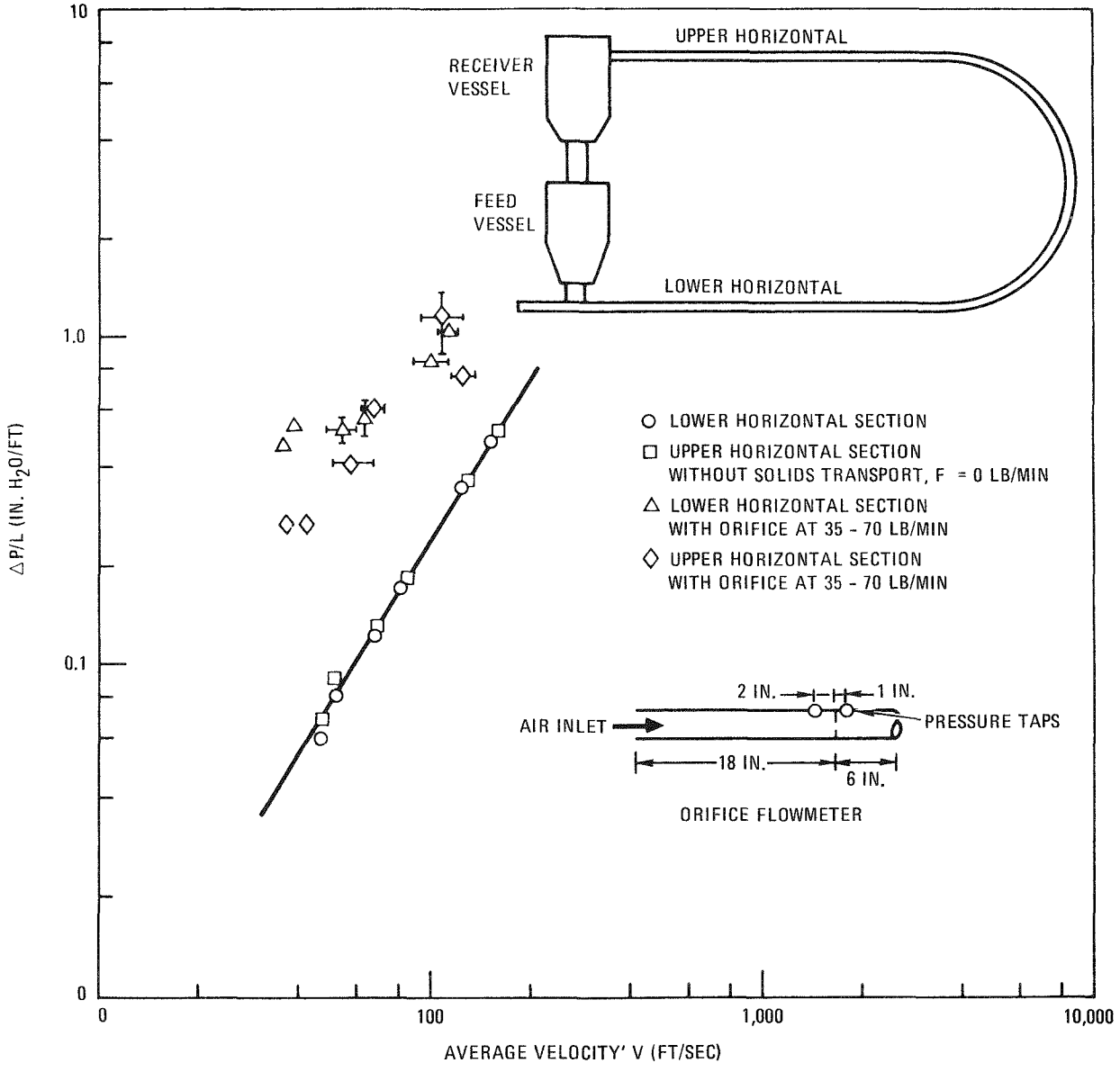

Fig. 3-2. Pressure drop per unit length for horizontal run

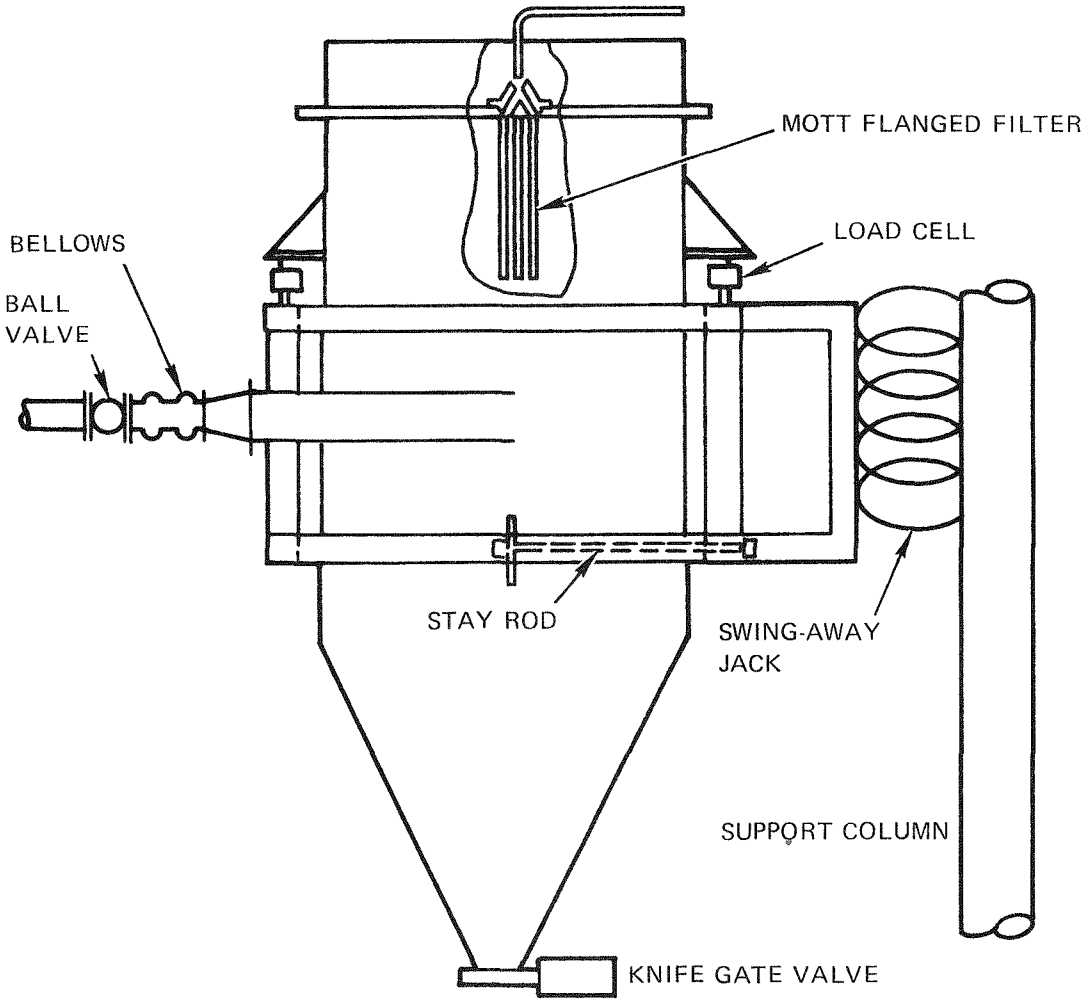

Fig. 3-3. Material weighing arrangement for prototype pneumatic transport system(s)

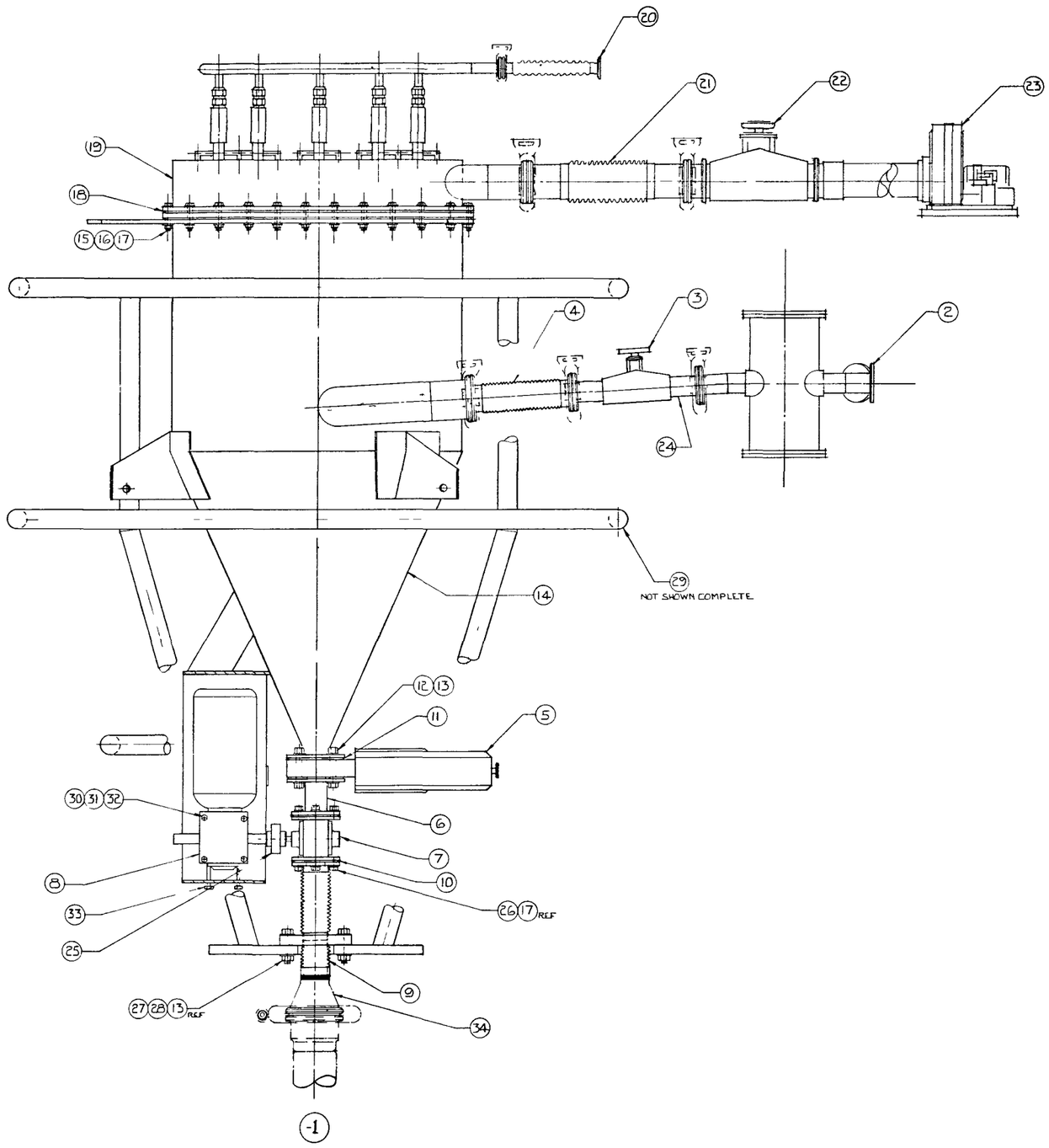

NOTE -

▽ GEAR MOTOR
MOTOR - ½ H.P N° FCM 012
GEAR REDUCER N° STF 225
SABINA ELECTRIC & ENGINEERING CO.
ORANGE, CALIF

▽ COUPLING - N° 40 B 12 FC
COUPLING BORES - ½ DIA x 1 DIA
CULLMAN WHEEL CO.
205 N HUEHL RD
NORTHBROOK ILL 60062

1	34	03018	REDUCER	
2	33		5/16-18 x 3 HEX HD BOLT	SST 18 8
4	32		3/8 FLAT WASHER	SST 18 8
4	31		3/8-16 HEX NUT	SST 18-8
4	30		3/8-16 x 1¼ HEX HD BOLT	SST 18-8
1	29	03044	BUNKER SUPPORT	
8	28	03046	5/8-11 HEX NUT	SST 18-8
8	27	03046	5/8-11 x 3 HEX HD BOLT	SST 18-8
8	26	03015	5/16-18 x 1 HEX HD BOLT	SST 18 8
1	25	03010	COUPLING	
3	24	03002	2 FERRULE TRICLOVER	
1	23	03039	BLOWER	
1	22	03037	BALL VALVE	
1	21	03035	BELLOWS	
1	20	03033	BELLOWS	
1	19	03040	FILTER PLENUM	
2	18	03021	GASKET	
68	17	03301.5 03302	5/16 FLAT WASHER	SST 18 8
30	16	03042	5/16 18 HEX NUT	SST 18 8
30	15	03042	5/16-18 x 2 HEX HD BOLT	SST 18 8
1	14	03041	BUNKER	
24	13	03011	5/8 FLAT WASHER	SST 18 8
8	12	03011	5/8-11 x 1 HEX HD BOLT	SST 18 8
2	11	03012	GASKET	
2	10	03016	GASKET	
1	9	03017	BELLOWS (OUTLET)	
1	8	03010	GEAR MOTOR	
1	7	03009	ROTARY VALVE	
1	6	03008	SPOOL PIECE	
1	5	03007	GATE VALVE	
1	4	03006	BELLOWS	
1	3	03003	BALL VALVE	
1	2	03001	DIVERTER VALVE	
	-1		ASSEMBLY	

Fig. 3-4. Bunker assembly

through the crushing, primary burning, and initial classification stages. By taking advantage of the differences in diameter and density of fissile and fertile particles, separation can be achieved through pneumatic classification.

In addition to separating the fissile and fertile particles, pneumatic classification has an additional location in the flowsheet. This place is in separating the whole unbroken TRISO particles from the SiC carbide hulls that remain as a solid stream after leaching. This separation will recover any whole particles that were not broken prior to burning in the secondary burner and will improve the recovery of fuel material in the flowsheet.

A topical report, "Pneumatic Classification of FSV Fuel Particles" (Ref. 3-1), has been published. The report describes a parametric study of the efficiency with which TRISO/TRISO fuel particles can be separated and relates efficiency and the cost penalty to the thorium fuel cycle resulting from crossover of the two fuel streams.

3.2.1. Prototype Pneumatic Classifier

The prototype line for head-end reprocessing incorporates a pneumatic classifier. The main column for the classifier has been designed, fabricated, and delivered. A variable-speed vacuum pump and feeder for the classification column have also been received. Installation is pending other construction for the prototype line.

3.3. SOLIDS PROPERTIES TESTING

Due to the nature of the head-end processes for reprocessing HTGR fuel, many areas exist that require handling of particulate systems. For this reason, the literature is constantly surveyed for better methods of handling particulate systems and for better methods of predicting the behavior of these systems. From this survey, several points have become evident.

1. The quality or performance of a process involving particulate systems hinges on the performance of the feeders and the bunkers above these feeders.

2. The feeder and its associated bunker cannot be treated separately.

3. Specific information on the behavior of materials similar to those encountered in the head-end flowsheet is almost nonexistent.

Because of the above points, a method was sought that would aid in the prediction of particulate behavior and in the design of the bunkers and the feeders associated with the flowsheet. A method that has enjoyed considerable success over the past few years is one developed by Jenike (Ref. 3-2). This method combines a theoretical approach developed from soil mechanics with empirical data gathered to support the theory. Through the use of this method combining theory with testing, the behavior of powders in bunkers and feeders can be predicted and used for designing the bunkers and the feeders.

In order to perform these tests on the particulate systems of the head-end flowsheet, equipment that had been perfected by Jenike was purchased. With this equipment the behavior of the unirradiated particulate system can be studied. Unfortunately, the effect of irradiation on these powders and their properties is not fully understood. For this reason parallel tests on irradiated material have been planned at the ORNL hot cells. These additional tests will allow the accurate prediction of the flowing properties for the irradiated particulates of the head-end process.

3.3.1. "Cold" Testing

The solids flow testing equipment is installed in a glove box fitted with humidity control equipment. The glove box contains the radioactive

(unirradiated) material and allows efficient handling of the equipment. The humidity control equipment provides the controlled atmosphere which is required due to the fact that characteristics of powders are dependent on their moisture content and thus the humidity of their environment.

An additional glove box has been attached to the existing unit to accommodate a tensile tester (described in Ref. 3-3).

During the construction period an electronic load cell was fitted to the flow factor tester. The electronic load cell replaced a pneumatic device and is expected to increase low end resolution of the apparatus and to eliminate ingress of dry air into the otherwise controlled atmosphere.

3.3.2. "Hot" Testing

Experiment data requests (ACC-ORNL-1 and ACC-GAC-0) have been prepared by Allied Chemical Corporation, Idaho (ACC) to answer technical questions concerning the "flowability" of irradiated versus unirradiated granular and powder systems in the head-end flowsheet. A description of the work being performed to answer ACC-GAC-9 has been sent to assist ORNL personnel in the procurement of equipment items necessary for parallel scoping experiments using irradiated material.

REFERENCES

3-1. deLesdernier, D., "Pneumatic Classification of FSV Fuel Particles," ERDA Report GA-A13135, General Atomic Company, June 30, 1975.

3-2. Jenike, A. W., "Storage and Flow of Solids," University of Utah Engineering Experiment Station Bulletin 123, March 1970.

3-3. "Thorium Utilization Program Quarterly Progress Report for the Period Ending May 30, 1975," ERDA Report GA-A13510, General Atomic Company, August 15, 1975.

4. FLUIDIZED-BED COMBUSTION

4.1. PRIMARY FLUIDIZED-BED COMBUSTION

The development program continued its focus on the 20-cm primary fluidized-bed burner. The reference configuration (Fig. 4-1) of the gas distributor and fines injection point has been finalized after successful operational testing of the system on the 20-cm primary burner. A 90°-included-angle perforated conical gas distributor has proven to be the optimum design. Pressurized dense-phase recycle of fines to the vertex gas entry resulted in the most successful operation and burning of fines of any of the systems tested to date. With this system, fines can be burned as fast as they are generated for beds with moderately high carbon concentrations.

The prototype primary vessel and the heating/cooling assembly design have been completed and drawings have been released for fabrication. Design of the fines recycle system can proceed now that verification of the system has been completed. The hoppers, lines, and controls have been sized; the final design is dependent upon selection of the hopper inventory monitoring system.

4.1.1. 20-cm Primary Fluidized-Bed Combustor

4.1.1.1. Burner Runs

Eleven runs (21; 22A, B, and C; 23 through 29) were performed in the 20-cm primary burner during the reporting period. In Run 21, a shallow 120°-included-angle perforated conical distributor was tested. The following runs used the dense-phase pressurized fines recycle system. The primary objective of these runs was to investigate fines burning capabilities during recycle to the bottom of both high- and low-carbon beds. Nine of the runs involved recycle injection tangentially into a 50°-included-angle

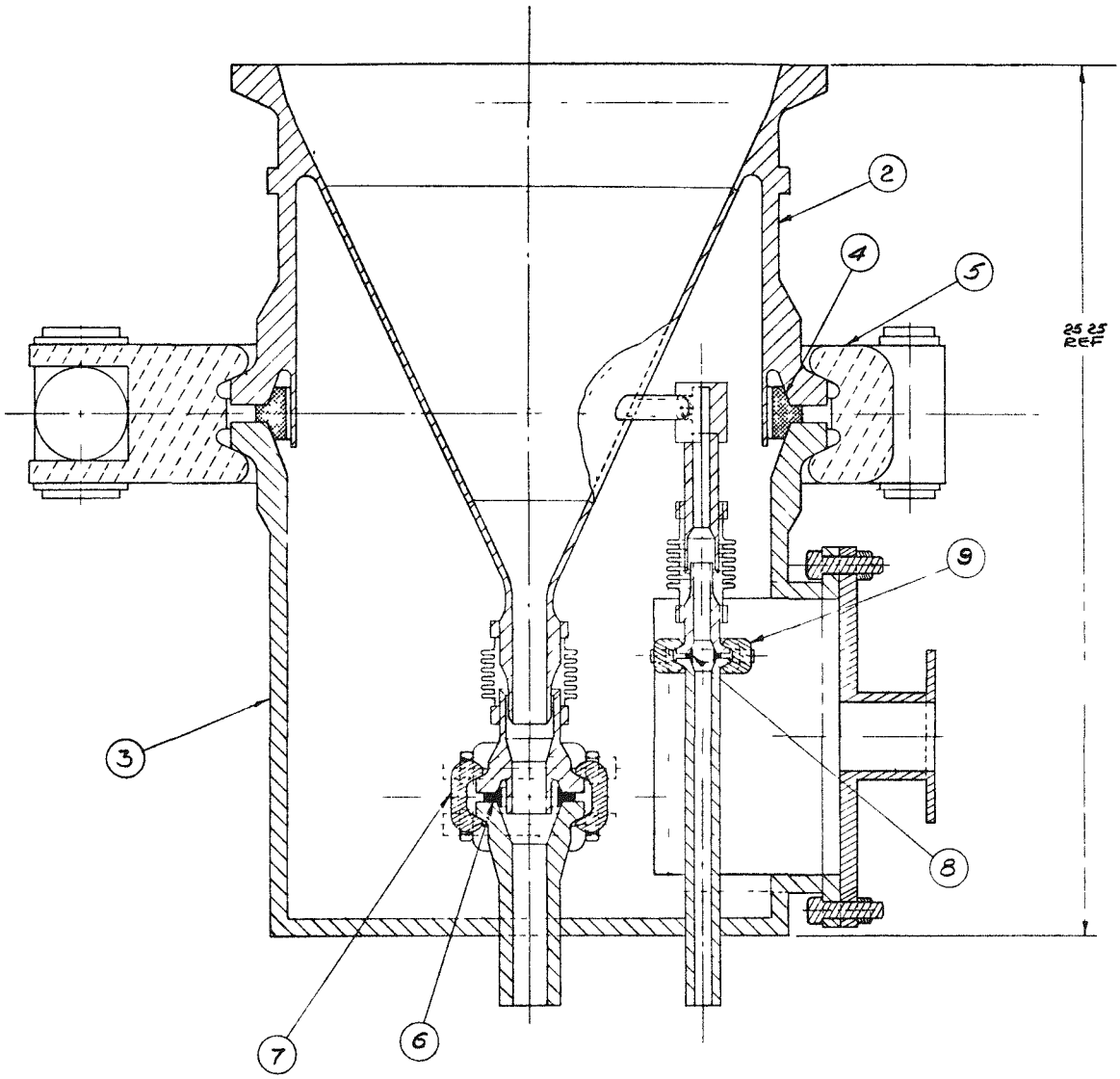

2. HUB AND CONE ASSEMBLY
3. LOWER CAP ASSEMBLY
4. SIZE 140 GRAYLOC SEAL RING
5. 14-IN. GRAYLOC SWING BOLT CLAMP
6. SIZE 14 GRAYLOC SEAL RING
7. 1-1/2-IN. GRAYLOC CLAMP
8. SIZE 4 GRAYLOC SEAL RING
9. 1/2-IN. GRAYLOC CLAMP

Fig. 4-1. Spool assembly, fluid bed, 40-cm primary burner

distributor. The tenth recycle run tested the prototypical configuration of fines recycle to the cone vertex gas line and also incorporated the prototypical 90° cone angle (Fig. 4-1).

The 120°-included-angle cone tested in Run 21 yielded very smooth operation with ≤3/16-in. feed. A thermocouple embedded in the gas plenum side of the perforated cone surface indicated 700° to 750°C (200°C less than a bed temperature measured about 3 in. from the thermocouple). A plenum thermocouple 1/2 in. below the cone surface registered 400°C, about 100°C lower than plenum temperatures in the runs with the steeper 50° cone. The embedded distributor thermocouple indicated 5° to 10°C temperature oscillations every 1 to 2 min during the early portion of the run. These oscillations smoothed out during the run, becoming insignificant after the particle concentration in the distributor area increased. The distributor allowed dumping the final bed at approximately 19 kg/min (1/2-in.-I.D. vertex). The only negative aspect noted with the 120° cone was the formation of brittle particle agglomerates around the periphery of several orifices and single particles fused into the plate surface. This evidence of material stagnation on the surface of the shallower cone indicated a requirement for a steeper cone angle.

Five shutdown runs (22A, B, and C, 23, 24) were required to achieve satisfactory operation of the recycle system. During these runs, it was found that the fines mass flow was very dependent on both the hopper outlet line size and the hopper pressurizing gas flow rates. Thus, recycle lines to the burner were sized at 0.49-in. I.D. In addition, it was found that large-sized graphite and/or particles that elutriate and reach the fines hoppers are likely to seriously hamper or block fines flow. As a result, the burner vessel was lengthened from 110 to 145 in. to provide additional deentrainment space.

Runs 25 through 28 investigated operation with recycle to both high-carbon (Run 25) and low-carbon (Runs 26 through 28) beds. Results showed

that fines burning in a high-carbon bed is insignificant; fines generation and accumulation are exceedingly high (∿40% of fresh feed weight). Appreciable fines burning will occur only late in the operating cycle after fresh feed flow is terminated and the bed carbon significantly decreases. When the bed carbon content approaches zero, above-bed fines burning will occur as long as the fines recycle flow is maintained. Such operation is difficult to control; temperature transients are very rapid once a large quantity of fines begin burning. Operation in low-carbon beds, however, results in appreciable fines burning during most of the operating cycle. In addition, fines generation is significantly reduced so that the fines residence time in the recycle hoppers is short enough to minimize heat loss before reentry to the burner. Control of the end-of-run above-bed burning was much easier with the reduced amount of recycling fines. Adjustments in the CO_2/O_2 ratio allowed the temperatures to be maintained at $\leq$1000°C while sustaining above-bed combustion. Wall temperatures remained below 900°C without cooling during the above-bed burning period This was apparently due to poor heat transfer to the walls from the burning dilute stream of fines.

Fines recycle during Runs 27 and 28 was maintained by an automatic timer, which controlled the hopper switching frequency and permitted fairly smooth operation. In both runs, fines heels totaling 10 kg (5 kg in each hopper) were utilized to provide a flow of fines to the burner upon the start of fresh feed flow. Fines inventories upon shutdown were ∿5.2 kg total (4.1 kg carbon) in Run 27 and ∿2.1 kg (0.8 kg carbon) in Run 28. This demonstrated the ability of the process to burn fines during the run at a rate surpassing that of the fines generation from the continuous fresh feed flow.

Observations made during the above-bed burning period of Run 25 indicated that a fines ignition mechanism existed other than the fines being heated to their ignition temperature by in-bed heat transfer. The fines spontaneously ignited immediately above a 12-kg particle bed that was

extinguished and had cooled to 400°C. The 450° to 550°C fines that were recycling through the bed were actually losing heat to the inert 400°C particles. The two fines ignition sources considered most possible in this situation are:

1. Some of the recycling fine particles were much hotter than the measured bulk temperature. These fines ($\geq$700°C ignition temperature) were igniting and propagating ignition to other fines.

2. The CO and O_2, always present to some degree above the bed, were igniting in small pockets and propagating ignition to the recycling fines.

In either case, the possibility that the in-bed recycle of fines is not necessary for fines ignition and burning implies that the mechanical complexity of the pressurized feeder may be unnecessary. Above-bed fines burning, feeding oxygen and recycling fines above the bed, may offer a mechanically simplier system. Above-bed burning and gravity fines recycle will be further investigated during the next quarter.

Run 29 tested recycle of fines into the cone vertex gas line instead of the mid-cone tangential injection used in prior runs. The cone used had a 90° included angle; this prototypical configuration worked well. The fines system did not plug or overpressurize at any time during the run. Plugging had occurred several times during each of the previous runs with the injection point exposed to the slugging bed solids. The 90° cone allowed good fluidization, and the cone surface indicated no solids fusion upon inspection after the run. Operating temperatures of the cone surface and plenum interior were $\leq$700° and $\leq$400°C, respectively. These temperatures were as low as those recorded during operation with the shallower 120° cone and were considered acceptable in terms of material integrity in long-term operation. Fines burning in Run 29 was again greater than the total generation/elutriation.

Most of the questions and problems with the dense-phase fines recycle system were resolved by testing with the final "reference" design discussed above. A sequenced pressurization system will be incorporated in the hoppers. This will allow more continuous pressures and, hence, more continuous fines flow into the bed. The mechanical requirements of sequential switching impose potential system reliability problems. However, these problems may be avoidable with above-bed recycle, which is simpler conceptually; future primary burner operation will be used to obtain data and determine if this configuration is feasible.

The accumulated experience in primary burning has settled many design questions. Some of the more important ones are summarized in the following sections.

4.1.1.2. Off-Gas Compositions

Data from operation of the 20-cm primary burner indicate changes in the CO/CO_2 ratio related primarily to fines recycle, bed carbon content, and bed temperature. Comparing runs with and without recycle of fines, the CO off-gas concentration appears 4 to 7% higher when fines are being recycled. Off-gas CO trends during runs with and without fines recycle show a major dependence on the amount of carbon in the bed. Run 27 had a higher bed carbon content than Run 28 and, hence, produced significantly higher off-gas CO. Changes in bed temperature have a marked effect on off-gas CO. Temperature changes of 40°C were accompanied by 3 to 5% changes in CO concentration (increasing temperature increases CO and vice versa). Off-gas CO averages ∿22% and reaches a maximum of ∿30% in runs with fines recycle.

4.1.1.3. Feeding

The recommended design for the primary burner fresh feed system consists of a rotary valve feeder and hopper located above the burner for top feeding. This system serves as a metering device for regulation of the

fresh feed rate to the burner. Compared with pneumatic and auger feed systems, which have also been tested, rotary valves represent a simpler design with less potential problems. With pneumatic systems sized for the required feed rate, bridging problems were observed. Augers performed acceptably but offer a larger surface for mechanical wear and particle breakage, while offering no advantage over a rotary valve. A supplemental knife gate is in the feed line to provide a positive air lock when required.

4.1.1.4. Gas Distribution

A 90°-included-angle perforated cone has proven to be the best distributor configuration for the primary burner. This particular angle was selected as the best trade-off considering the following points:

1. The steeper angle cone ran at a hotter temperature than the shallower cones (50° cone ran 100° to 150°C hotter than the 90° and 120° cones) and local combustion intensity within the steeper cone is considered more severe, making temperature excursions and oscillations with large fresh feed more significant.

2. The shallower cone (120°) has shown solids agglomeration and fusion to the distributor surface around the periphery of several orifices.

3. Correlations for flow of solids in conical air pad devices indicate that an 80° to 120° included angle yields the best solids flow properties (Ref. 4-1). Operation of a 90° cone has been most satisfactory. The 90° cone ran as cool as the 120° cone and indicated no surface stagnation problems.

Agglomerates were noted in final beds of runs with both the 50° cone and the 120° cone and were felt to be due to low gas flows at startup. The primary difference noted was that the 50° cone surface was polished smooth

around each orifice and showed no solids fused to the plate. The 120° cone surface was not as smoothly polished; a few orifices showed definite signs of solids stagnation and fusion to the plate. A 90° cone is felt to be the best design as it allows the coolest distributor operation together with good solids movement at the plate surface, avoiding agglomeration and fusion on the plate.

The orifice diameter has been set at 0.035 in. Smaller distributor orifices tend to plug with SiC particles, and larger orifices allow excessive quantities of particles to drain into the plenum.

4.1.1.5. Product Removal System Design

The recommended design of the primary burner product removal system consists of an actuated knife-gate valve (variable orifice) located below the perforated conical distributor. Product removal is thus controlled by varying the cross-sectional area open at the knife gate.

With a batch operating cycle, burner product is removed at the end of the operating cycle and is immediately transported to the product hopper. Pneumatic transport tests on the 20-cm primary burner product line have indicated that particle breakage is minimized by increasing both the product batch size and rate of mass transport through the system. Thus, a variable orifice knife gate will allow both a rapid product dump and a metering capability.

A 0.5-in.-I.D. conical distributor vertex allows dumping high particle concentration final beds at up to 20 kg/min but bridges with fresh feed size material. A 1-in.-I.D. vertex allows dumping of -3/16 in. fresh feed size material at about 10 kg/min with no plugging. Since a burner operating in a production facility must have the capability to dump a charge of fresh feed in case of equipment failure, the 1-in.-I.D. vertex has been used in the 40-cm prototype design. In addition, the 1-in. vertex allows

much higher particle mass transport than does the 1/2-in. vertex, further decreasing particle breakage.

4.1.1.6. Continuous Versus Semicontinuous Product Removal

Product removal and the subsequent transport of product must be performed in such a way as to minimize fuel particle breakage. Since particle breakage during pneumatic transport is strongly dependent on product batch size and mass flow rate, it is desirable to transport material quickly and in large quantities. This is most easily accomplished by a rapid, end-of-cycle whole-bed product dump when operating with a batch operating cycle. For longer batch operating cycles, when more than one whole bed of particles is processed, a "semicontinuous" series of product dumps is recommended where the rate and quantity of each particle dump are maximized.

Particle breakage during pneumatic transport with continuous product removal would be considerably larger than that with batch product removal. In addition, without tail-end burning for reduction of carbon content, a continuous product stream would likely contain a significant amount of carbon. From a control standpoint, both the product removal rate and the fresh feed rate would have to be integrated. Operation in this manner could result in significant fluctuation in bed composition and a greater possibility of process upsets. Continuous product removal is not recommended.

4.1.1.7. Bed-To-Wall Heat Transfer

Heat transfer measurements were made in the 20-cm primary burner. The average bed-to-wall heat transfer coefficient, h_i, during steady-state combustion is on the order of 95 Btu/hr-ft^2-°F (540 W/m^2-°C) at 900°C average bed temperature and 3 ft/sec superficial gas velocity. Local h_i measurements as high as 100 to 110 Btu/hr-ft^2-°F (567 to 624 W/m^2-°C) have

been taken near the bottom section of the fluid bed where the distributor mixing effect and graphite burning are more significant. As burning progresses, the h_i gradually decreases as more fuel particle product accummulates. At the end of burning, the h_i is on the order of 50 to 60 Btu/hr-ft^2-°F (283 to 340 W/m^2-°C).

A special experimental h_i measurement for a 2% carbon particle bed in the 10-cm secondary burner indicated that a particle bed has an h_i around 40 to 50 Btu/hr-ft^2-°F (227 to 283 W/m^2-°C) at 800°C bed temperature, further confirming the decrease of h_i at the end of the run.

Table 4-1 shows h_i as a function of time during a typical burner run without fines recycle. The h_i during startup is not available with the present startup technique.

4.1.1.8. Wall-To-Air Heat Transfer

The wall-to-air film coefficient is highly dependent on air superficial velocity at the vessel wall and is also dependent on the vessel wall geometry (i.e., the type of fin and pattern). The present 20-cm primary burner has 7/8-in. by 1/4-in.-O.D. pins (13 pins/row and 32 rows over a 56-in. burner length) on the outer vessel surface. The air film coefficient as a function of time and superficial air velocity during a burner run is also included in Table 4-1.

4.1.1.9. Fluidization Studies

Several beds of varying size distributions and compositions were fluidized in a glass mockup of the 20-cm primary burner to investigate the parameters affecting quality of fluidization. Five 30-kg beds ranging in composition from -3/16 in. fresh feed (17 wt % particles) to 100 wt % particles were investigated at 0 to 3 ft/sec gas velocity with the results and observations discussed below. Results indicated considerably different

TABLE 4-1
HEAT TRANSFER COEFFICIENTS UNDER STEADY-STATE PRIMARY BURNING[a]

Time After Startup (min)	Mean Bed Temperature (°C)	Overall Heat Transfer Coeff., U_i (Btu/hr-ft^2-°F)	Average Bed-To-Wall Coeff., h_i (Btu/hr-ft^2-°F)	Superficial Gas Velocity (ft/sec)	Wall-To-Air Film Coeff., h_o (Btu/hr-ft^2-°F)	Cooling Air Log Mean Superficial Velocity (ft/sec)
98	893	27.4	94	3.0	38.0	76
133	895	27.8	96	3.0	38.7	76
279	867	22.9	81	3.0	30.2	62
328	915	16.0	53	2.7	20.7	45

[a]Data from Run 15 of 20-cm primary burner: heat transfer height is 59 in., bed weight during steady-state combustion is ∿40 kg, and no fines recycle.

fluidization behavior as bed particle concentration was varied. In general, beds of medium particle concentration require less gas velocity for good mixing than beds of very high or low particle concentration.

Figure 4-2 shows the height to which the bed solids slug. Eruption of these slugs throws particles even higher, but the dimensions of the column used limited higher measurements. Additional column height has been ordered to extend these tests.

Qualitative observations made during the course of this cold work were thought to be representative of actual hot operation in terms of bed behavior above the area of the distributor. However, past experience during hot operation has indicated that small (1000 to 2000 μm) particle agglomerates tend to form in the perforated cone at gas velocities $\leq$3 ft/sec. This agglomerate formation suggests that the good mixing seen in this cold work is not typical of hot operation. However, it should be noted that in the cold work the formation of slugs, and the resulting violent solids mixing, was observed to occur 10 in. or more above the perforated conical distributor. Particle movement below this point may have been considerably poorer or even nonexistent at the distributor surface at velocities significantly less than 3 ft/sec. This may be due to segregation of the largest bed material in the distributor area.

Since heat transfer in a hot distributor cone is directly related to particle motion, minimum or optimum fluidizing gas velocities must be determined experimentally in a hot burner. In similar fashion, the above-bed phenomena observed in the cold work (e.g., large particle eruption, fines elutriation) would actually be less severe than in a hot burner due to the gas volume increase and subsequent velocity increase associated with combusion to CO ($1/2\ O_2 \rightarrow CO$), which can be as much as 25% depending on the temperature. Also, it is not known what effect a large, continuously recycling fines stream would have in terms of bed mixing or upper- and above-bed phenomena. Thus, the results of this cold work are thought to

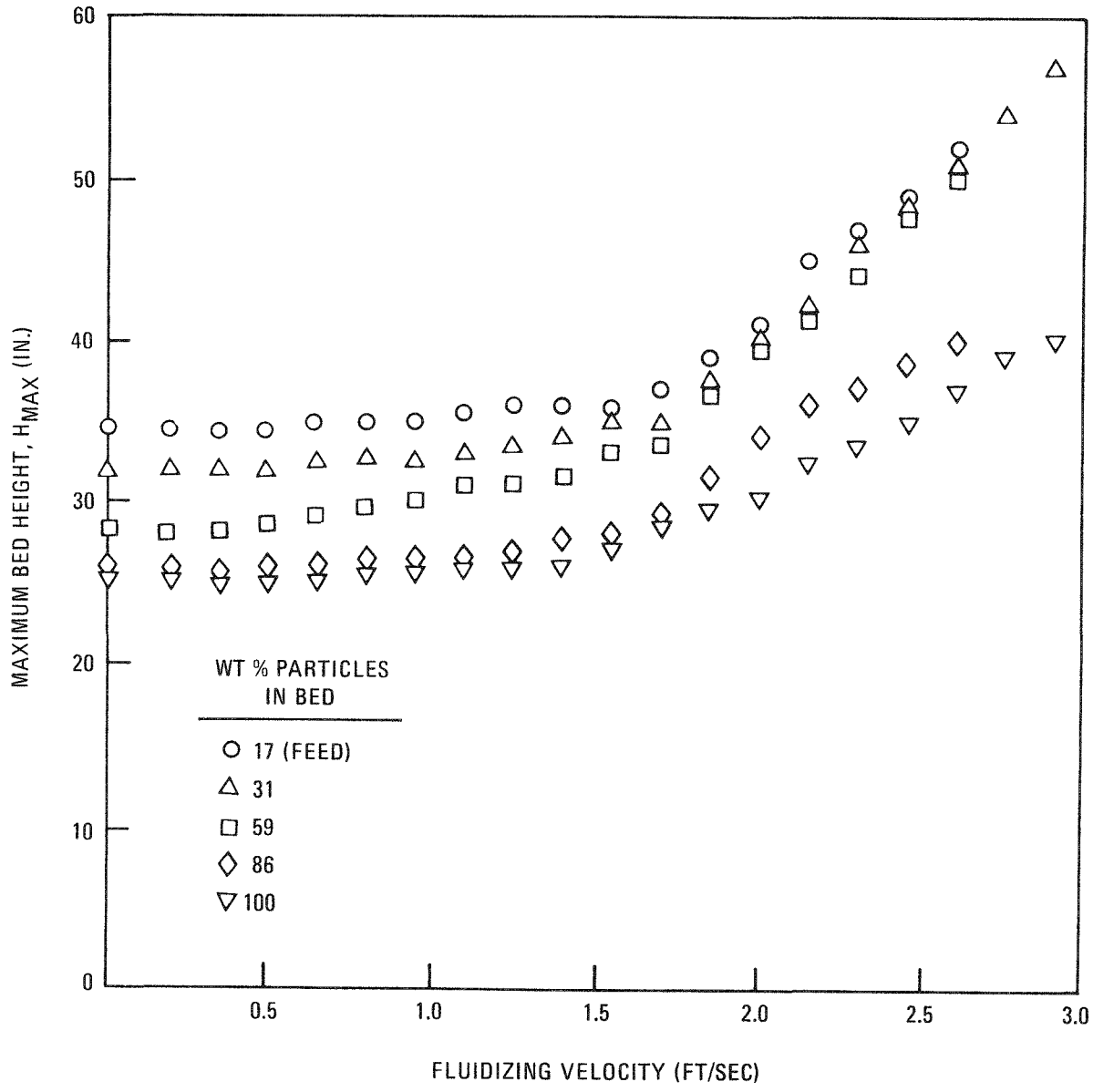

Fig. 4-2. Maximum bed height versus gas velocity for 30-kg beds

provide good qualitative information but only approximate quantitative information.

Other pertinent conclusions obtained were that the 1/2-in. vertical thermowell appears to have no effect on the bubble pattern and mixing in the bed. As shown in Fig. 4-3, the gas required for complete mixing of a bed is minimized when the bed particle concentration is ∿60 to 90 wt %. This, of course, would also depend on the fresh feed graphite (≤3/16 in.) size distribution which, in the case of this cold work, came from the same batch. In addition, initial bubbling and bed expansion apparently occur at lower velocities in beds with ∿60 wt % particles than in fresh feed or in particle-rich beds.

Depending on the size and quantity of graphite in the bed, there will always be a range of fluidizing gas velocities where almost complete bed segregation occurs; that is, a fines layer will be found at the surface of the bed above a layer of larger graphite which, in turn, exists above a particle bed. Complete mixing will be achieved only at a considerably higher gas velocity.

Measured product removal rates through the 1-in. vertex ranged from 165 g/sec for the 17% particle bed to 365 g/sec for the 100% particle bed. However, these data were acquired with almost no fluidizing gas flow and with a slight vacuum from the ventilation system. Under normal operating conditions, these rates would be considerably higher and well within the range of rates required for minimal particle breakage in the pneumatic transport system.

On the basis of the results of this cold work, future work in the hot 20-cm primary burner will continue to be performed at velocities of ∿3 to 4 ft/sec.

Future cold work in the glass mockup will include investigation of:

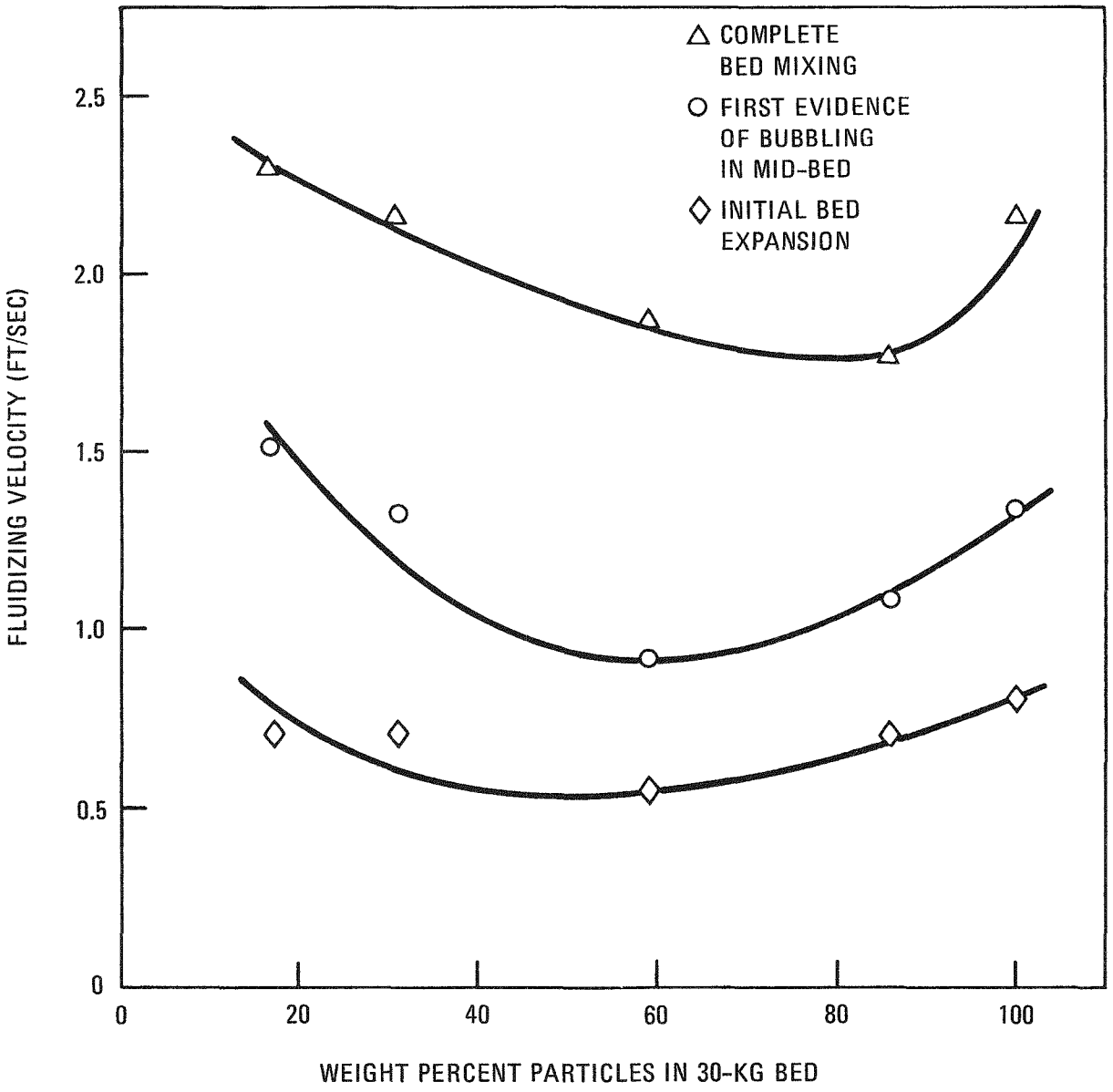

Fig. 4-3. Fluidizing velocity versus bed composition for 30-kg beds

1. Effect of bed weight on fluidization.

2. Effect of maximum feed size on fluidization.

3. Minimum bubbling and minimum fluidization phenomena.

4. Maximum product removal rates acquired under normal operating conditions.

5. Vertex/plenum gas flow combinations for gas jet mixing of solids low in the burner; applies to startup operation with induction heating.

4.1.1.10. 20-cm Primary Burner Design and Modification

The 20-cm primary burner is to be rebuilt to incorporate many of the prototype design features to verify the design parameters on a scaled-down basis; the cooling jacket will be of the pin-fin design and heat fluxes for the cooling jacket and for the induction heater between the susceptor and vessel wall will be similar to those for the prototype burner. The distributor design will have the same included angle and pressure drop as the prototype burner with a product removal line scaled down to provide similar gas velocities during burner operation. This will limit the loading rate to the transport system and will cause particle breakage rates higher than would be obtained with larger capacity (prototype) equipment but is necessary to maintain the vertex/plenum gas ratio of the conical distributor equivalent to that used for the prototype. This ensures that fluidization phenomena will be similar.

4.1.2. Prototype Primary Burner

4.1.2.1. Heating System Design

Thermal analysis for the two-section induction coil indicates the desirability of a heater made up of two independent 36-in. zones. The

lower zone 36-in. induction coil is capable of maintaining the tail-burning particle bed at ∿800°C when heat loss from fines carryover is neglected. Figure 4-4 represents the results of a computer calculation using a relaxation method to obtain the maximum attainable bed temperature in the tail-burning phase when the bed material is predominately fuel particles. The steady-state portions of the temperature curves indicate that the output of a 125-kW motor-generator (M-G) set to this lower zone is adequate under the present design conditions. Actually, the limiting factors in maintaining a higher bed temperature are the bed-to-wall heat transfer coefficient [on the order of 45 Btu/hr-ft^2-°F (255 W/m^2-°C)] and the heat losses from fines carryover. The ability of the induction heater to maintain the bed temperature above 800°C during the burnout phase with fines recycle has not been verified experimentally. Heat losses attributable to fines recycle depend on the fines burn rate, as well as the recycle mass flow rates and temperature. Further evaluation of the burnout phase, including fines recycle, will depend on the availability of experimental data from the 20-cm primary burner.

The 36-in. lower zone is adequate for startup of the bed with the reference operating cycle with a 125-kW power output from the M-G set. The startup transients in Fig. 4-5 indicate the 0.7 fuel element bed will be ready for ignition in approximately 60 min or less. However, startup transients for the 6-ft "whole bed" case with a 36-in. induction coil indicate that with a power input of 115 kW to the susceptor, the bed will reach a steady-state value of approximately 700°C in approximately 2 hr. Figure 4-6 represents this startup transient. The lower attainable bed temperature is attributed to the additional heat transfer losses to the unheated portion of the bed and to the burner wall. The capability of one 36-in.-long coil is therefore marginal for any beds larger than the reference startup case. The induction heating system will therefore be a two-stage system consisting of two 36-in.-long sections designed for 125-kW output each from the M-G set.

The induction heater vendor, Tocco Company, has recommended the use of parallel control of the two zones, that is, separate control stations for

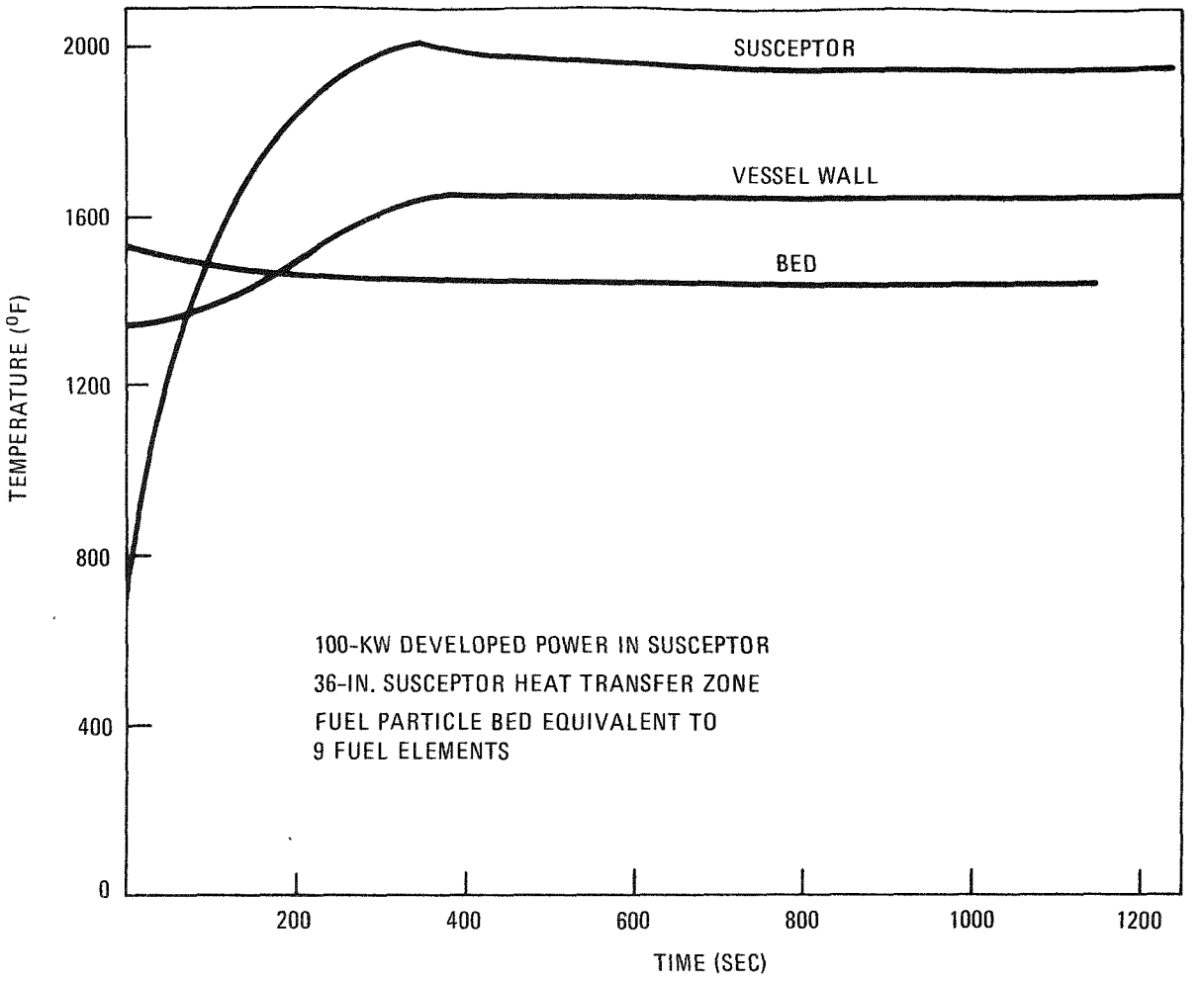

Fig. 4-4. Induction heating tail-burning "steady-state" temperature

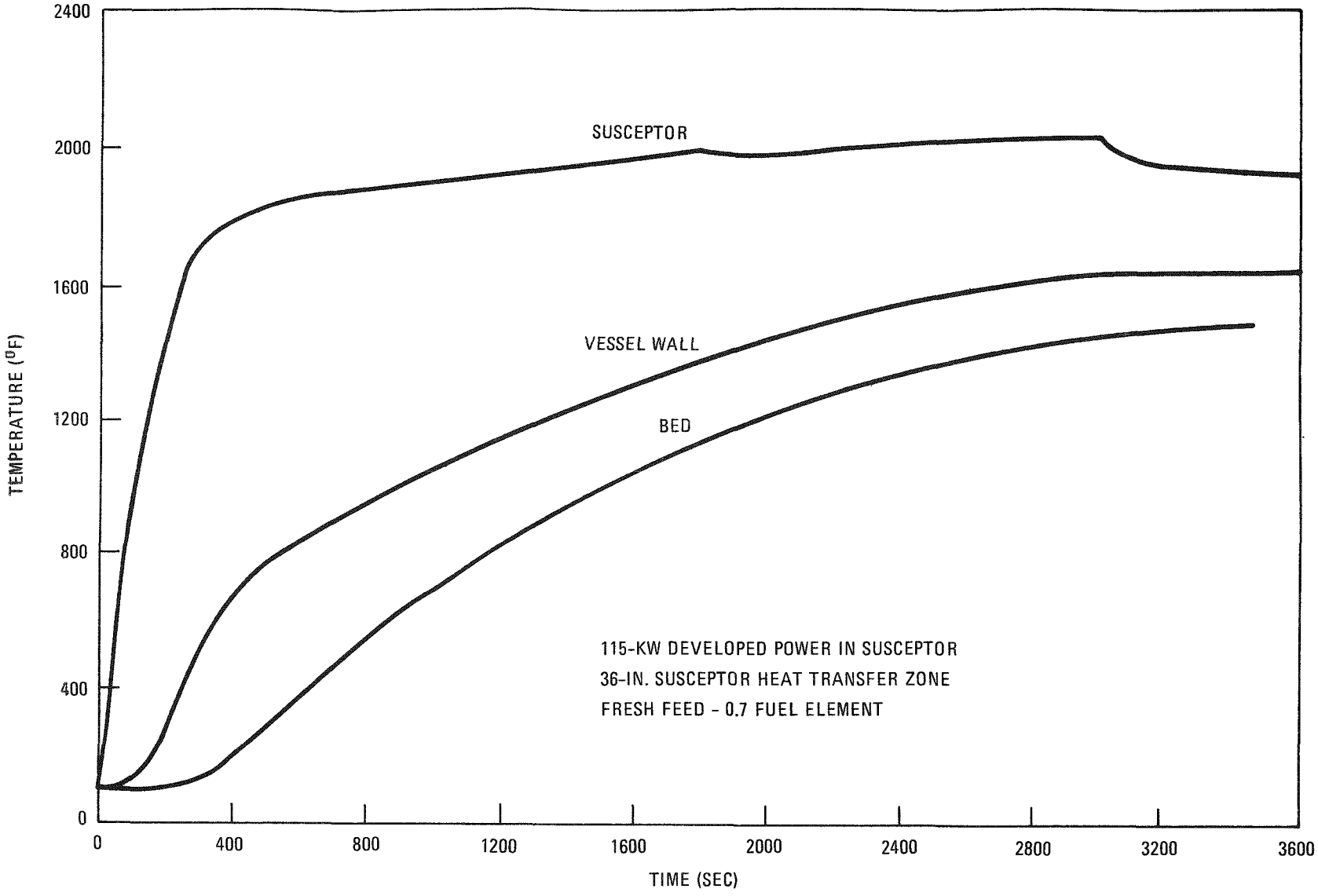

Fig. 4-5. Normal startup transients with a 36-in. coil

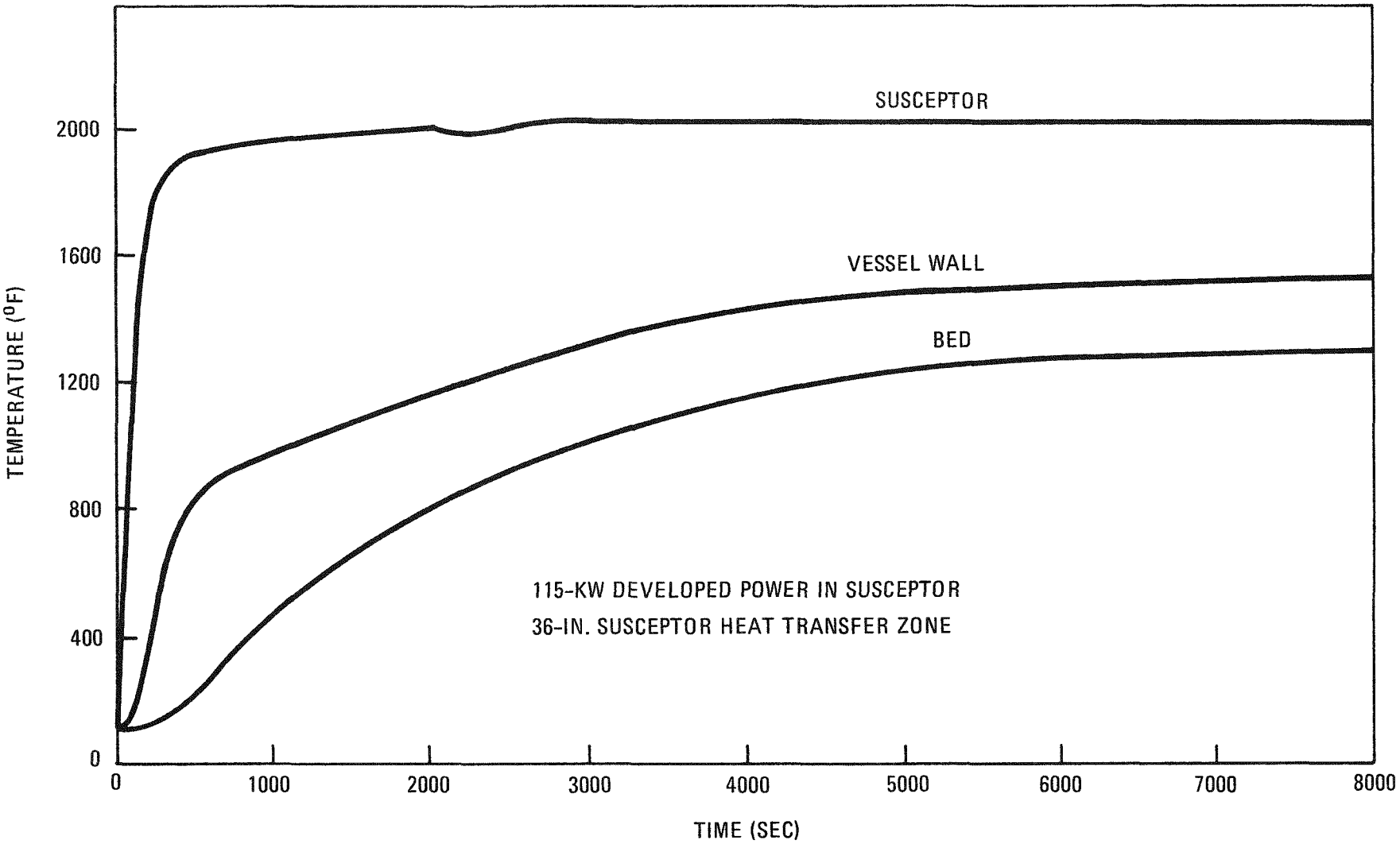

Fig. 4-6. Whole bed startup with a 36-in. coil

each coil running off the same M-G set. The original 72-in.-long coil will be split into two 36-in.-long sections, with each section designed for 50% of the output of the M-G set. The factors listed below were evaluated while arriving at the major coil design and fabrication parameters listed in Table 4-2. These factors affect coil design, including tubing size, number of turns, and the coil support system.

1. Requirements for the coil cooling water and the recirculating pump pressure head.

2. Requirement for the circuit balancing capacitor (as well as the coil terminal voltage and the space requirement).

3. Material availability and unit length (for example, available 1-in. tubing comes in 12-ft lengths, while 7/8-in. tubing comes in 60-ft lengths).

4. Minimum coil spacing requirement.

4.1.2.2. Heating/Cooling System Fabrication

After the completion of structural analysis, the heating/cooling assembly was released for fabrication. Delivery is expected in early November. Subassemblies currently being fabricated include:

1. Exhaust plenum mounting plate

2. Upper intake lifting plate

3. Lower intake plenum assembly

4. Insulation bonnet assembly

5. Cap insulator assembly

TABLE 4-2
INDUCTION HEATING COIL DESIGN PARAMETERS
40-CM PRIMARY BURNER

Coil size	7/8-in. O.D. 0.065-in. wall
Number of turns	29 turns/section
Coil spacing	1/4-in., even distribution 1/2-in. gap between sections
Coil terminal voltage at full power (250 kW)	520 V
Support legs	8 each, 1-1/2-in. x 2-in. depth, transite 4 studs on each turn
Capacitors (300 kVAR each)	3 capacitors/section
Coil supply	Lead will be held in position by insulating clamps to the coil
Cutting coil	Cutting coil crossover tube will be held in position by insulating clamps

Figures 4-7 through 4-10 show some of the above parts in various stages of fabrication.

4.1.2.3. Installation

The cooling air blower and accessories have been received and plans for installation are under way. An architectural layout of cooling duct, heat exchanger, and induction heater components is being prepared in an effort to avoid interferences between equipment and instrumentation when equipment installation is fully under way. The cooling air blower will be installed in a closed vault to minimize noise.

4.2. SECONDARY FLUIDIZED-BED COMBUSTION

4.2.1. 10-cm Secondary Fluidized-Bed Combustor

The induction heating system and the automatic control system were evaluated during the reporting period, with recommendations made for scaleup to larger burners.

One burner run was made to measure internal heat transfer coefficients. A second run was made to oxidize BISO ThO_2 particles needed for work being performed in connection with the leacher.

4.2.1.1. Evaluation of Induction Heating Systems

Induction heating has been selected as the heating system for the secondary burning operation (Ref. 4-2). Induction heating is defined as the heating of a conducting material in a varying magnetic field due to its internal losses; in the case of Hastelloy X, internal losses are due to eddy currents induced in the metal by transformer coupling action.

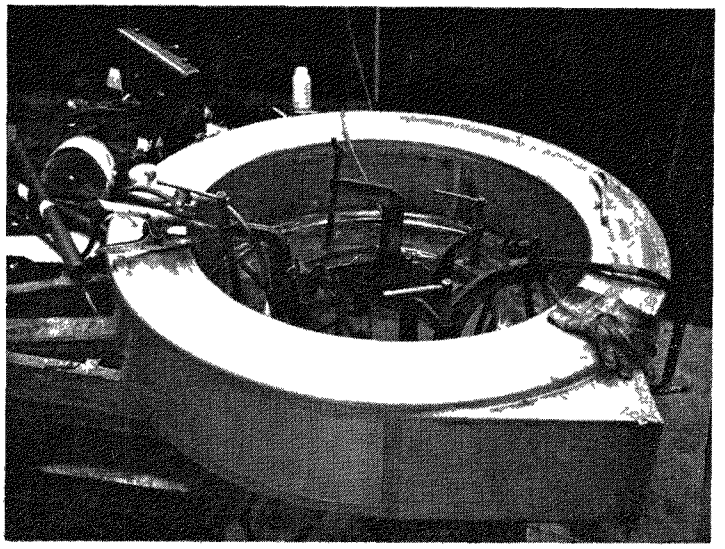

Fig. 4-7. Lower intake plenum assembly (Part No. 5244040-1)

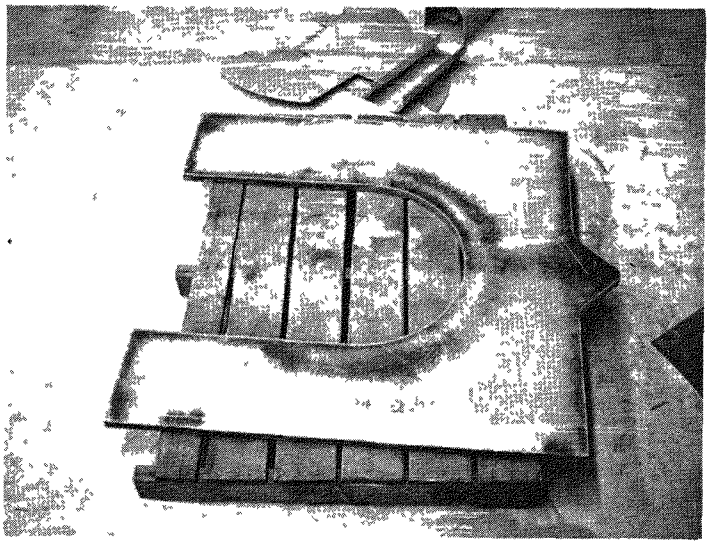

Fig. 4-8. Upper intake lifting plate (Part No. 5244047-1)

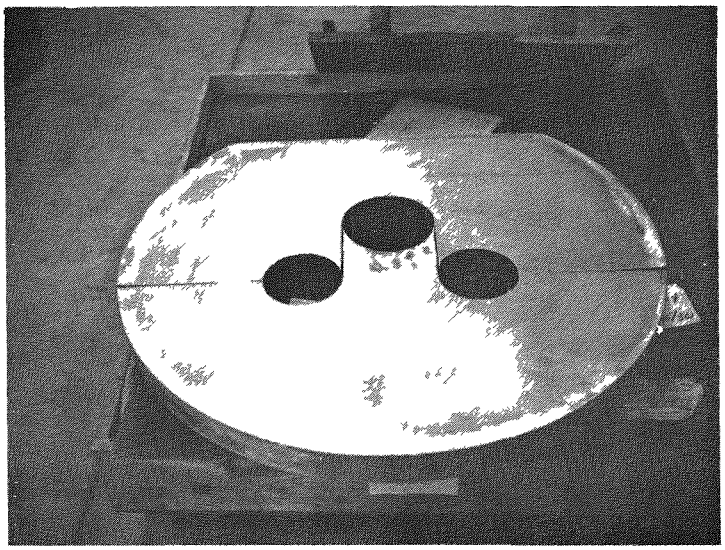

Fig. 4-9. Cap insulator assembly (Part No. 5244061-1)

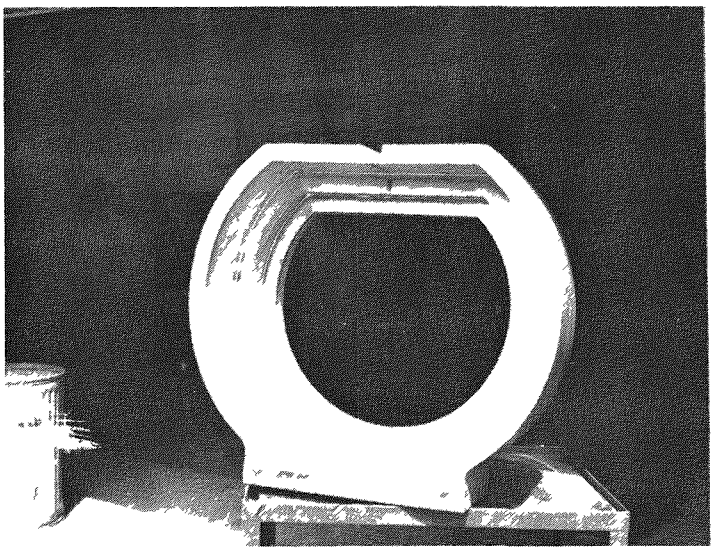

Fig. 4-10. Insulation bonnet assembly (Part No. 5244063-1)

Three induction coil designs have been used on the 10-cm secondary burner during a total of thirteen burner runs. The induction heating system was identical in all runs except for the differences in coil design. The general layout of the system is shown in Fig. 4-11. The motor-generator area is shown in Fig. 4-12, and the burner area is shown in Figs. 4-13 and 4-14. The basic operation of the system is as follows:

1. The motor-generator produces 10,000 cycles/sec AC current at 0 to 440 V, with a maximum power level of 30,000 W at 440 V (68.2 amp). The motor-generator is water cooled to remove mechanically and electrically produced heat. It is actuated by a magnetic starter. Regulation of the motor-generator output is accomplished by varying the field from approximately 0 to 55 V. The voltage required for the field is supplied by a magnetic amplifier to allow use of an automatic controller in adjusting the generator field. The field voltage required to yield maximum generator current output increases as the load (in this case the burner) changes temperature.

2. High frequency contactors are used for absolute shutoff of high-frequency current to the coil.

3. An autotransformer reduces the high-frequency supply voltage before it reaches the coil. The autotransformer is water cooled.

4. A water-cooled capacitor, parallel to the burner coil, electrically balances the system such that the phase angle is at a minimum and realized power is thus maximized. Water-cooled copper bus bars connect the capacitor to the coil, which is also water cooled.

The first coil used was a 53-turn, 30-in.-long solenoid coil made of 3/8-in. copper tubing. The coil was made by TOCCO as part of the initial

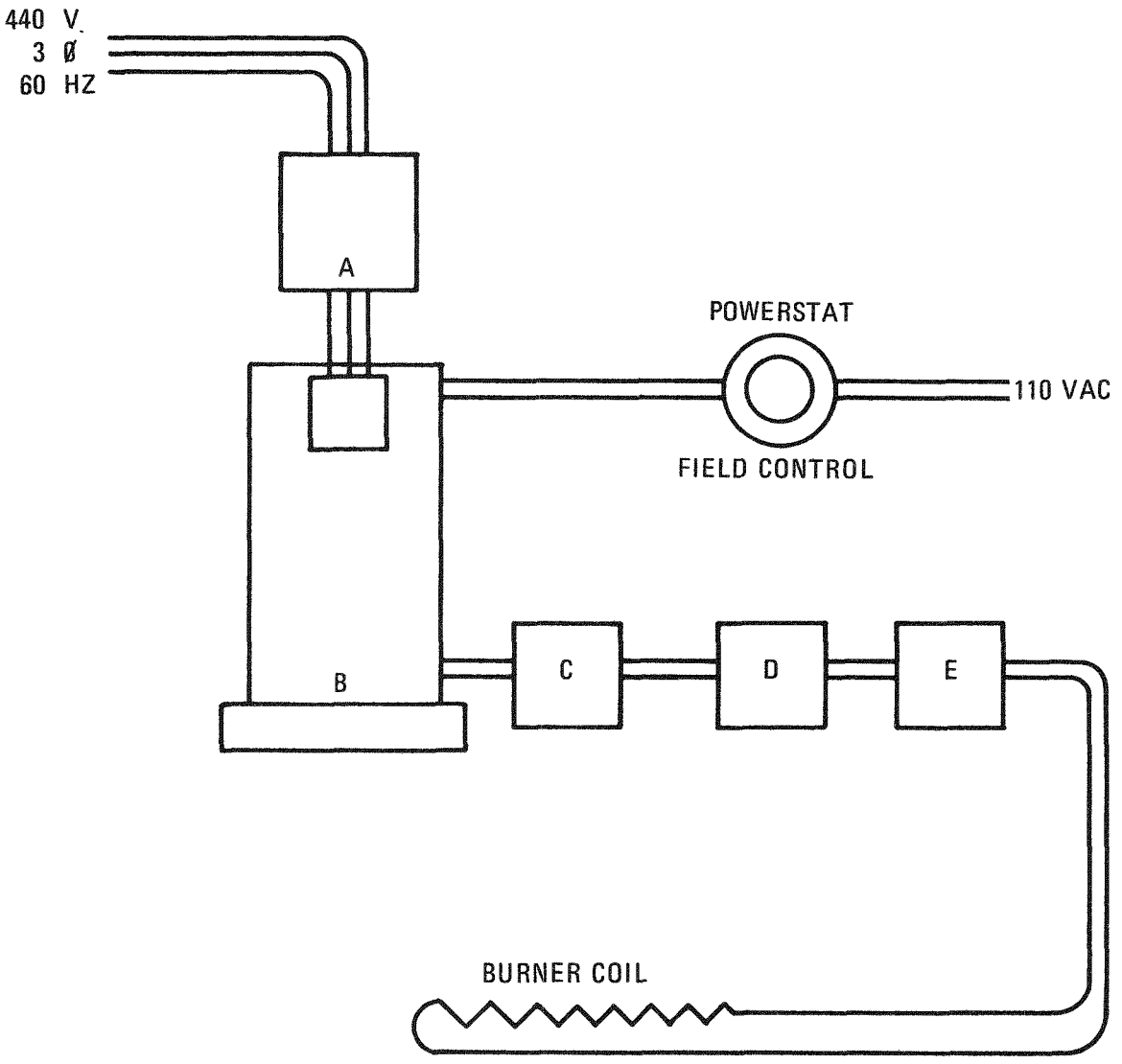

A STARTER
B 30-KW MOTOR GENERATOR
C CONTACTORS
D TRANSFORMER
E CAPACITOR

Fig. 4-11. General layout of induction heating system

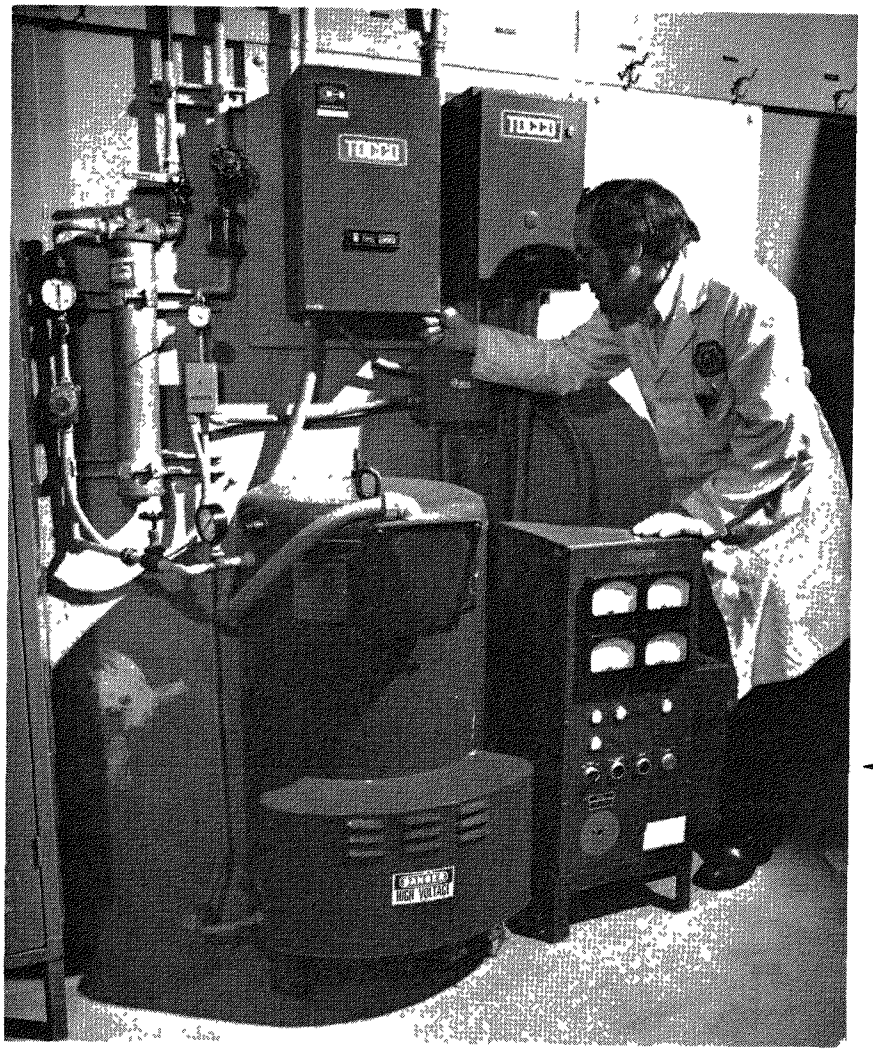

Fig. 4-12. Motor-generator system

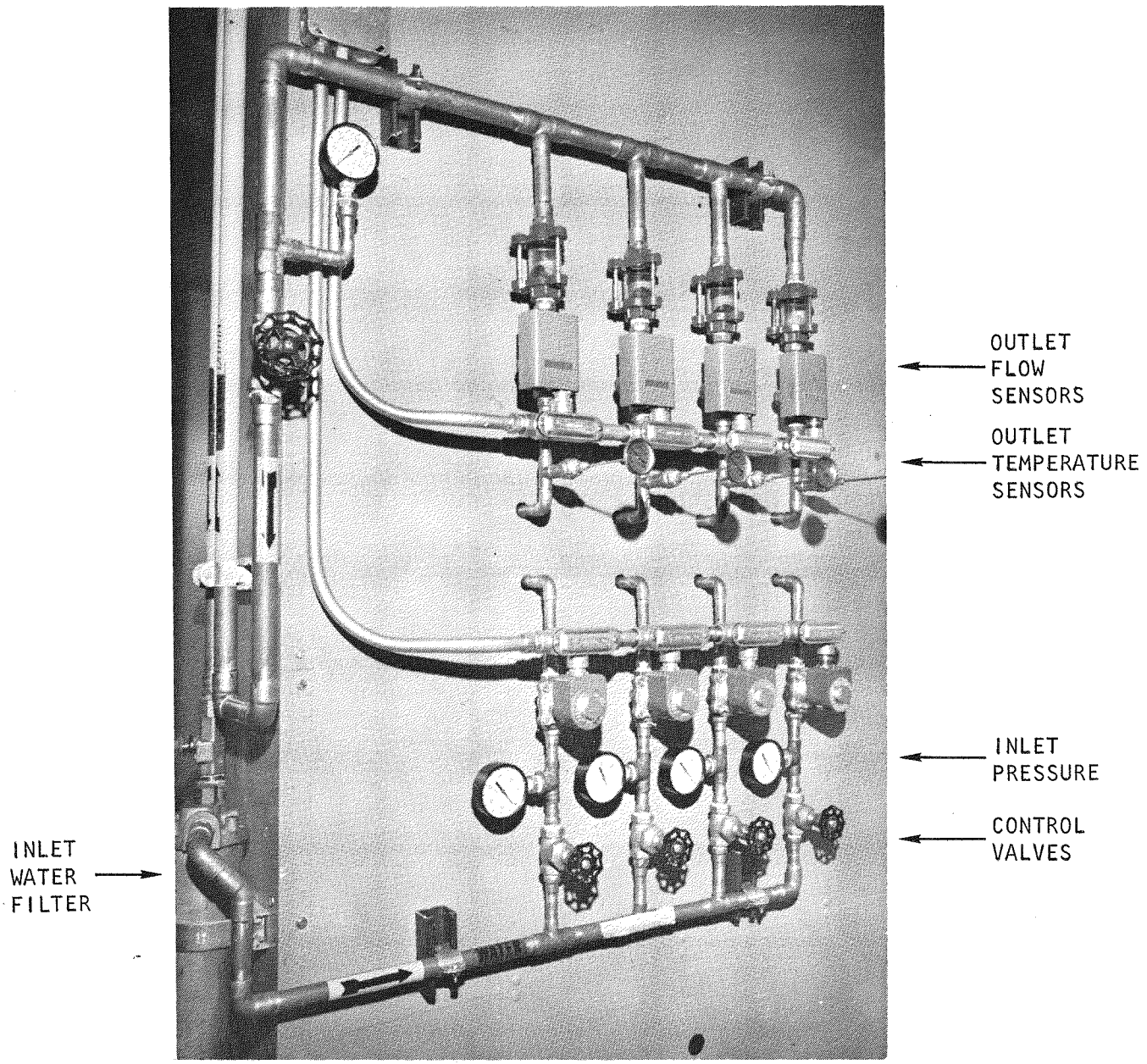

Fig. 4-13. Water-supply manifold

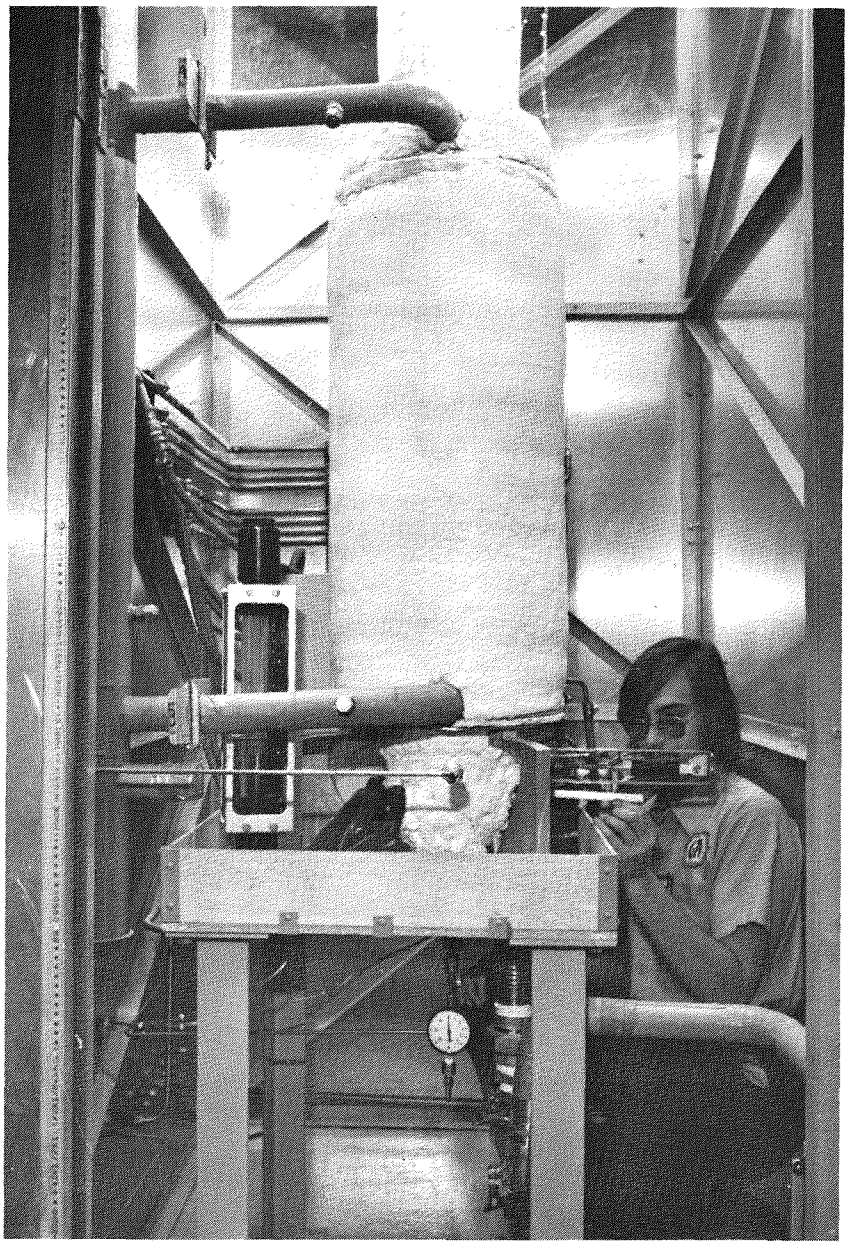

Fig. 4-14. Induction-heated secondary burner

purchase order and was tuned at the TOCCO facility prior to shipping to GA. The air gap between the 4-in. Schedule 40 Hastelloy X tube and the coil was 0.30-in. The coil was insulated only on the outside so that the copper tubing was bare on the side toward the burner tube. The outside insulation consisted of 2 in. of Fibrefax with a stainless steel outer jacket (10-in. diameter). The end plates of the stainless jacket were 2 in. from the end coil turn. No appreciable heating of these end plates due to susception from induction coil end effects was noted. Heating occurred only by convection and radiation from the burner tube. The coil was balanced by setting the autotransformer at a turndown ratio of 0.8/1 and setting the capacitor at 154 kVA. The coil cooling water flow was 2.3 gal/min.

The initial heatup rate using this coil indicated that 18 kW were being dissipated in the burner tube as heat. The remaining 12 kW were taken up by resistive losses in the coil, autotransformer, capacitor, and lead line from the motor-generator set. Since these readings were taken essentially at ambient temperatures, heat losses to the surroundings were negligible. The tube could be heated to 900°C, at which time the heat losses to the water-cooled coil via radiation were up to 18 kW, thus bringing the tube temperature to a steady state.

This coil was used in burner Runs 37 and 38. After combustion was stabilized with the tube at 900°C, the 18 kW of power loss to the coil with the motor-generator set off was enough to remove sufficient heat, even at peak burn rates, to keep the tube at 900°C. Because of this ample cooling capacity, no cooling air was required in the vicinity of the coil.

A second coil was built to enable 1/8 in. of asbestos insulation to be placed between the coil and the burner tube to reduce radiant heat losses. This coil was built with a 6.5-in. I.D. such that it could be slipped around the burner tube over the existing flanged ends. The coil was 28 in. long with 12 turns (the number of turns was determined by shunting to get the correct impedance) and was made of 3/8-in. copper tubing. There was a

1-in. air gap between the coil and the burner tube. The coil cooling water flow was 2.3 gal/min. The coil was insulated on the outside by 3 in. of Fibrefax, which was held in place by a 13-in.-diameter stainless steel jacket. The initial 10-in.-diameter jacket suscepted too much power from the coil and the jacket was therefore enlarged to reduce the induced power. The jacket and plates (located 2 in. from the coil end turns) were originally stainless steel. These plates got very hot due to induced current from the coil and were therefore changed to transite. The end plates are not required to be mechanically strong, but only to seal the cooling air flow. Transite is therefore acceptable and this material exhibits no heating due to induction effects.

This coil was balanced at a transformer turndown ratio of 0.8/1 and 539 kVA of capacitance. The initial heating rate with this coil indicates 23 kW dissipated in the tube, with the remainder as coil and peripheral electrical equipment resistive losses. The steady-state tube temperature with this coil configuration was ∿850°C without a fluid bed.

To check induced power in the support rods for the prototype burners, a test was made by embedding a thermocouple in a 1/2-in. stainless steel rod positioned 1/2 in. from the present coil. No appreciable induction heating of the rod was noted; the only heatup observed was from convection.

Burner Runs 39 through 46 utilized this second coil design. This coil was capable of holding the bed temperature during tail burning to 800°C, yielding acceptable product carbon contents.

The present coil design is a basic departure from earlier work in that the coil now suscepts onto a cylinder that is placed concentrically around the burner tube. The previous coils suscepted directly on the burner tube. This new coil was installed for the purpose of prototype design verification (both primary and secondary). As documented in Ref. 4-3, the larger burner heating systems will be more efficient with an intermediate susceptor.

The susceptor plate heating system for the 10-cm secondary burner was designed using the same procedures as used for the prototype burner. As shown in Fig. 4-15, the susceptor is a 7-in.-I.D., 34-in.-long cylinder made from 1/8-in.-thick RA-333. The susceptor has removable end plates to seal cooling air flow, as well as to allow removal of the susceptor over the 6-1/2-in. burner flanges. The susceptor outer surface is insulated with 1-1/2-in. of WRP-X moldable insulation; a 26-in.-long, 10-turn helical induction heating coil made from 3/4-in. copper tubing surrounds the insulation. One field cutting copper coil is located at each end of the induction coil, adjacent to the end plates. These cutting coils serve to block the induction field from coupling to the end plates and dissipating heat therein.

Heating tests were made using the empty burner tube. Figure 4-16 shows the time-temperature plot of the susceptor and the tube.

The present heating system has been used to make four secondary burner runs (47, 48, 49, and 50). This system is capable of holding the bed at 775°C during tail burning (a period of low combustion just prior to the end of the run). This temperature is slightly less than that for the second coil design, but still yields acceptable product carbon contents. The most important result of using this susceptor plate system is the data obtained, mainly on heatup transients and steady-state idling of the fluid bed, that can be used to verify the prototype burner design. These data are currently being analyzed to verify design of the prototype burners. Heat-transfer coefficients, burner end losses (fines heat transport to filter areas), and induction coil design parameters (coil spacing, coil tube size, etc.) are being determined.

In conclusion, induction heating has proved to be a versatile, trouble-free operation as used on the 10-cm secondary burner. The three coil designs tested have all yielded workable heating rates. Support was given to the prototype design effort by the installation of a susceptor plate

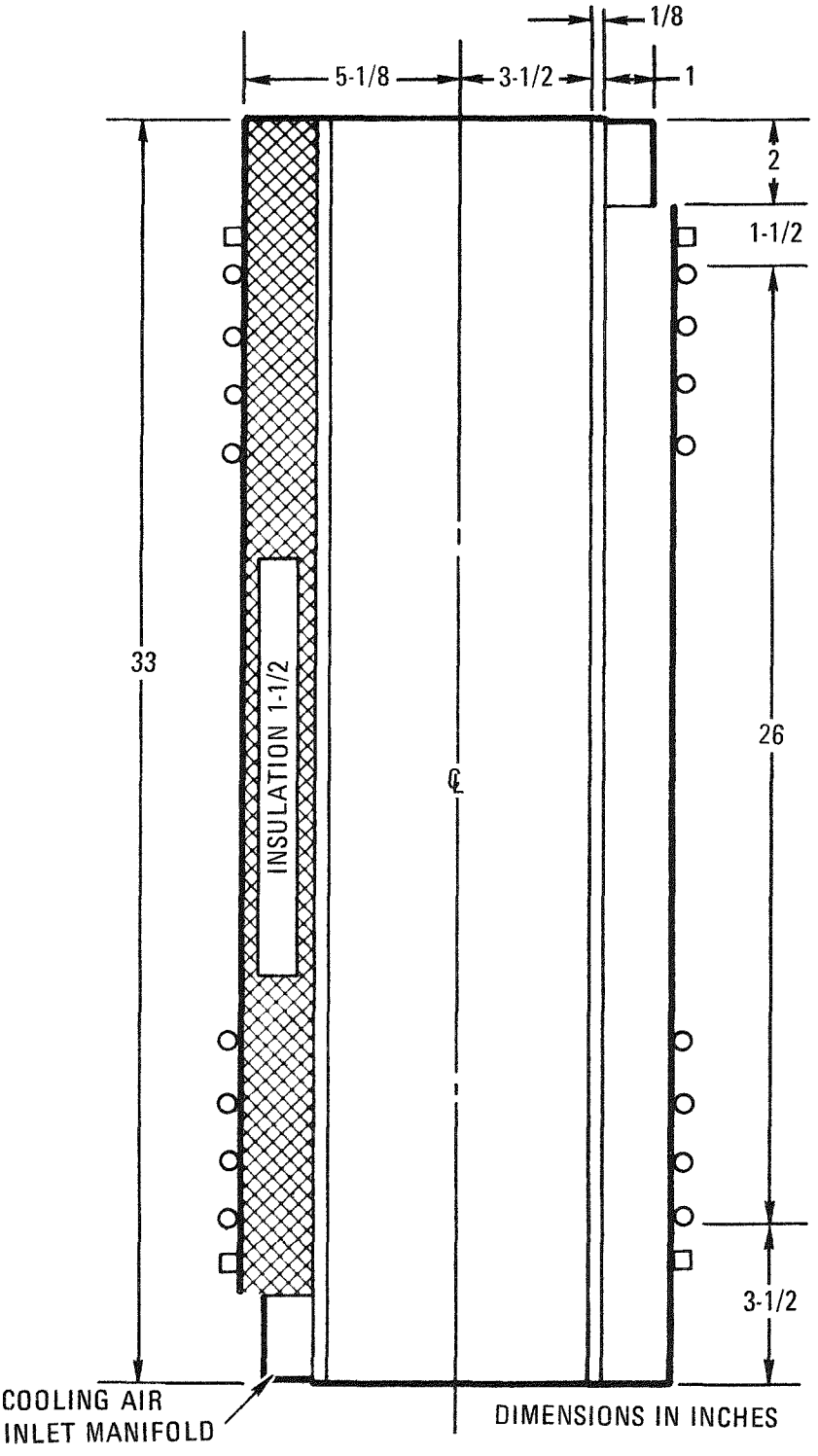

Fig. 4-15. Susceptor-coil assembly

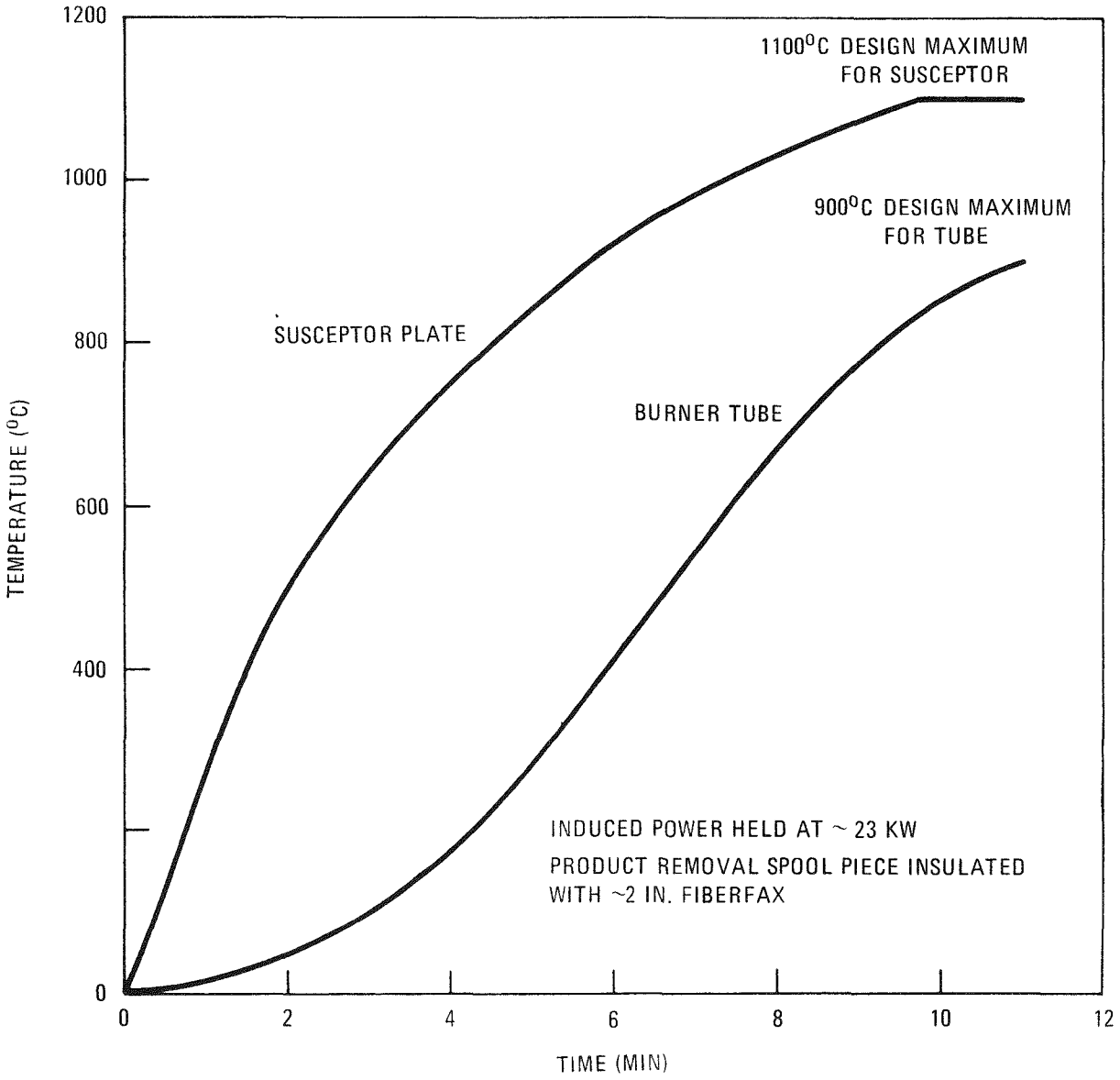

Fig. 4-16. Empty tube heating transient

heating system. All indications are that there will be no problems in the use of an induction heater on larger burners.

The only future work to be done on the 10-cm secondary burner is in fulfillment of a GA-ACC commitment; this entails use of a water recirculator system on the induction heating coil. A fixed amount of water, containing a neutron poison in a concentration to be determined by ACC, will be circulated and the chemical stability of the poison will be examined.

4.2.1.2. Evaluation of the Automatic Control System

The 10-cm secondary burner was operated manually during many runs. When the operating mode became sufficiently well known, automation of the batch cycle was begun in steps. The first steps were to test individual control loops, leaving other systems in a manual mode. At present, all the control loops are being utilized in each burner run. This section discusses the hardware requirements of the control systems, their performance during burner runs, and an alternative method that has been considered.

The secondary burner operates as a batch combustor, burning an initial bed of crushed fuel particles to a low-carbon ash of ThO_2 and SiC. The basic operating steps are as follows:

1. Preheat: Preheat the burner tube to 900°C with a 40 SLPM CO_2 purge. Actuate filter blowback.

2. Feed: Add crushed feed using the gravity pneumatic feeder.

3. Startup: When the bed heats up to 700°C, introduce O_2 as a ramp from 40 to 100 SLPM in a 6-min period. Decrease CO_2 flow to 0.

4. Main burn: Control the bed temperature at 900°C using cooling air flow modulation. Filter chamber cooling air is on demand (when filter temperature is >400°C).

5. Tail burn: Change inlet flows to 60 SLPM O_2 and 40 SLPM CO_2 when the bed begins to burn out, as evidenced by a drop in off-gas CO concentration below 2%. Hold bed temperature as close to 900°C as possible.

6. Shutdown: When the bed is sufficiently low in carbon (as seen by the balance of O_2 in = O_2 out), switch to pure CO_2 inlet flow and cool the bed to 500°C.

7. Cleanout: Pneumatically transport the product through the high-temperature bed removal system. Include burner cleanout procedures to remove heel from distributor plate surface.

The heating and cooling instrumentation is shown in Fig. 4-17. The heater is actuated to bring the burner tube to 900°C without raising the susceptor temperature over 1100°C or the bed temperature above 900°C. There are ∿15°C dead bands on the temperature set points. Thus, the bed is held as close to 900°C as possible using induction power whenever it is required throughout the run. Burner cooling is on demand when the bed temperature exceeds 900°C. This cooling system holds the bed to a 20°C overshoot when it is actuated in a run. Filter cooling is actuated when the filter temperature is above 400°C, which is generally during the entire main burning portion of the run.

The gas inlet flow is controlled at preset values and is changed by the "trips" listed with the basic operating steps. For example, when the bed is heated to 700°C, the flow changes to allow an O_2 ramping procedure for startup. The flow control system is shown schematically in Fig. 4-18. In practice, this system keeps the flows at the preset ±2 SLPM, which is more than sufficient accuracy.

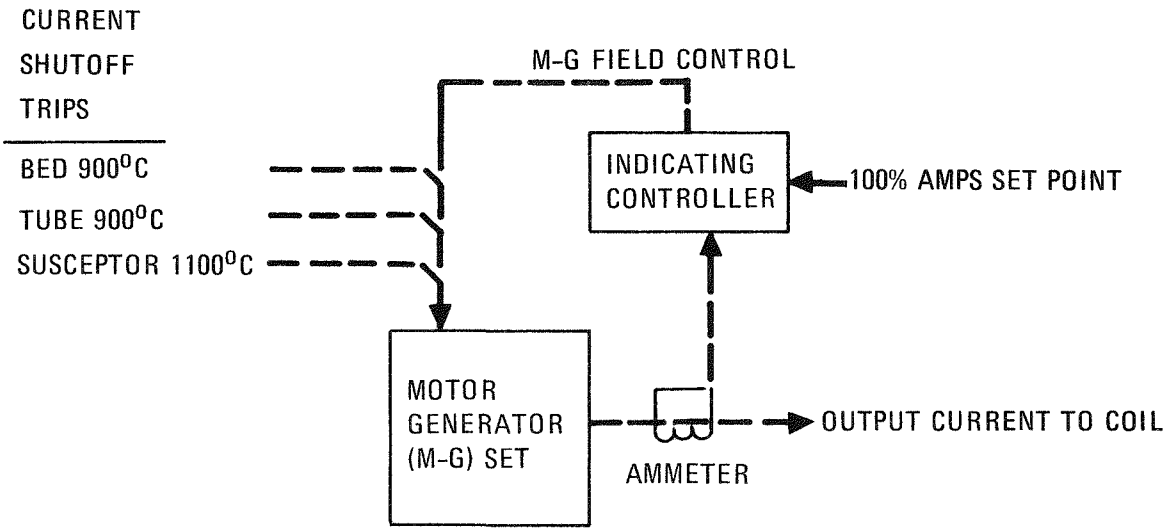

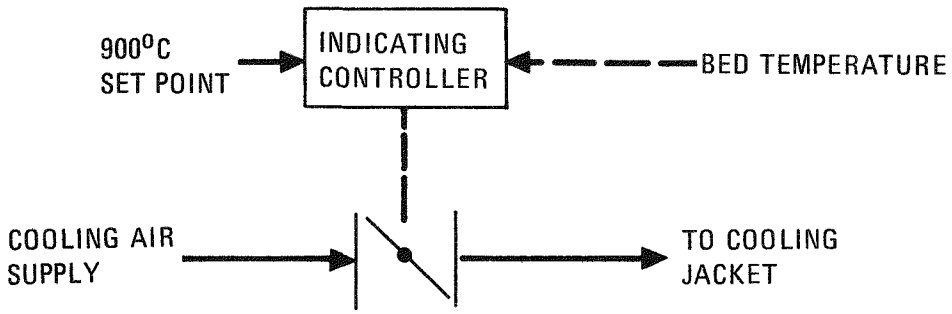

Fig. 4-17. Heating and cooling controls

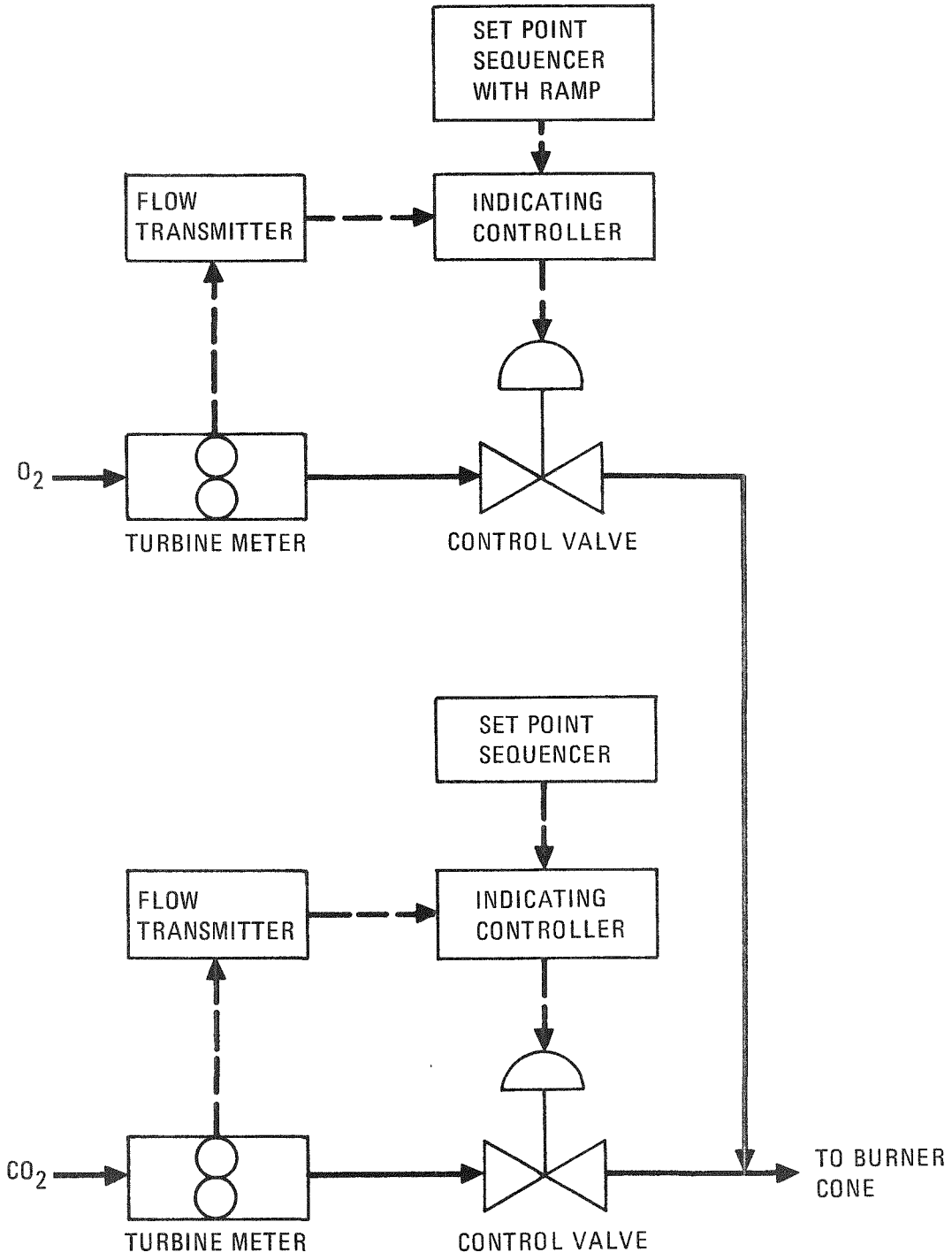

Fig. 4-18. Gas flow controls

Auxiliary system controls include the following:

1. The filter blowback system consists of two timers; one sets the blowback pulse duration and the other sets the frequency of blowback (Ref. 4-4).

2. Feeding the burner requires actuating the gas flows required for feeder operation for preset times. It also requires opening and closing the appropriate ball valves for feed hopper isolation (Ref. 4-5).

3. Removal of product requires a cycle of actuating the pneumatic transport pump, opening the product valve, and performing steps for burner cleanout (Ref. 4-6).

These three systems are presently actuated manually but are quite amenable to cycle timers for automated usage.

Burner Run 49 was made using automatic gas flow systems as well as the automatic heating and cooling systems. The auxiliary systems were manually actuated.

The gas flows deviated a maximum of ±1 SLPM in the run. This type system is expected to work well as it is a simple feedback situation.

The heating system was held at an output amperage at 100% during all demand periods. The temperature of the susceptor will normally affect this amperage as much as 20 to 30% if not suitably controlled. The susceptor temperature controlled the heating demand during the tube preheat portion of the run. The burner wall controlled the demand during bed heating and ignition. Cooling was called for intermittently through the main burn portion. The bed temperature kept the induction heater de-energized during

that period. In tail burning, the susceptor was the limiting temperature.

No problems were encountered throughout the run, indicating the suitability of the system during normal operation. Should a problem develop, adequate means are available for correction. If a bed temperature were to rise above 900°C, the cooling air would increase until the bed temperature decreased. Air flow at 30% of capacity is capable of cooling the bed 50°C/min. Full cooling should result in at least 100°C/min bed cooling rates. Bed temperatures over 950°C actuate an alarm such that appropriate operator action can be taken.

The only other control mode that has been considered is the oxygen-flow bed-temperature feedback loop as utilized on the primary burner. The advantage of this control mode is that it has a faster response to temperature upsets, although this response may be considerably faster than is actually necessary. The startup must still be coordinated via an O_2 ramping mode, in this case followed by switching to temperature feedback control of O_2 after ignition. During the tail burning portion, the temperature feedback would have to be terminated to avoid driving the O_2 flow to maximum when the temperature falls off. This feedback O_2 control would thus be operable only during the main burning portion. Burner cooling would have to be fixed, with incremental adjustments possible if the temperature could not be held at 900°C by O_2 flow alone. The induction heating system would be identical to the present system. Inlet CO_2 flow would be controlled in a similar manner to that presently used. The only real difference with this mode of control is that during the main burn portion, bed temperature would be controlled by O_2 flow instead of by cooling air flow. Because there has been no indication that this is required (upsets should be self correcting at a workable speed with the present system) and because changing control modes in the middle of a run is a complication, this method is not used or recommended.

In conclusion, the 10-cm secondary burner automatic control system has been selected as the most desirable of two options. It has worked well whenever used in burner runs and will be used in future experimental plans. This system is being incorporated, in principle, in the prototype secondary design; no problem areas are anticipated.

4.2.1.3. Burner Run 50

In Run 50, 14 kg of feed were used to perform heat transient tests over a 2-day period. This bed was then burned down to low carbon content (0.5%). A Hastelloy X in-vessel filter had been installed prior to the run as part of a corrosion study to compare Hastelloy X with stainless steel. Product transport was complicated by an improperly seated filter, but resumed normally upon replacement of the filter.

The 14 kg of TRISO fertile particles were crushed through the double-roll crushing system. The size distribution of this feed is shown in Fig. 4-19.

After the heat transients were completed, the bed was heated to 775°C and ignited as in previous runs. Filter cooling and blowback were then actuated, keeping the maximum filter temperature to 720°C and the maximum filter pressure drop to 9 in. H_2O. The filters were cooled to 580°C prior to breakthrough of the O_2 front from the bed. Final bed burnout was at 780°C.

The final bed was cooled to 300°C while fluidized with 100 SLPM CO_2. With the pneumatic transport system actuated, the product valve was opened for product withdrawal. The pump suction vacuum rapidly went from 8 to 22 in. Hg and stayed at this level, indicating a blockage. External equipment checks gave no clue as to the cause. The burner was shut down and left for 3 days (over a weekend). Inspection then indicated that the small pump prefilter was heavily clogged with product. Following replacement of this

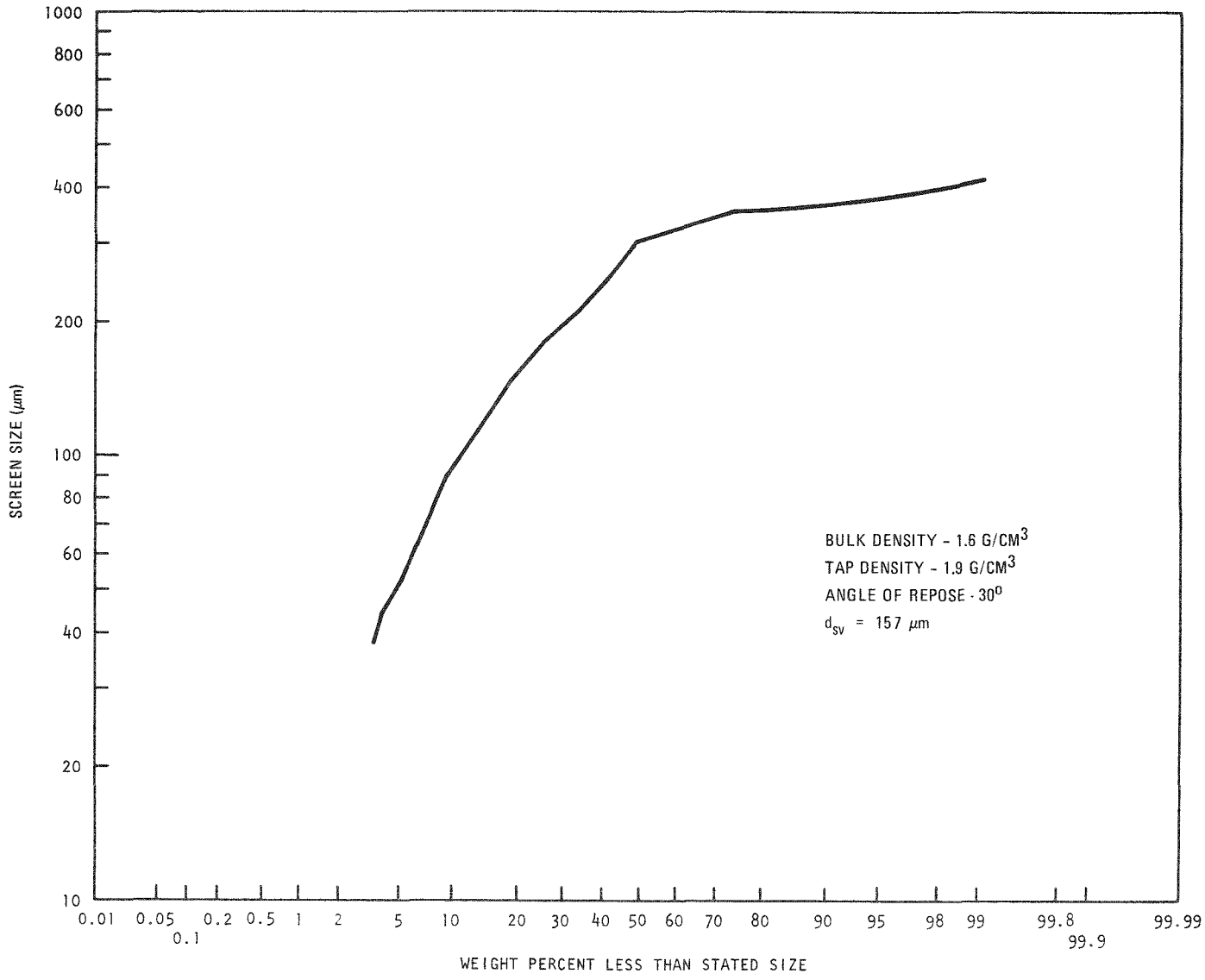

Fig. 4-19. Size distribution of Run 50 sample crushed feed

filter and the receiver filter, the remainder of the product was transported normally. It appears that the receiver filter had not seated properly and allowed a large amount of the initial product to fill the pump prefilter, thus stopping air flow.

It is important to note that even under these adverse conditions, the secondary burner product transport system was rendered operable after the problem was corrected. In this case bulk material was picked up off the bottom of the pipe after it had "salted out," which is much more difficult than normal transport and thus demonstrates the flexibility of this system.

The product contained 0.5 wt % burnable carbon; the size distribution is shown in Fig. 4-20.

4.2.1.4. BISO ThO_2 Particle Burnback

Sixty kilograms of BISO ThO_2 particles were oxidized in the 10-cm secondary burner to provide ThO_2 kernels for work being performed in connection with the leacher. The initial bed contained 14 kg of feed. The remaining feed was added continuously until all 60 kg were in the burner. Peak burn rates were ∿60 g C/min displaced from the burner. The product contained ∿8% carbon, most of which was extremely fine carbon that was trapped in the filter chamber during the final portion of the run. This carbon was removed from the burner after the ThO_2 kernels so that the kernels for use in leaching were low in carbon (0.02%).

The ThO_2 kernels were of the sol-gel type and were prepared by Oak Ridge National Laboratory. The kernels were BISO coated at GA. The total weight of the particles was 60 kg [21.5 kg carbon coatings (buffer and PyC) and the balance ThO_2].

The first startup attempts were made by induction heating of 20 kg of feed to 800°C and then trying to fluidize and ignite the bed. The gas

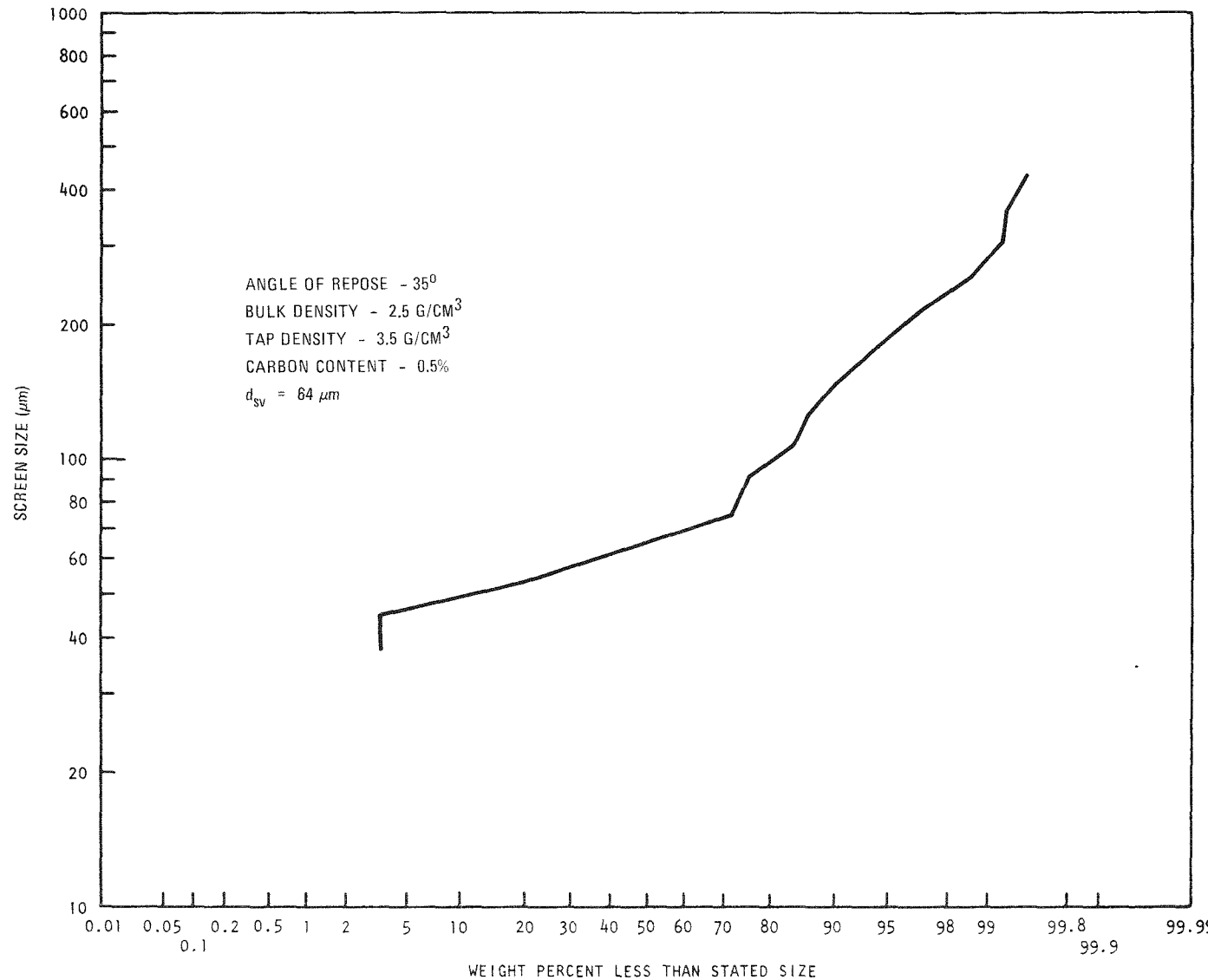

Fig. 4-20. Size distribution for Run 50 product

flows would have been sufficient to fluidize the bed if the entire bed had been at 800°C; however, the portions of the bed above and below the heated zone were cool (<300°C) and fluidization of these areas required much higher flows (higher than the capability of the gas supply system).

The next startup utilized a higher capacity gas supply to enable low-temperature fluidization, with successful results. A 14-kg bed (which just fits into the induction heating zone) was heated to 800°C, fluidized, and ignited using ∿250 SLPM inlet flow (40% O_2). When the entire bed reached 900°C, the total flow was reduced (because of reduced gas requirements at higher temperatures) to 160 SLPM (65% O_2) for main burning.

During main burning, carbon was consumed at a rate that required addition of about 150 g of particles per minute to hold the bed carbon inventory constant (letting the ThO_2 inventory increase). Batches of 3 kg were added at 20-min intervals. This was found to be unsatisfactory because of the instability induced by adding the cold charge. In one instance the bed was extinguished due to quenching by the feed and had to be restarted. Following reignition, 1-kg bed batches were added every 5 to 10 min.

Combustion was stable for the remainder of the run, with cooling air required intermittently for bed temperature control. About 1 to 2% O_2 bypassed the bed during the main burning portion. This is probably due to the large particle size, which leads to a low carbon surface area for gas contact, as well as the short bed length (2 to 3 ft) and the low reaction kinetics of the PyC and O_2.

Filter blowback was a 1-sec pulse every 10 sec. The maximum lower filter temperatures were 500°C, and the peak filter pressure drop was 16 in. H_2O.

When combustion decreased at the end of the run, the heater was reactivated to hold the bed temperature at 800°C. Gas flow was gradually

changed to 160 SLPM of O_2. When combustion products ceased to exit the burner, the gas flow was switched to 160 SLPM of CO_2, and the bed was cooled for product removal.

The pneumatic transport system was actuated and the product valve was opened 1/4 in. This resulted in a very high rate of product exiting through the valve, which could not be handled by the transporter and caused the transport line to plug. The burner was then emptied manually.

The product contained very low carbon until the very last portion, which had ∿3 kg of very fine carbon. Evidently, at the gas flows required to fluidize the particles, this very fine carbon could not re-enter the bed for combustion and was held in the filter chamber until the bed was emptied. This suggests that a fines recycle system such as will be used in the prototype primary burner will be required in BISO particle combustion. In-vessel filters, as used in this run, will not allow complete fine carbon burning with a BISO particle bed.

The clean ThO_2 kernels will be used in leaching tests.

4.2.2. Prototype Secondary Burner

The prototype secondary burner system design is being finalized; stress analysis of the package is nearly complete.

The system will be divided into three subsystems for fabrication purposes:

1. Burner assembly (includes the main Hastelloy X burner vessel with semiremote Grayloc flange assemblies, the filter chamber and plenum section, and the lower spool piece with the product removal valve assembly).

2. Heating and cooling system (includes the induction heating system with a susceptor plate, all sheet metal works for the forced air cooling jackets and plenums, and the burner insulation).

3. Burner support frames (include frameworks for the burner and for the heating and cooling system).

Quotations for secondary burner fabrication work are being solicited. Receipt of the long-lead components is continuing.

4.2.2.1. Stress Analysis

Stress analysis on the burner assembly and the support frame has been completed. Analysis on the heating and cooling system is continuing.

The analysis of the burner vessel assembly indicated that to meet ASME Section VIII, Division 1 requirements, thicker flanges were required at both the burner upper cap and the lower spool piece. The number and size of bolts used had to be increased. The bolts at the lower spool piece have been changed from stainless steel to Hastelloy X in order to maintain proper sealing between the flanges at high temperatures.

As a result of the stress analysis, many reinforcing gussets in the support framework have been eliminated, which simplifies the design and fabrication.

4.2.2.2. Internal Heat Transfer Coefficient

As the burning process continues, changes occur in the composition and physical parameters (such as particle size, density, and heat capacity) of the bed material. The fluidizing characteristics of the feed and the final product material are quite different (Ref. 4-7). The heat transfer mechanism is also different. The feed material will have less convection and

conduction heat transfer due to its larger particle size but will have larger radiative heat transfer due to its heavier slugging, while the opposite will be true for the smaller product material. The net effect, therefore, is a rather constant heat transfer during the burning process. An internal heat transfer coefficient of 80 Btu/ft^2-hr-°F (454 W/m^2-°C) has been consistently used for design purposes.

The internal heat transfer coefficients for both the feed and the product materials have been measured using the 10-cm secondary burner with an induction heater. The results for the product material were reported in Ref. 4-8.

The results for the fresh feed material are shown in Fig. 4-21. The heat transfer coefficient does not significantly change with temperature below 600°C. At temperatures above 600°C, there is a marked increase in the heat transfer coefficient with temperature. This is probably due to increased radiation heat transfer at high temperatures.

Another reason for a higher heat transfer coefficient at higher bed temperatures may be the change in particle size during the course of the experiment. The experiment was carried out from a low temperature (400°C) to a high temperature (775°C) and also from a high velocity to a low velocity at constant temperature. At temperatures above 600°C, a substantial amount of CO appeared in the off-gas as a result of the following reduction reactions:

$$ThC_2 + 4CO_2 \rightarrow ThO_2 + 6CO$$

$$CO_2 + C \rightarrow 2CO$$

Due to the pyrophoric nature of the ThC_2, these reactions might have reduced the particle size and affected (increased) the heat transfer coefficient. The degree of contribution of this particle size effect is not

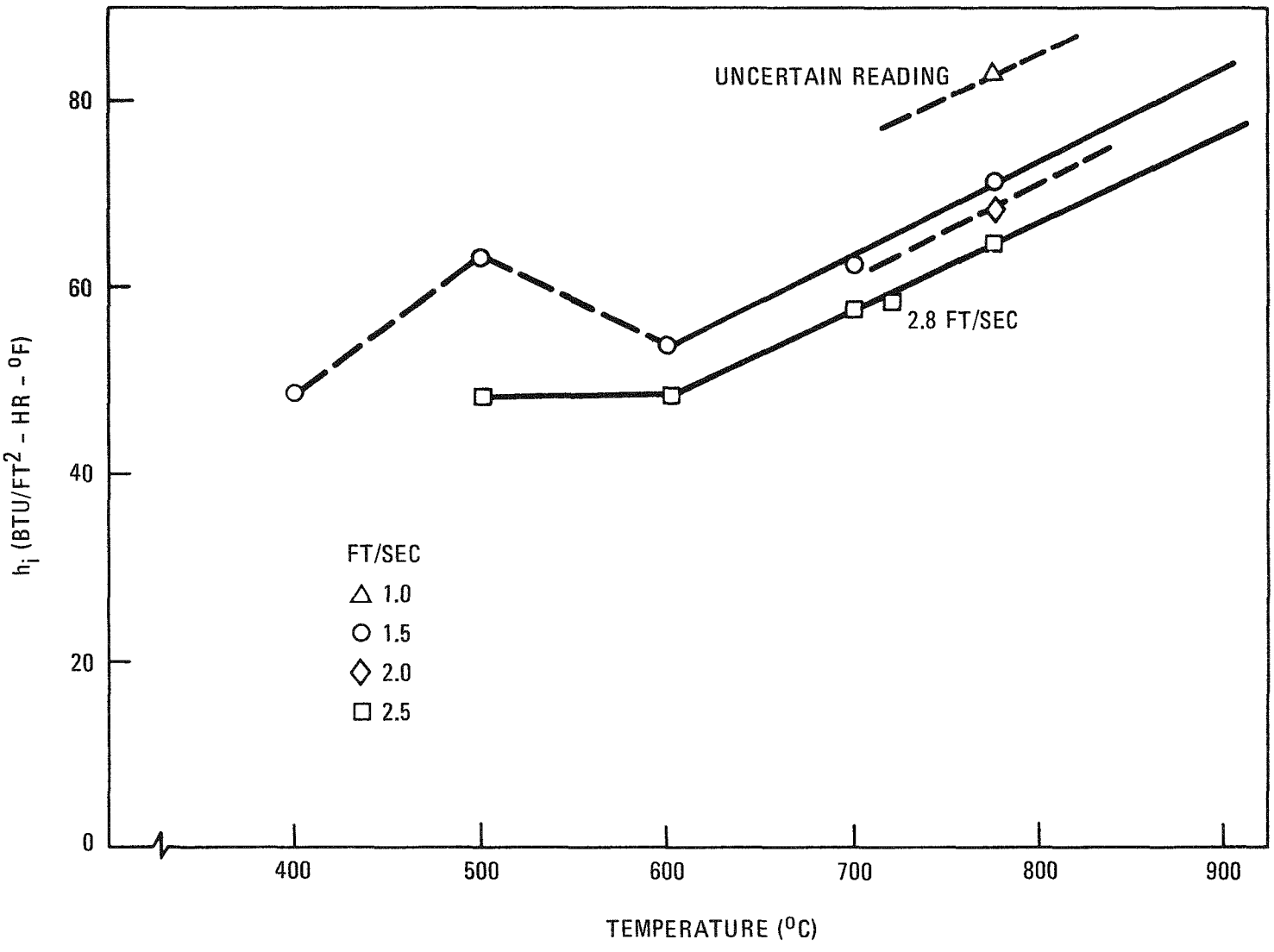

Fig. 4-21. Heat transfer coefficient versus temperature for fresh feed material

certain since no particle size distribution was determined after the experiment. However, considering the fact that the heat transfer coefficient increased rather linearly at temperatures above 600°C while the CO content in the off-gas increased almost exponentially, this effect may not have been significant.

The effect of fluidizing velocity on the internal heat transfer coefficient is also shown in Fig. 4-22. A general trend of slightly decreasing heat transfer with increasing fluidizing velocity is observed. Poor solid mixing due to heavier slugging at higher velocities may be the cause of this phenomenon.

The results of the experiment verify the prototype design bases and can be summarized as follows:

1. The internal heat transfer coefficient for the feed material at 900°C and normal operating velocity (∿2 ft/sec) is on the order of 80 Btu/ft^2-hr-°F (454 W/m^2-°C).

2. The internal heat transfer coefficient for the product material at normal operating conditions is on the order of 70 Btu/ft^2-hr-°F (397 W/m^2-°C).

3. During the main burning period, a higher fluidizing velocity does not greatly reduce the heat removal rate; thus, higher velocities can be used to increase the burner throughput.

4. The heat transfer coefficient does not change significantly from feed to final product due to a change in heat transfer mechanism (a cancelling effect of the radiative and nonradiative heat transfer).

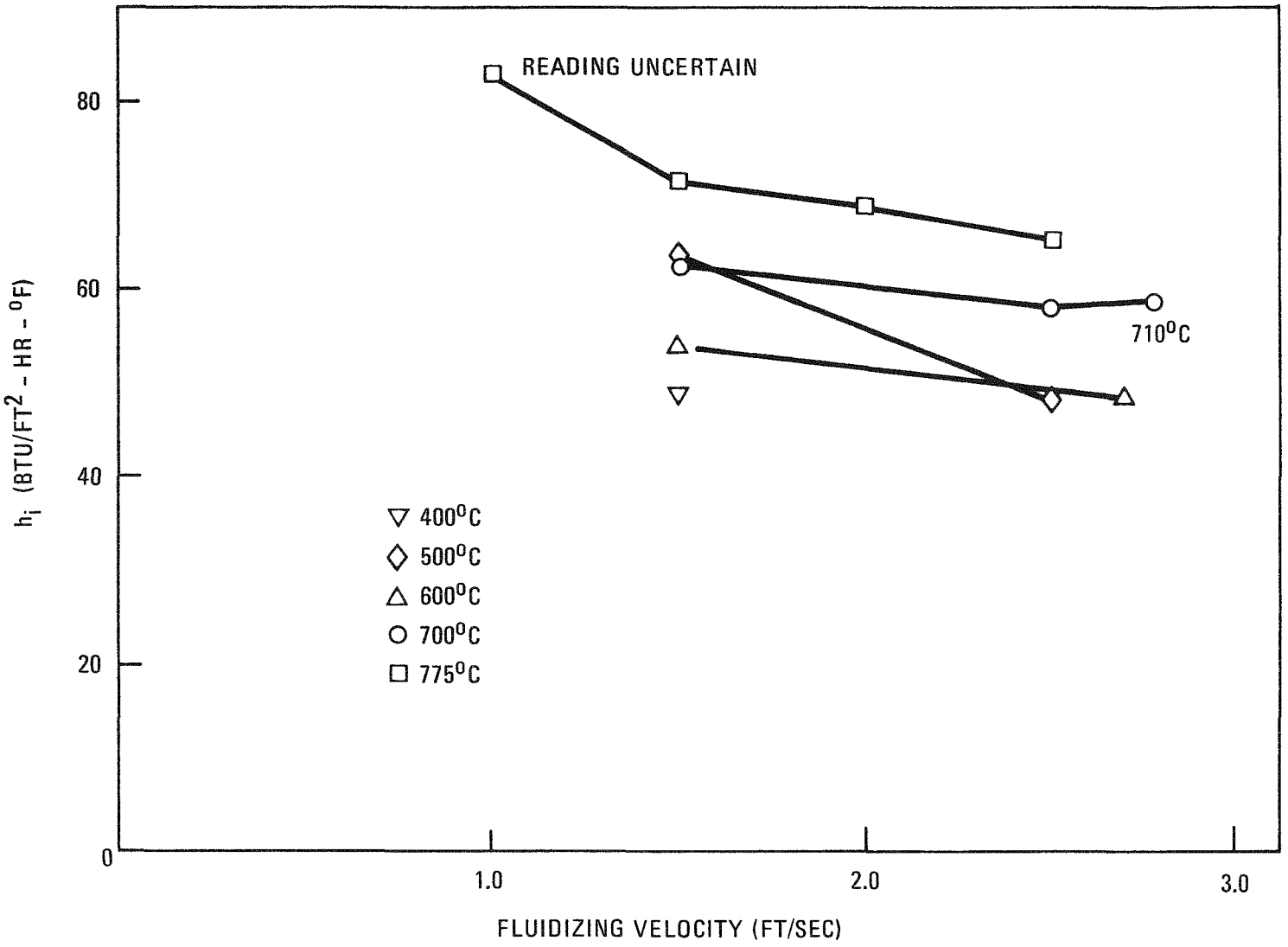

Fig. 4-22. Internal heat transfer coefficient versus fluidizing velocity

4.2.2.3. Burner Automatic Control

The burner automatic control scheme for the 2° burner using air cooling as the main control was reported in Ref. 4-8. The control will be performed using a Diogenes process control system manufactured by Rosemount. Detailed process interface module (PIM) and control function matrix (CFM) loop configurations have been worked out.

REFERENCES

4-1. Jenike, A. W., "Storage and Flow of Solids," University of Utah Engineering Experimental Station Bulletin 123, March 1970.

4-2. "Base Program Quarterly Progress Report for the Period Ending November 30, 1973," USAEC Report GA-A12818, Gulf General Atomic Company, December 28, 1973.

4-3. "Thorium Utilization Program Quarterly Progress Report for the Period Ending November 30, 1974," USAEC Report GA-A13255, General Atomic Company, February 15, 1975.

4-4. Rickman, W. S., "Evaluation of In-Vessel Off-Gas Filter System on the 10-cm Secondary Burner," General Atomic unpublished data, April 21, 1975.

4-5. Rickman, W. S., "Evaluation of a Gravity-Pneumatic Feeder System for Secondary Burners," General Atomic unpublished data, January 31, 1975.

4-6. Rickman, W. S., "Evaluation of a High-Temperature Bed Removal System Integrated with a Pneumatic Transport System for Use on Secondary Burners," General Atomic unpublished data, April 4, 1975.

4-7. "Thorium Utilization Program Quarterly Progress Report for the Period Ending August 31, 1974," USAEC Report GA-A13178, General Atomic Company, October 31, 1974.

4-8. "Thorium Utilization Program Quarterly Progress Report for the Period Ending May 31, 1975," ERDA Report GA-A13510, General Atomic Company, August 15, 1975.

5. AQUEOUS SEPARATION

5.1. SUMMARY

Eleven separate runs on dissolution of crushed, burned-back TRISO coated ThC_2 particles are reported for the quarter. Because of rapid dissolution of the ThO_2 burner product and wide variation in analyses on the thorium content of the feed material, initial experiments have not measured differences in dissolution rate as a function of process parameters. Two of the runs included 4.5% carbon in the feed. The presence of the carbon had no significant effect on dissolution rates.

In several runs, high thorium losses (up to 15%) to the insols were observed. Correlation of run data suggests thorium precipitation may have occurred. Available solubility data on the $Th(NO_3)_4 - HNO_3 - H_2O$ system indicate no thorium crystallization should have occurred. Laboratory-scale tests made to measure the effect of aluminum and fluoride present in the leacher solution on thorium solubility indicate their presence would not cause the apparent precipitation. Tests are needed to determine if other materials which may be present in the leacher feed could account for the observed behavior.

It has been demonstrated that two-stage leaching where fresh Thorex acid is used to reduce thorium content of the insols can be used, but greater time cycles and process complications will result.

Steam-jet transfer is being investigated as a method of removing mother liquor - insols slurry from the leacher. Results of these tests are encouraging, but further work is required to prevent occasional suction leg plugging.

5.2. LEACHING

5.2.1. Leaching Runs 95 Through 100, 102, and 103

Leaching Runs 95 through 100, 102, and 103 were conducted to determine if increased air sparge rates could increase the dissolution rate of crushed, burned-back, TRISO coated ThC_2 particles. The 13-cm-diameter leacher (Fig. 5-1) was used for all runs in this study. Each run in this series consisted of dissolving ∿4 kg of "82-kg composite" burner ash, (described in Ref. 5-1, pp. 5-4 and 5-5) in ∿12 liters of Thorex solution [13M HNO_3, 0.05M HF, 0.1M $Al(NO_3)_3$]. The air sparge rate for Runs 95 through 99 and 102 was set at 18 standard cubic feet per hour (SCFH). The sparge rate for Runs 100 and 103 was set at 6 SCFH.

Slurry samples taken during Runs 99 and 100 were analyzed for thorium. The slurry samples for Runs 102 and 103 were filtered and the filtrate was submitted for analysis. Filtration avoids additional dissolution of the thoria in the cooled mother liquor between the time the sample is drawn and the time it is analyzed. The slurry samples allow the extent of dissolution to be calculated from material balances at interim points during the run.

The operating and analytical data and the overall material balances are given in Tables 5-1 and 5-2, respectively. Dissolution curves are shown in Fig. 5-2.

The dissolution curves in Fig. 5-2 show substantial scatter of the data. An error analysis that accounts for the uncertainty in the feed material thorium content, the mother liquor thorium content, and the mass of Thorex charged shows that the amount of scatter obtained is not to be unexpected. When the errors are accounted for, the resulting value

TABLE 5-1
LEACHER OPERATING DATA AND SAMPLE ANALYSIS RESULTS, RUNS 95 THROUGH 100, 102, AND 103

	95[a]	96	97	98	99	100	102	103
Burner ash charged, kg	3.971	3.998	4.000	4.000	4.000	4.000	3.822	4.043
Thorex charges, liters	11.94	11.94	14.83[b]	13.92[b]	11.70	12.23	11.46	12.02
Air sparge rate, liters/min	8.49	8.49	8.49	8.49	8.49	2.83	8.49	2.83
Leaching time at boiling point, hr	2.0	1.0	1.8	1.0	5.25	4.0	4.0	3.75
Insolubles after leach (dry weight), g	1021	1056	955	845	950[c]	1096[c]	681[c]	1010[c]
Mother liquor	13.03 l[d]	14.52 l[d]	15.69 l[d]	(e)	19.30 kg[f]	18.78 kg[f]	19.12 kg[f]	19.27 kg[f]
Burner ash, wt % Th	61.4[g]	59.85[h]	65.6[h]	66.42[h]	60.0[g]	65.3[g]	63.4[g]	61.81[h]
Insolubles, wt % Th	0.83[g]	0.84[g]	0.78[g]	6.8[g]	2.02[g]	11.50[g]	3.9[g]	14.04[h]
Mother liquor, thorium analysis	206.5 g/l	173.4 g/l	158.1 g/l	(e)	0.139 g/g[f]	0.128 g/g[f]	0.124 g/g[f]	0.133 g/g[f]
Heaters used	3 electrical	3 electrical	Steam	4 electrical	Steam + 4 electrical	4 electrical	Steam + 4 electrical	Steam + 4 electrical

[a] Leacher run number.

[b] Thorex was diluted by water leakage into Thorex storage tank.

[c] Approximately 100 g insols removed with slurry samples not accounted for.

[d] Includes some wash water.

[e] Mother liquor volume lost in a spill.

[f] Based on average of last seven mother liquor samples, all of which show nearly complete dissolution.

[g] Analysis based on Thorin colorimetry.

[h] Analysis based on gravimetric determination using an oxalate precipitation of thorium.

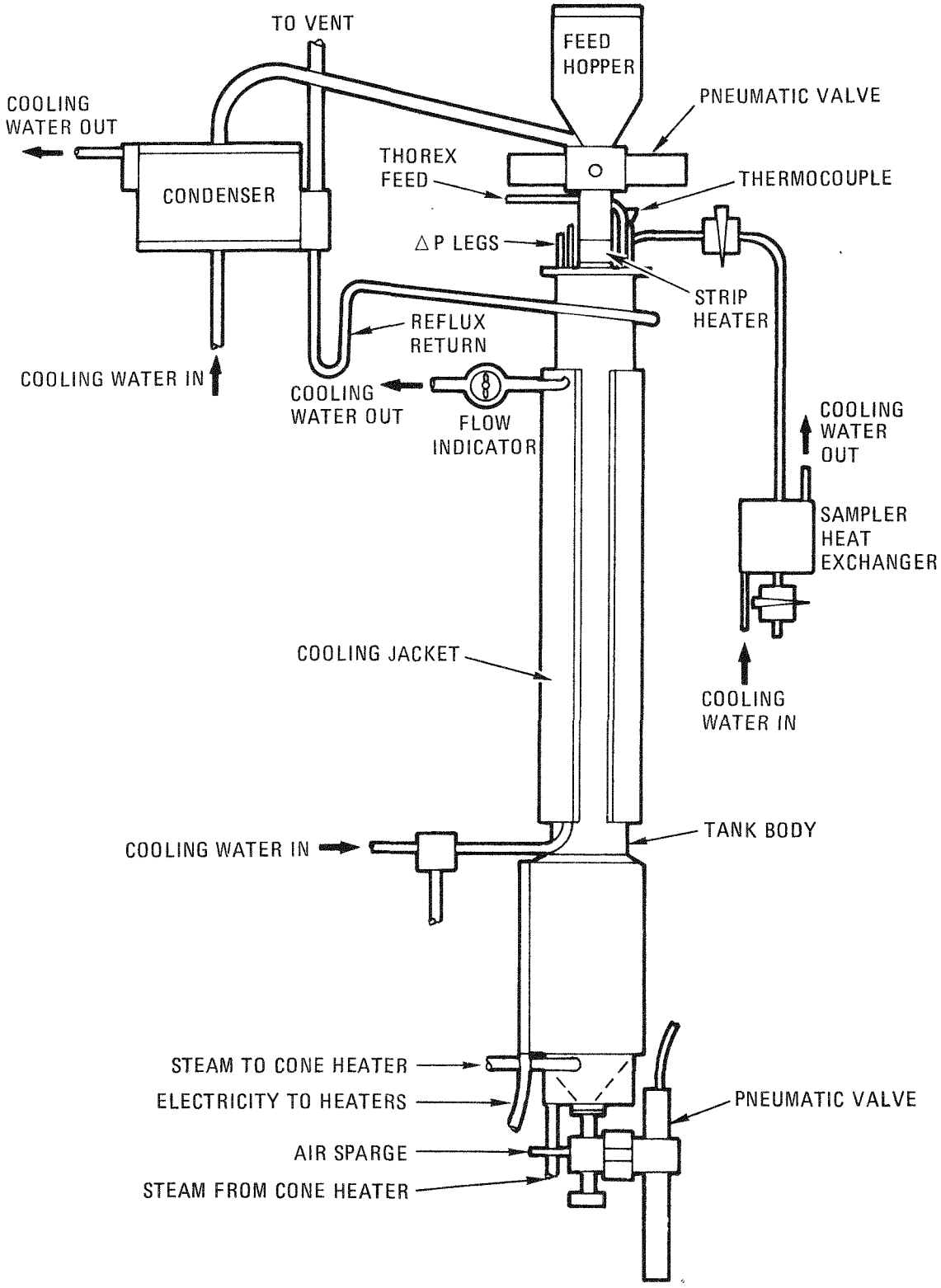

Fig. 5-1. 13-cm-diameter leacher arrangement

TABLE 5-2
OVERALL THORIUM MATERIAL BALANCES, RUNS 95 THROUGH 100, 102, AND 103

	95[a]	96	97	98	99	100	102	103
Thorium input, g burner ash	2438	2393	2624	2657	2400	2612	2423	2499
Thorium output, g								
In mother liquor	2691	2518	2481	--	2686[b]	2401[b]	2378[b]	2564[b]
In insolubles	8	9	7	57	19	126	27	142
Total	2699	2527	2488		2705	2527	2405	2706
Material balance closure,[c] wt %	110.7	105.6	94.82	--	112.7	96.7	99.26	102.6
Percent dissolution (mother liquor)[d]	110.4	105.2	94.55	--	111.9	91.9	98.1	108.3
Percent dissolution (insols)[e]	99.67	99.62	99.73	97.85	99.21	95.21	98.89	94.32

[a] Leach run number.

[b] Based on average of last seven mother liquor analyses, all of which show nearly complete dissolution.

[c] (Total output/input) x 100.

[d] $\left(\frac{\text{Output in mother liquor}}{\text{Input}}\right) \times 100.$

[e] $\left(\frac{\text{Input} - (\text{output in insols})}{\text{Input}}\right) \times 100.$

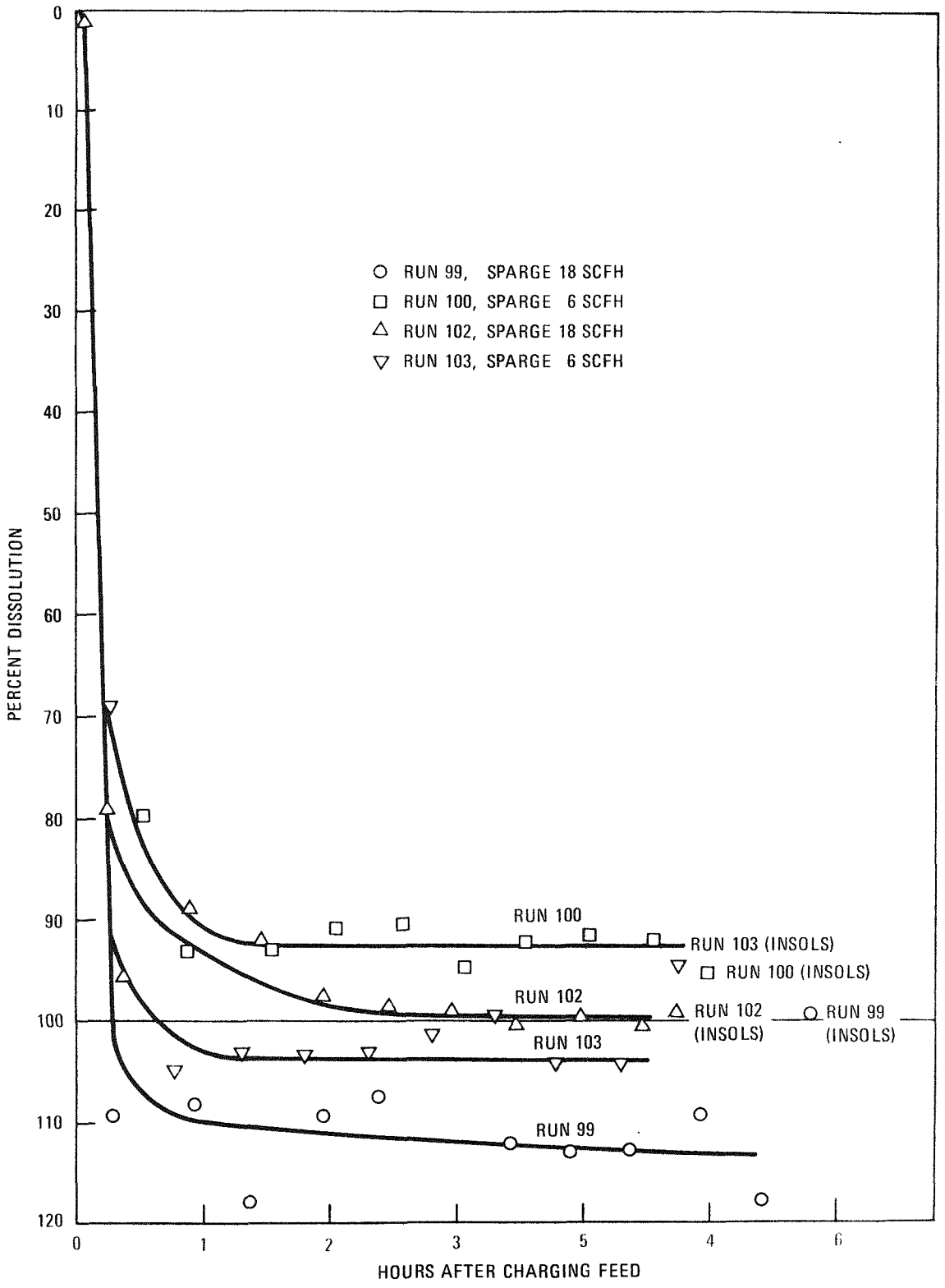

Fig. 5-2. Effect of sparge in dissolution of 82-kg composite material

reported for percent dissolution may be in error by ±7%. Most of the error results from the uncertainty of the thorium content in the feed material.

No observable or significant differences in dissolution could be seen in the dissolution of the 82-kg composite using sparge rates of 6 and 18 SCFH. Minor differences may have been obscured by the rather large experimental error. It should be noted, however, that once the slurry has started boiling, most of the agitation is provided by the boiling action. The steam heater alone can cause a vaporization rate corresponding to about 115 SCFH. The agitation produced by boiling action is largely dependent upon the location of the heaters, but the steam-jacketed cone (Fig. 5-3) is located at the bottom of the leacher where mixing would be most effective.

There is a wide variation in the thorium content found in the insoluble material (insols) from Runs 95 through 100, 102, and 103. A similar variation ranging from 0.38% Th to 21.35% Th was reported for prior Runs 82, 83, and 85 through 93 (Ref. 5-1).

No correlation between thorium content in the insols as a function of time, sparge rate, mass of feed charged, mass of Thorex charged, heat input, or analytical technique could be found. Error introduced by improper rinsing of the insols in the centrifuge basket, a maximum of about 1% of the thorium charged, does not account for the variations. The only correlation which could be developed was that the thorium content increased with decreasing temperature of the product slurry at the time it was dumped into the centrifuge (Fig. 5-4).

A possible explanation for this correlation is that thorium precipitated during the cooling period. Figure 5-5 (from Ref. 5-2) shows the ternary phase diagram for the thorium nitrate - nitric acid - water system at 25°C. Laboratory experiments (Section 5.6.1) have verified that this diagram is valid for the leacher mother liquor even with fluoride ions,

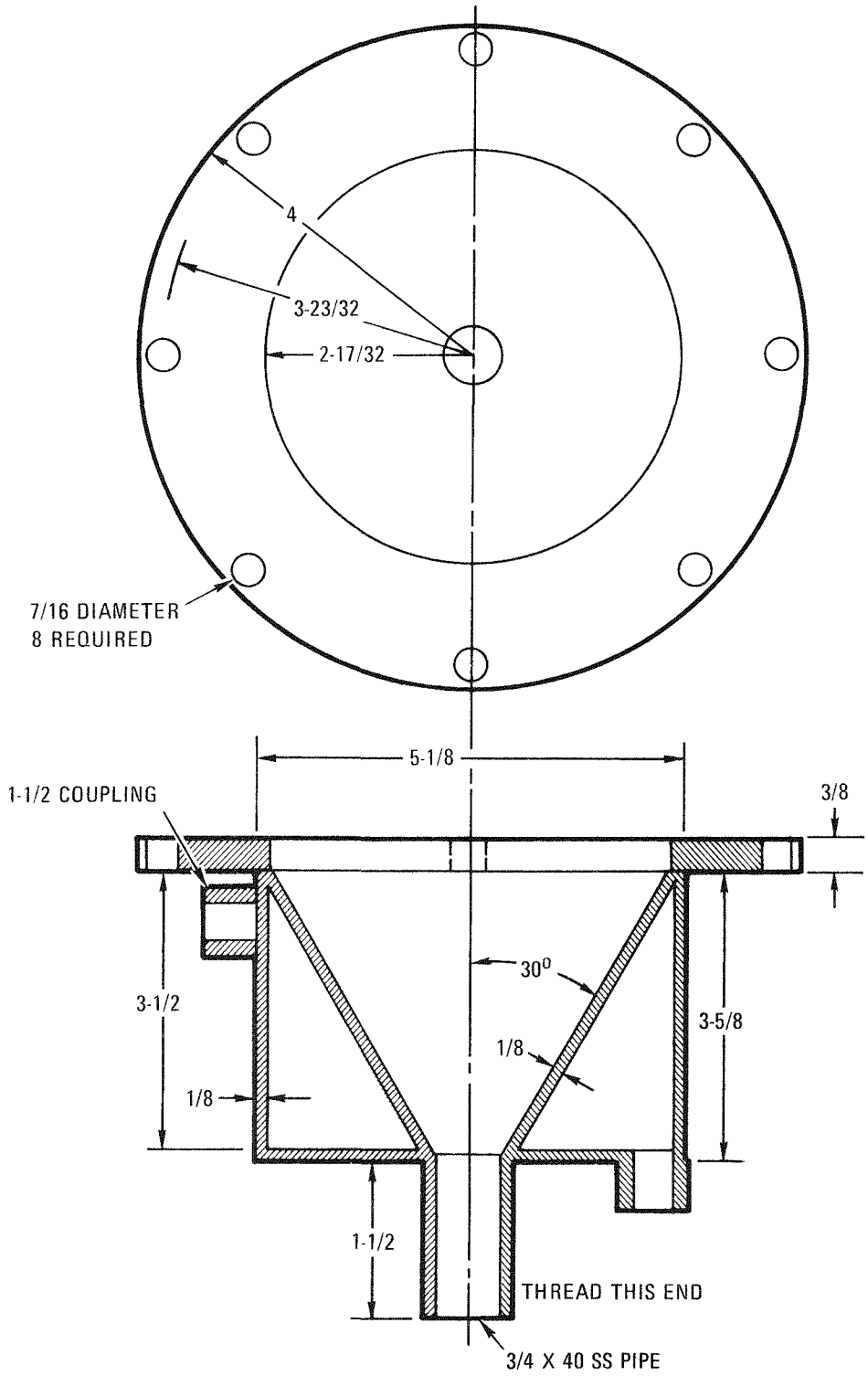

Fig. 5-3. Details of steam jacket on 13-cm-diameter leacher cone

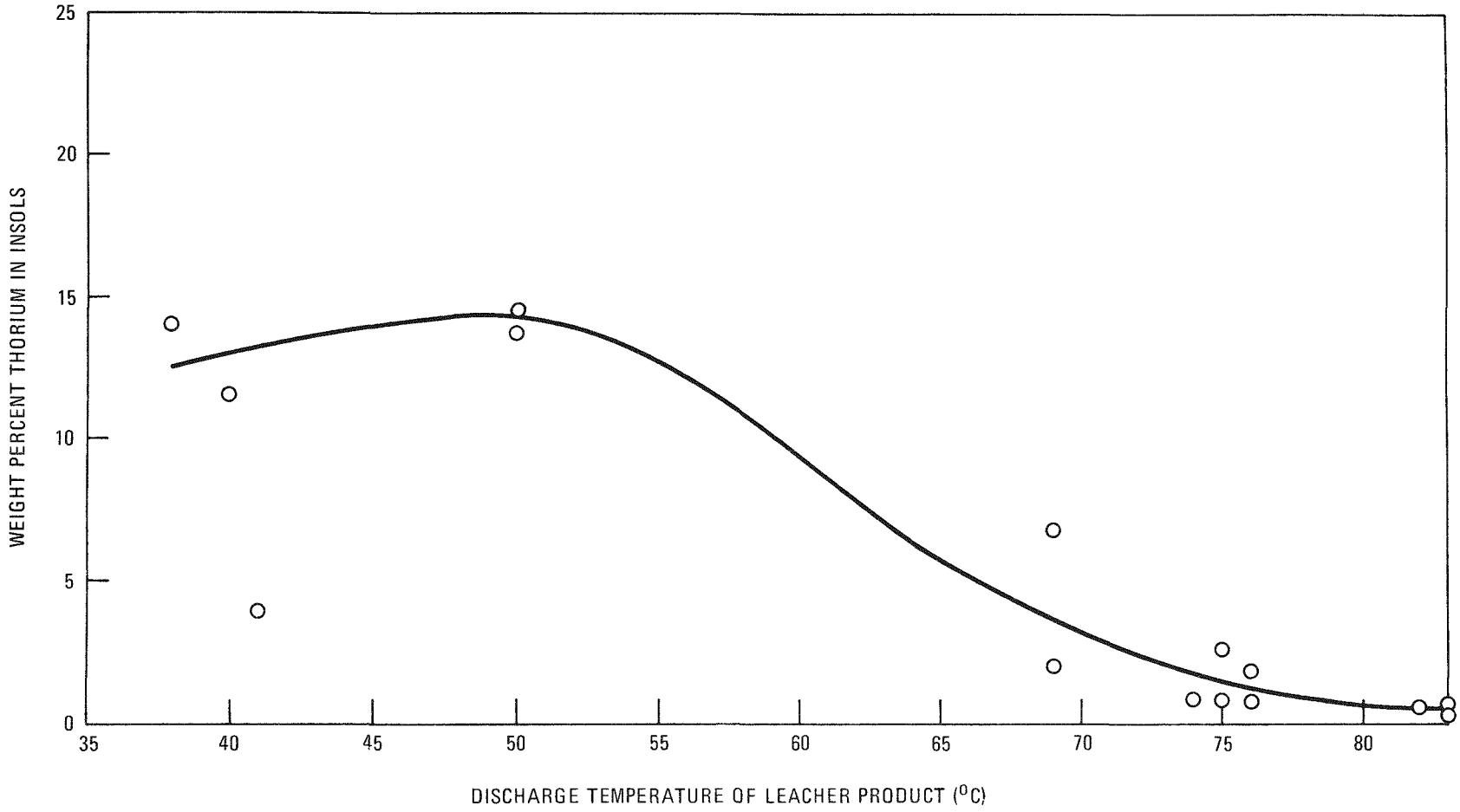

Fig. 5-4. Trend showing increasing thorium content in insols with decreasing discharge temperature

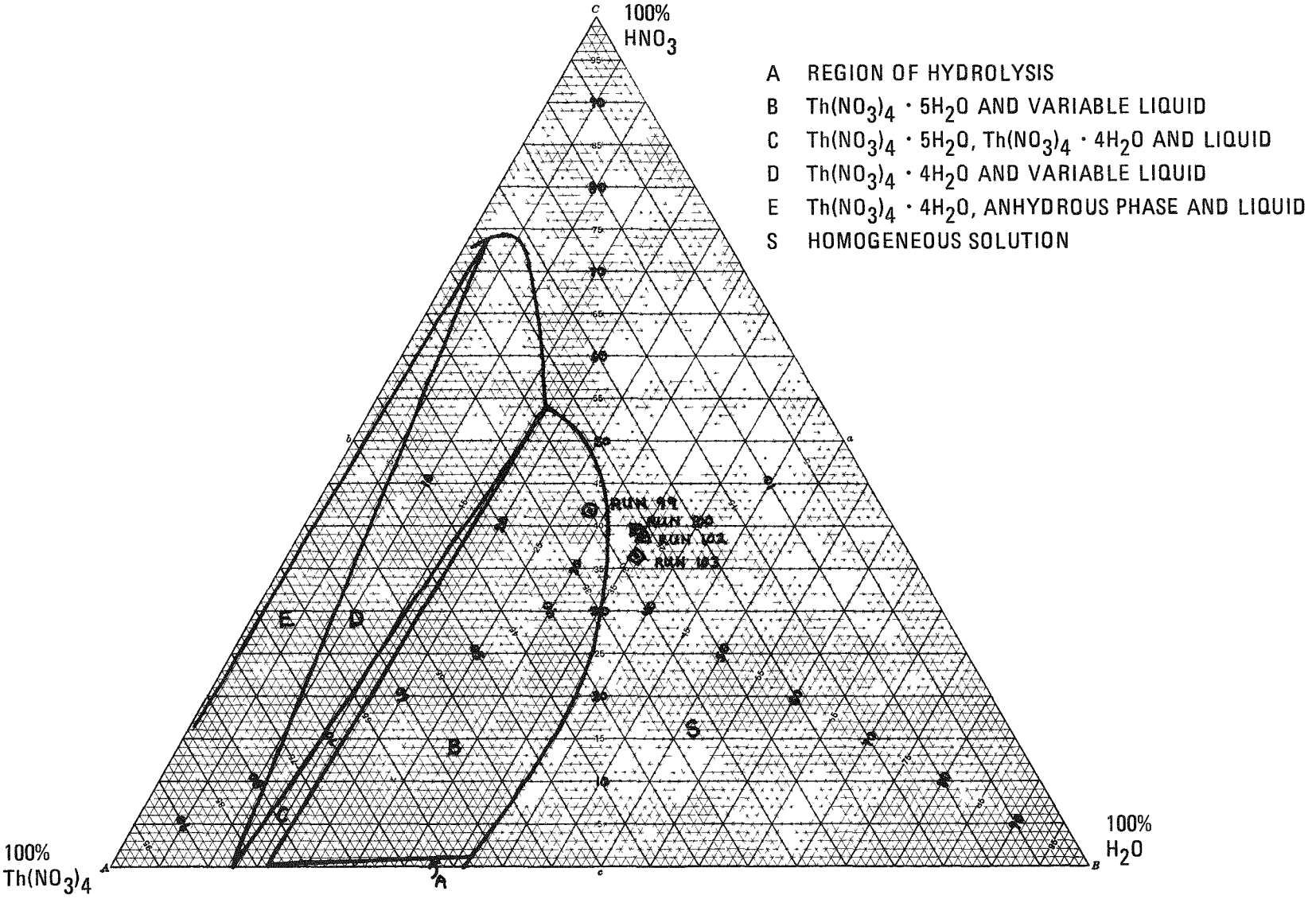

Fig. 5-5. $Th(NO_3)_4$ - HNO_3 - H_2O system at 25°C (Reprinted with permission from "The System Thorium Nitrate - Water - Nitric Acid at 25°C and the Hydrates of Thorium Nitrate," J. R. Ferraro, L. I. Katzin, and G. Gibson, J. Am. Chem. Soc. 76, 909 (1954), Fig. 1, p. 910. Copyright by American Chemical Society.)

aluminum nitrate, and silicon carbide hulls present. The mother liquor compositions from Runs 99, 100, 102, and 103 are located on this phase diagram. The mother liquor composition for Run 99 shows that thorium nitrate will precipitate. The compositions for Runs 100, 102, and 103, however, indicate that precipitation did not occur.

The explanation of thorium nitrate precipitation is presently the only plausible explanation for variations in thorium content in the insols. Based strictly upon the mother liquor compositions, precipitation did not occur. There may be other factors, however, such as concentration gradients, the presence of other extraneous salts in the particular burner ash composite, and the introduction of dry nitrogen for sparging, that could induce precipitation. The problem of potential precipitation, therefore, must be studied further.

The cooling step is required in the leacher operating procedure when steam jet transfer is used for product removal. On the basis of experiments described further in Section 5.2.4, a maximum slurry temperature of 30°C is recommended for smooth transfers and for minimizing the chances of plugging the suction tube of the jet.

In summary, the following conclusions are made for this series of leaching runs:

1. There are no significant differences in the dissolution of 82-kg composite feed (a composite of crushed, burned-back TRISO ThC_2 particles from several burner runs) with air sparge rates of 6 and 18 SCFH in the 13-cm-diameter leacher.

2. Most of the agitation in the 13-cm-diameter leacher is probably provided by vaporization once the boiling point is reached.

3. The limit of accuracy for determining the extent of dissolution is about ±7% of the thorium charged. This is a substantial margin of error, and efforts will be made to reduce this margin.

4. The initial dissolution rate of 82-kg composite material is very rapid. About 80 to 90% of the thorium dissolves within a half-hour after being loaded.

5. A possible reason for variations in the thorium content in insols from various runs could be that thorium precipitates while the leacher product is being cooled.

5.2.2. Leaching Run 104

Leaching Run 104 was made to provide preliminary information for two-stage leaching operations of crushed, burned-back TRISO coated fertile particles. This run consisted of leaching the insols from several previous runs in fresh Thorex solution. Two-stage leaching was simulated by combining the dissolution curve for releached insols, Run 104, with a typical dissolution curve for the fertile secondary burner ash.

Run 102, summarized in Section 5.2.1, was chosen to be the basis for the first stage of the two-stage process because it had the best material balance closure (99.3%) of several previous runs. Run 104 consisted of charging about 4 kg of insols, containing 147.5 g thorium, from previous leaching runs that utilized 82-kg composite burner ash (Ref. 5-1) in 12 liters of Thorex [13M HNO_3, 0.05M HF, 0.1M $Al(NO_3)_3$]. The dissolution rate data from Run 104 were then plotted with the data from Run 102 as though Run 102 was terminated at the time when 147.5 g of thorium remained undissolved. The combined plot is shown in Fig. 5-6.

The operating and analytical data and overall material balances from Run 104 are given in Tables 5-3 and 5-4, respectively. The dissolution

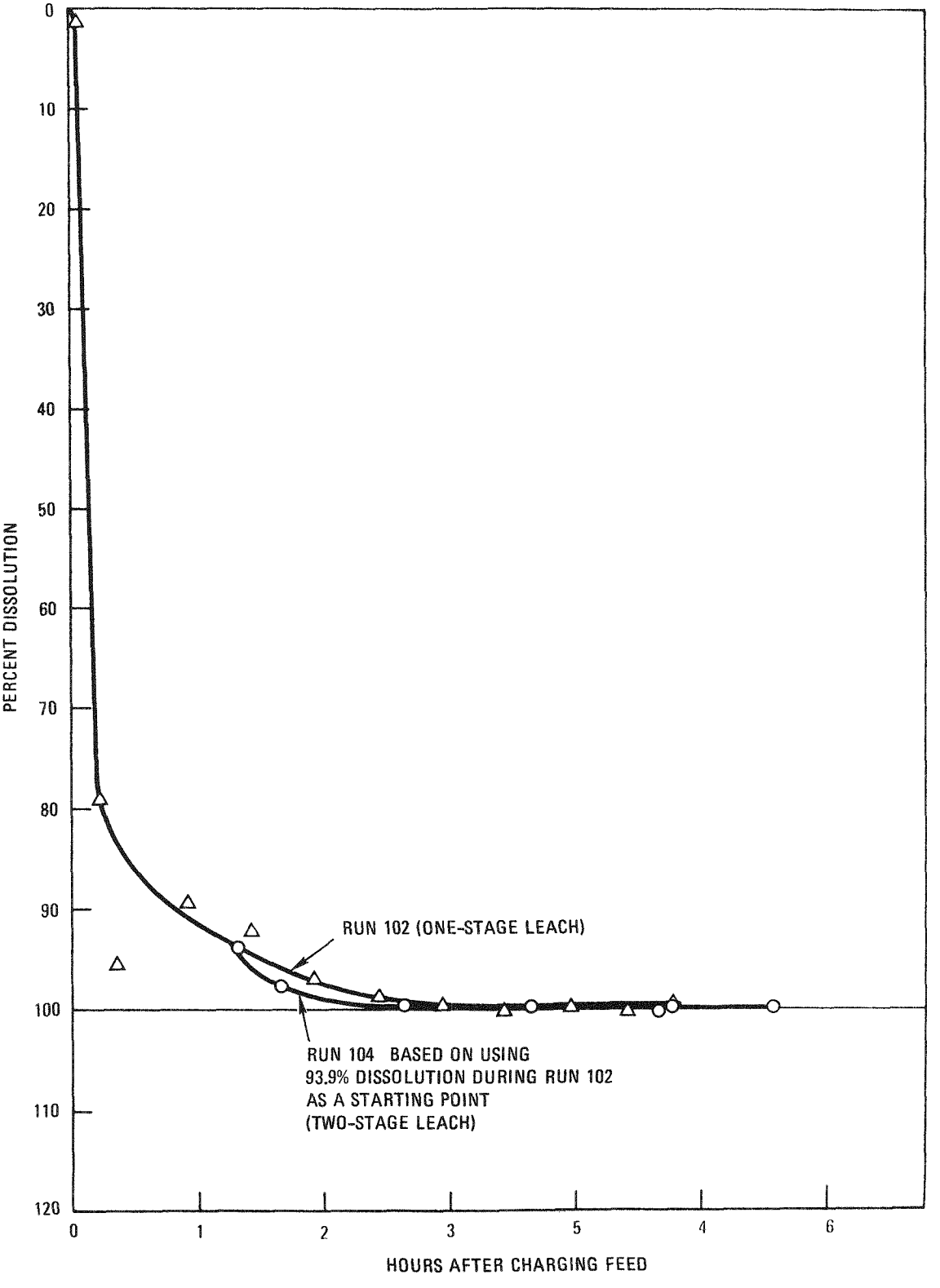

Fig. 5-6. Simulated dissolution curve for two-stage leaching

TABLE 5-3
LEACHER OPERATING DATA AND SAMPLE ANALYSIS RESULTS, RUN 104

Feed material, g	4390
Thorex, liters	11.98
Air sparge rate, liters/min	8.49
Leaching time at boiling point, hr	3.3
Insolubles after leach (dry weight),[a] g	3936
Burner ash, wt % Th	3.36
Insolubles, wt % Th	0.06
Heaters used	4 electrical + steam jacket

[a] Approximately 50 g insols removed with slurry samples not accounted for.

TABLE 5-4
OVERALL THORIUM MATERIAL BALANCE, RUN 104

Thorium input, g	147.5
Thorium output, g	
In mother liquor[a]	147.2
In insolubles	2.4
Total	149.6
Material balance closure[b]	101.4
Percent dissolution (mother liquor)[c]	99.80
Percent dissolution (insols)[d]	98.37

(a) Based on last mother liquor sample taken.

(b) (Total output/input) x 100.

(c) $\left(\frac{\text{Output in mother liquor}}{\text{Input}}\right) \times 100.$

(d) $\left(\frac{\text{Input - (output in insols)}}{\text{Input}}\right) \times 100.$

curve for Run 104 alone (Fig. 5-7) shows that the thoria remaining in the insols after the first leach of burner ash dissolves rapidly when fresh Thorex is used to leach these insols a second time.

Figure 5-6 shows that a two-stage leaching operation can provide 99% dissolution of the original thorium with a minor time savings. The overall dissolution time cycle of a two-stage operation would be increased, however, because the operation is more complex and requires more operating steps.

The only significant advantage that was found in favor of two-stage leaching with ash from carbide fuel particles was the low residual thorium content of the insoluble material. The thorium content of the insols for the single-stage leach was 3.9 wt %, corresponding to 98.9% dissolution. For the two-stage process, however, it was only 0.06 wt %, corresponding to 99.9% dissolution. Two-stage leaching has yet to be tested with feed derived from ThO_2 fuel particles.

5.2.3. Leaching Runs 105 and 107

The objective of leaching Runs 105 and 107 was to determine the effect of combustible carbon upon the dissolution of crushed, burned-back, TRISO coated ThC_2 particles. The 13-cm-diameter leacher (Fig. 5-1) was used for both runs. The feed material for Run 105 was split from the burner ash product from secondary burner Run 42 (Table 5-5) and contained 4.5% combustible carbon. The feed for Run 107 was also split from secondary burner Run 42 ash but was pan-burned in an electric furnace for 30 hr at temperatures of about 825° to 950°C. For both runs, about 4 kg of ash were leached with 12 liters of Thorex [13$\underline{M}$ HNO_3, 0.05$\underline{M}$ F^-, 0.1$\underline{M}$ $Al(NO_3)_3$]. The air sparge rate was set at 14 SCFH. All four electrical heaters and the steam heater were used to boil the slurry in Run 105. In Run 107, only two electrical heaters and the steam heater were used. Slurry samples were taken throughout both runs in the manner described in Section 5.2.1.

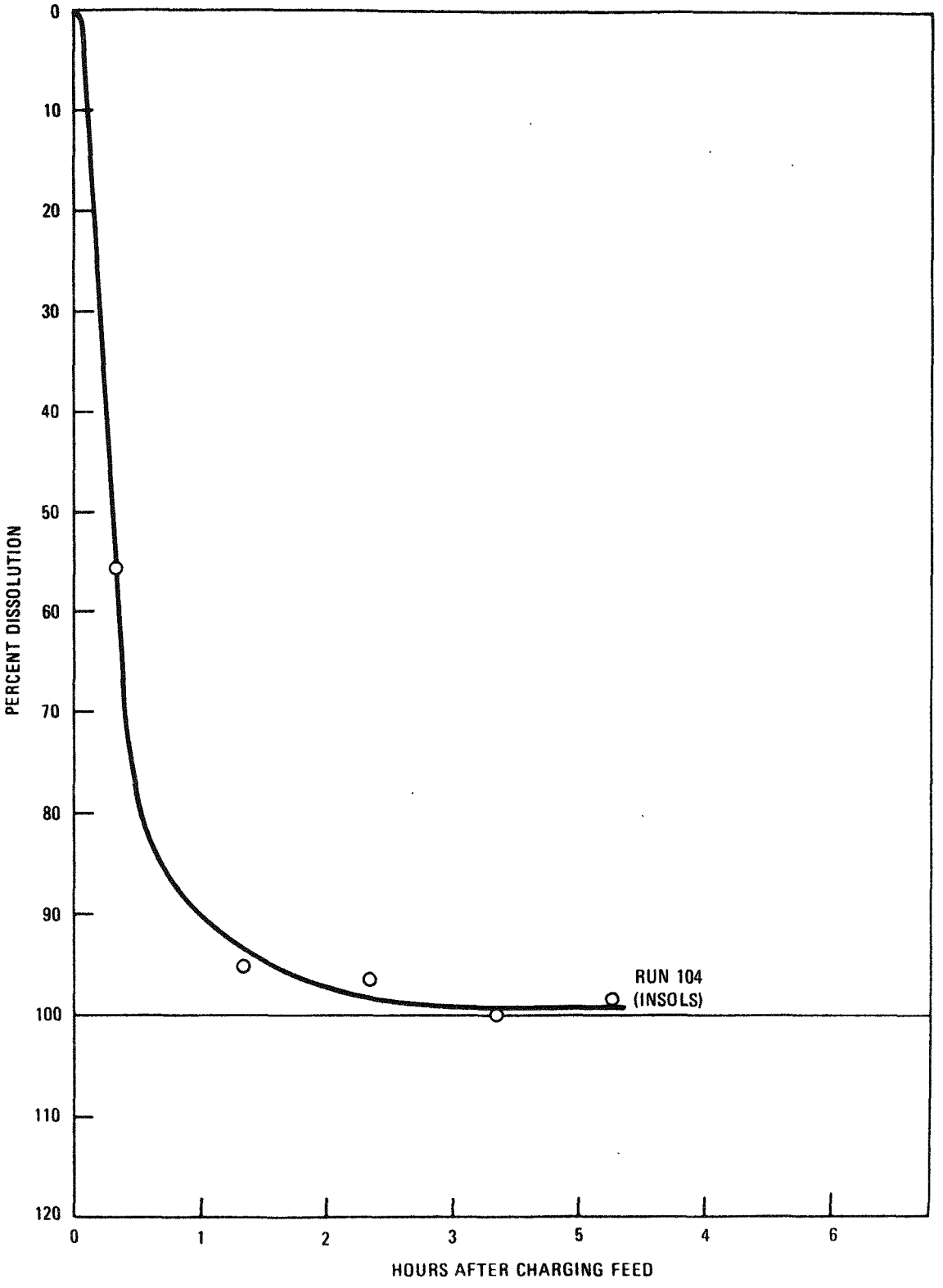

Fig. 5-7. Dissolution curve for Run 104 using insols as feed material

TABLE 5-5
SIZE DISTRIBUTION OF SECONDARY BURNER RUN 42 ASH

Screen Size (μm)	Material Retained on Screen (wt %)
420	2.4
355	1.0
300	1.0
250	1.6
212	3.0
180	3.8
150	4.2
125	5.0
106	4.5
90	9.0
75	8.5
63	11.0
53	19.0
45	15.0
38	1.0
Pan	10.0

The operating and analytical data and the overall material balances are given in Tables 5-6 and 5-7, respectively. The dissolution curves shown in Fig. 5-8 indicate that the feed material with carbon present dissolved slightly slower than the pan-burned material. The difference is quite small, however, and is within the limits of experimental error. It is therefore concluded that the presence of up to 4.5% combustible carbon is not detrimental to the dissolution rate.

The final thorium concentration in the insols from Run 105, indicating 98.1% dissolution, is slightly higher than from Run 107, which indicates 99.89% dissolution. The presence of carbon may slightly decrease the extent of dissolution near the end of the dissolution process. This difference is not attributed to the possible thorium nitrate precipitation reported in Section 5.2.1. The slurry discharge temperatures of Runs 105 and 107 were 70° and 24°C, respectively, and the thorium content of the mother liquor from Run 107 was higher than that from Run 105. Both of these variations would tend to cause a difference in the insols thorium content in reverse order of that observed.

The errors in the value reported for percent dissolution for Runs 105 and 107 are 2.7 and 1.7%, respectively. This is a marked improvement from the 7% error reported for Run 103 (Section 5.2.1). The improvement is attributed to the improved sampling technique for the feed material. Previously, a 1- to 2-g sample was split from the feed. This resulted in a standard deviation of 2.59% in the thorium analysis. For Runs 105 and 107, three 5- to 10-g samples were split from the feed. This requires fewer solids sample splits of small quantities. The analytical results gave standard deviations of 0.15 and 0.25%. The major source of error in Runs 105 and 107 is attributed to the mother liquor samples rather than the feed samples.

The carbon in the feed material was the result of an incomplete secondary burner run. In the event of a similar incomplete secondary burner run

TABLE 5-6
LEACHER OPERATING DATA AND SAMPLE ANALYSIS RESULTS, RUNS 105 AND 107

	105[a]	107
Feed material, g	3912	4191
Thorex, liters	11.74	12.04
Air sparge rate, liters/min	6.6	6.6
Leaching time at boiling point, hr	4.6	2.6
Insolubles after leach (dry weight),[b] g	1109	971
Burner ash, wt % Th	60.71	65.23
Insolubles, wt % Th	4.07	0.35
Heaters used	Steam + 4 electrical	Steam + lower 2 electrical

[a] Leach run number.

[b] Approximately 100 g insols removed with slurry samples not accounted for.

TABLE 5-7
OVERALL THORIUM MATERIAL BALANCES, RUNS 105 AND 107

	105[a]	107
Thorium input, g	2375	2734
Thorium output, g		
In mother liquor[b]	2388	2730
In insolubles	45	3
Total	2433	2733
Material balance closure[c]	102.44	99.96
Percent dissolution (mother liquor)[b,d]	100.55	99.85
Percent dissolution (insols)[e]	98.10	99.89

[a] Leach run number.

[b] Based on average of last seven mother liquor analyses, all of which indicated nearly complete dissolution.

[c] (Total output/input) x 100.

[d] $\left(\frac{\text{Output in mother liquor}}{\text{Input}}\right) \times 100.$

[e] $\left(\frac{\text{Input} - (\text{output in insols})}{\text{Input}}\right) \times 100.$

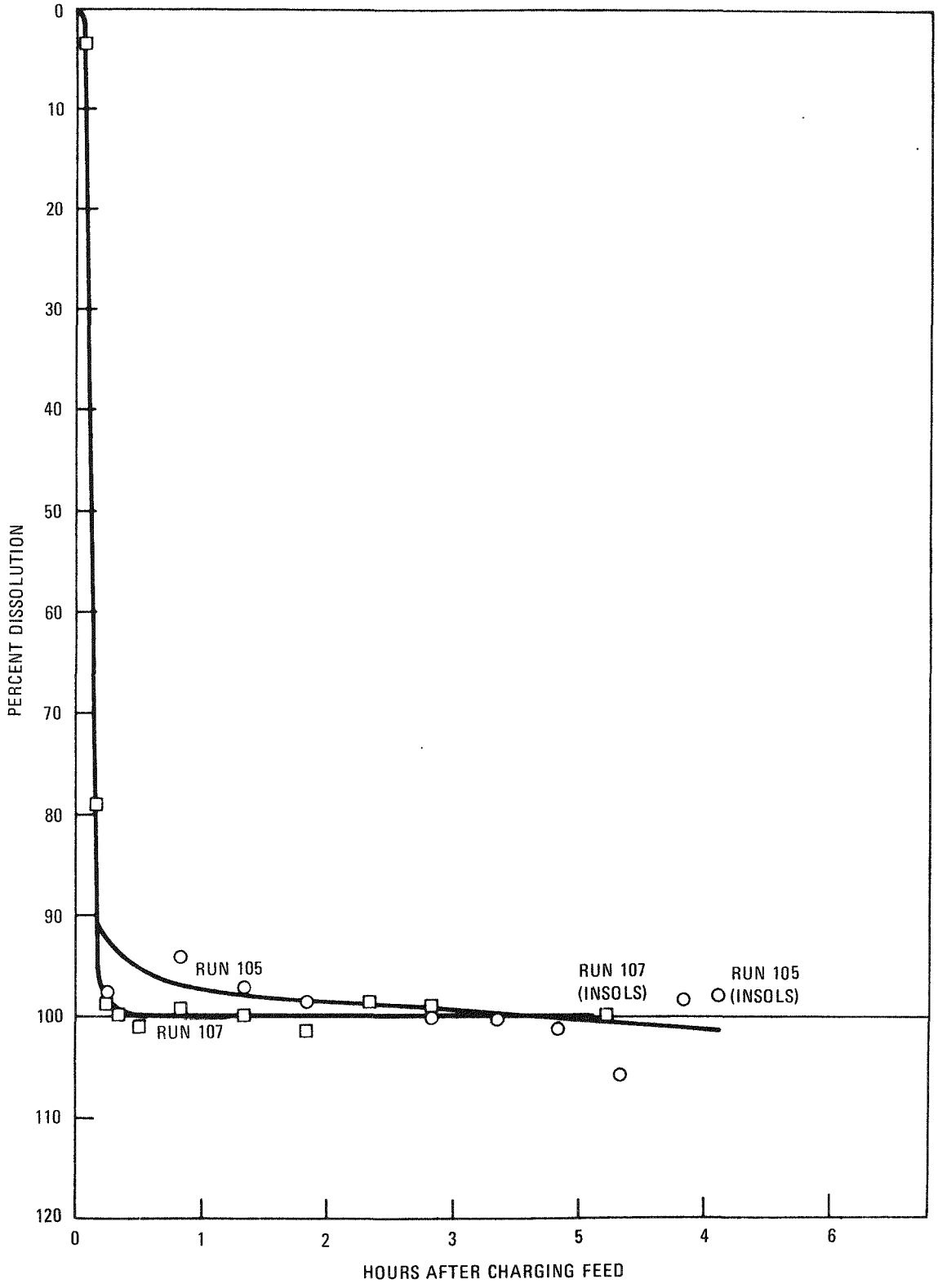

Fig. 5-8. Dissolution curves for Run 105 (with 4.5% carbon) and Run 107 (no carbon)

in a commercial plant, this study shows that the material can be leached without increasing the dissolution time cycle. However, difficulties could be created in subsequent steps (solvent extraction and waste processing). Any carbon in the form of ThO_2 or UC_2 will result in the formation of organic compounds, including oxalic and mellitic acids, in the leachate (Ref. 5-3). In the solvent extraction process, the resultant organic compounds can lead to undesirable emulsion formation, create special waste management problems (Refs. 5-3, 5-4), and decrease zirconium decontamination (Ref. 5-5).

5.2.4. Steam Jet Transfer Tests for Leacher Product Removal

Steam jet Runs 8 through 11 were performed with varying initial slurry temperatures to determine the effect of temperature upon transfer characteristics. Particular attention was given to plugging incidents since these are extremely important in evaluating the reliability and ease of maintenance of remote steam jet operations. Some operating experience with the steam jet transfer apparatus was gained during several transfers that were made for centrifuge experiments and were not recorded as steam jet transfer runs. In order to further develop the background of plugging incidents, this experience is included in this section.

The horizontal suction jet was used to transfer the slurry from the left tank to the right tank as shown in Fig. 5-9. The liquid used for all runs was 50 liters of 38 wt % $NaNO_3$ solution having a specific gravity of 1.30. The slurry contained 69 g SiC hulls per liter of solution. Saturated steam at 90 psig was used for the motive force.

In all runs the solids were added to the liquid and the mixture was then sparged to provide mixing similar to the mixing action in a leacher. The sparge was turned off, the solids were allowed to settle for 10 min, and the manometer readings were then taken. In Runs 8, 9, and 10, there was no additional mixing after the 10-min settling period. In Run 11, the

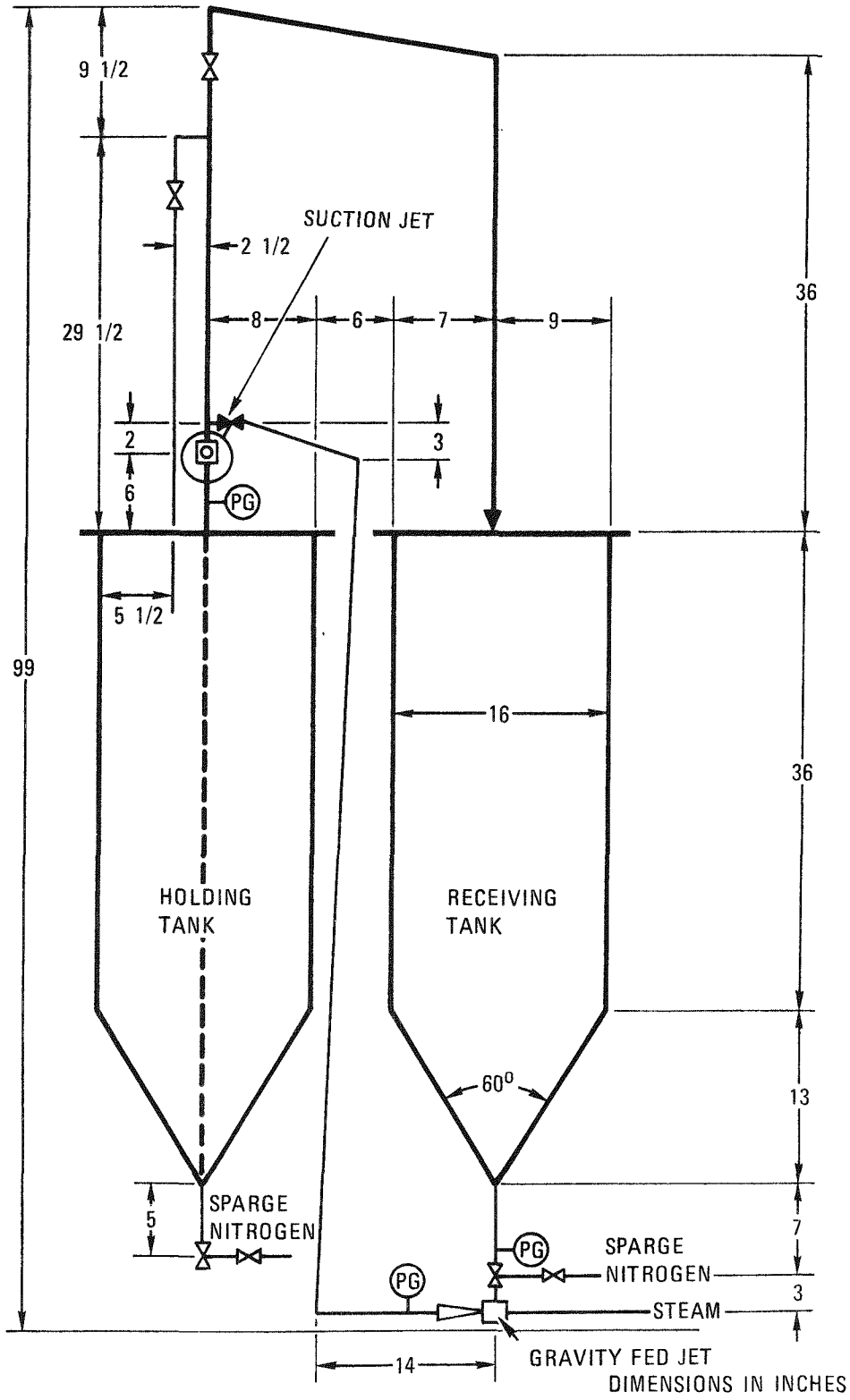

Fig. 5-9. Steam-jet transfer apparatus

slurry was sparged at 12 SCFH just prior to the transfer; the sparge was shut off again for the transfer.

The runs made for centrifuge experiments that also added to steam jet operating experience utilized similar procedures except that some transfers were made using the gravity-fed jet (Fig. 5-9).

The results of Runs 8 through 11 are given in Table 5-8. Descriptions of these runs and of the operating experience gained from transfers that were for centrifuge test runs are summarized in Table 5-9.

Increasing the slurry temperature from 25° to 50°C causes a small decrease in the transfer rate. A definite correlation between slurry temperature and plugging incidents was not obtained. The suction tube of the jet plugged repeatedly at slurry temperatures of 40°C; however, some successful runs have been made at 40°C and one successful run has been made at 50°C. A run made at 60°C resulted in a plug that could not be cleared. No plugging incidents occurred in the suction jet configuration with slurry temperatures below 40°C. It should be noted that the successful run made at 50°C was done immediately after sparging the slurry at 12 SCFH. This indicates that sparge flow is desirable to keep the solids from settling and compacting in the bottom of the tanks.

Most plugs in the suction jet configuration occurred in the suction tube. This tube was cleared with steam pressure by closing the valve in the discharge line and letting steam leak through the jet nozzle. This forces the plug backwards through the suction tube. The procedure is readily adaptable for clearing plugged suction tubes in remotely operated full-scale leachers by using the configuration shown in Fig. 5-10. There was one plug, however, that could not be cleared with 100-psig steam pressure, and the suction tube had to be replaced.

The gravity jet, shown in Fig. 5-9, was used in preparation for centrifuge runs. This jet plugged repeatedly when the slurry was admitted to

TABLE 5-8
DATA FROM STEAM-JET RUNS 8 THROUGH 11

Run	Sparge (SCFH)	Slurry Temp (°C)	Temp Rise (°C)	Dilution[a] (%)	Transfer Time (min)	Mass Liquid Holdup (g)	Mass Solid Holdup (g)
8	0	24	14	1.6	222	59	46
9	0	31	13	1.5	224	--	627
10	0	40	20	2.4	231	--	47
11	0[b]	50	12	1.4	248	20	328

[a] Calculated from enthalpy balance based on heat capacity of 0.721 Btu/lb-°F for 38 wt % $NaNO_3$ solution.

[b] Slurry sparged at 12 SCFH immediately prior to run.

TABLE 5-9
STEAM-JET TRANSFER OPERATING EXPERIENCE

Run	Jet Used (see Fig. 5-9)	Slurry Temp (°C)	Remarks
1	Suction	24	Transfer successful.
2	Suction	25	Transfer successful.
	Gravity	--	Plugged jet. Cleared jet with water spray. Second attempt successful.
	Suction	--	Plugged jet when using a polyethylene discharge line. Cleared jet with water spray. Replaced polyethylene line with stainless steel line. Second attempt successful.
3	Suction	23	Transfer successful.
	Gravity	--	Plugged jet. Cleared jet with water spray. For second attempt, steam was turned on first, and then the valve was slowly opened; transfer successful.
	Suction	44	Plugged jet. Cleared jet with water spray. Second attempt successful.
4	Suction	23	Transfer successful.
	Gravity	--	Turned on steam first. Transfer successful.
	Suction	39	Transfer successful.
5	Suction	22	Transfer successful.
	Gravity	--	Transfer successful.
	Suction	43	Transfer successful.
6	Suction	22	Transfer successful.
	Gravity	--	Transfer successful.
	Suction	--	Transfer successful.

TABLE 5-9 (Continued)

Run	Jet Used (see Fig. 5-9)	Slurry Temp (°C)	Remarks
7	Suction	38	Transfer successful.
	Gravity	--	Transfer successful.
	Suction	50	Plugged suction tube. Cleared with water spray. Also plugged suction tube on second attempt. Cleared suction tube with 50-psig steam pressure and cooled to 25°C. Third attempt successful.
8	Suction	24	Transfer successful.
	Gravity	--	Transfer successful.
	Suction	--	Transfer successful.
9	Suction	31	Transfer successful.
	Gravity	--	Transfer successful.
	Suction	--	Transfer successful.
10	Suction	40	Plugged suction tube. Cleared with 100-psig steam.
		42	Plugged suction tube again. Cleared with 100-psig steam.
		44	Plugged suction tube again. Cleared with 100-psig steam.
		46	Plugged suction tube again. Cleared with 100-psig steam. Sparged slurry for 2 hr at 14 SCFH. Turned off sparge and let settle 10 min.
11	Suction	50	After letting solids settle 10 min, sparged slurry at 12 SCFH for 2 min immediately prior to transfer. Transfer successful.
	Suction	60	Sparged immediately prior to run. Plugged suction tube. Could not be cleared with 100-psig steam. Replaced suction tube.

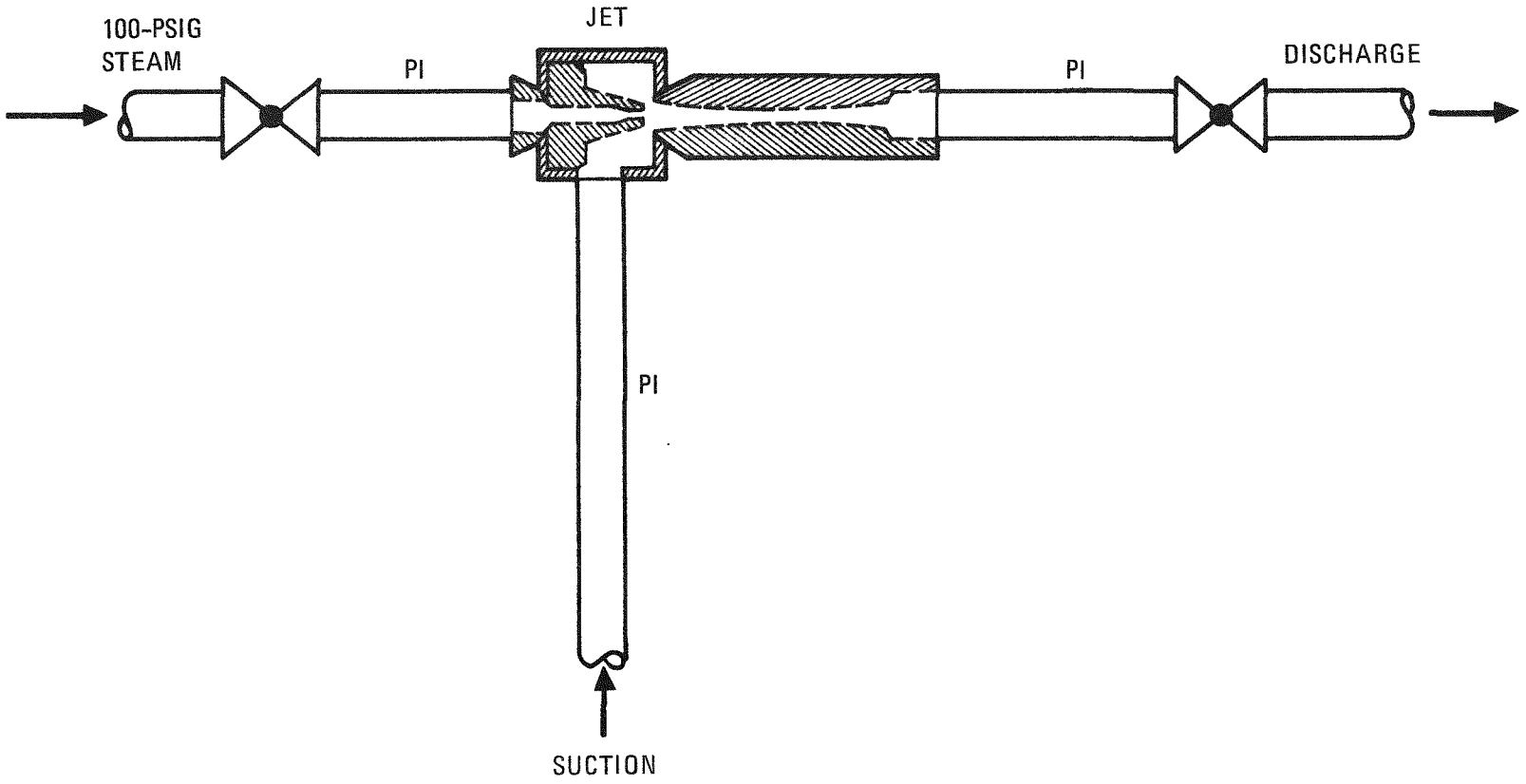

Fig. 5-10. Recommended steam-jet configuration

the jet before the steam pressure was turned on. A gravity jet is not recommended for use in remote commercial leachers because a dump valve is needed below the leacher to keep the slurry out of the jet. This valve would require remote maintenance and could not be removed when the leacher is full.

5.3. INSOLS DRYING

Eight batch insols dryer runs (Runs 12 through 19) were made in the insols drying system (Fig. 5-11) to establish the effect of feed moisture content on the drying cycle. During these runs constant drying gas inlet temperature and flow rate were maintained. All runs were successfully completed and yielded a free-flowing solids product, although the Dynapore distributor became plugged over the duration of the run series and will require further investigation.

Results of this series of dryer runs are presented in Table 5-10. These data and the least-square fit of the data are plotted and compared to former dryer runs in Fig. 5-14. As can be seen from the plot in Fig. 5-14, the total cycle time can be considered linear with respect to the initial feed moisture content. Deviation from linearity results from poor mixing of the solids during the run. This poor mixing effect is very evident in Run 18, where a large slug formed that took considerable time to dissipate.

Through visual examination and operating experience, it can be generalized that feeds of lower moisture content result in more predictable drying cycle times, as well as better overall operation of the unit.

When this series of runs are compared to former runs at the same gas flow rate but 100°C inlet gas temperature, it is evident, as expected, that the drying time is reduced by a factor of two for the 200°C inlet gas temperature. Overall operation of the system seems improved, and solids mixing is better at the higher temperature.

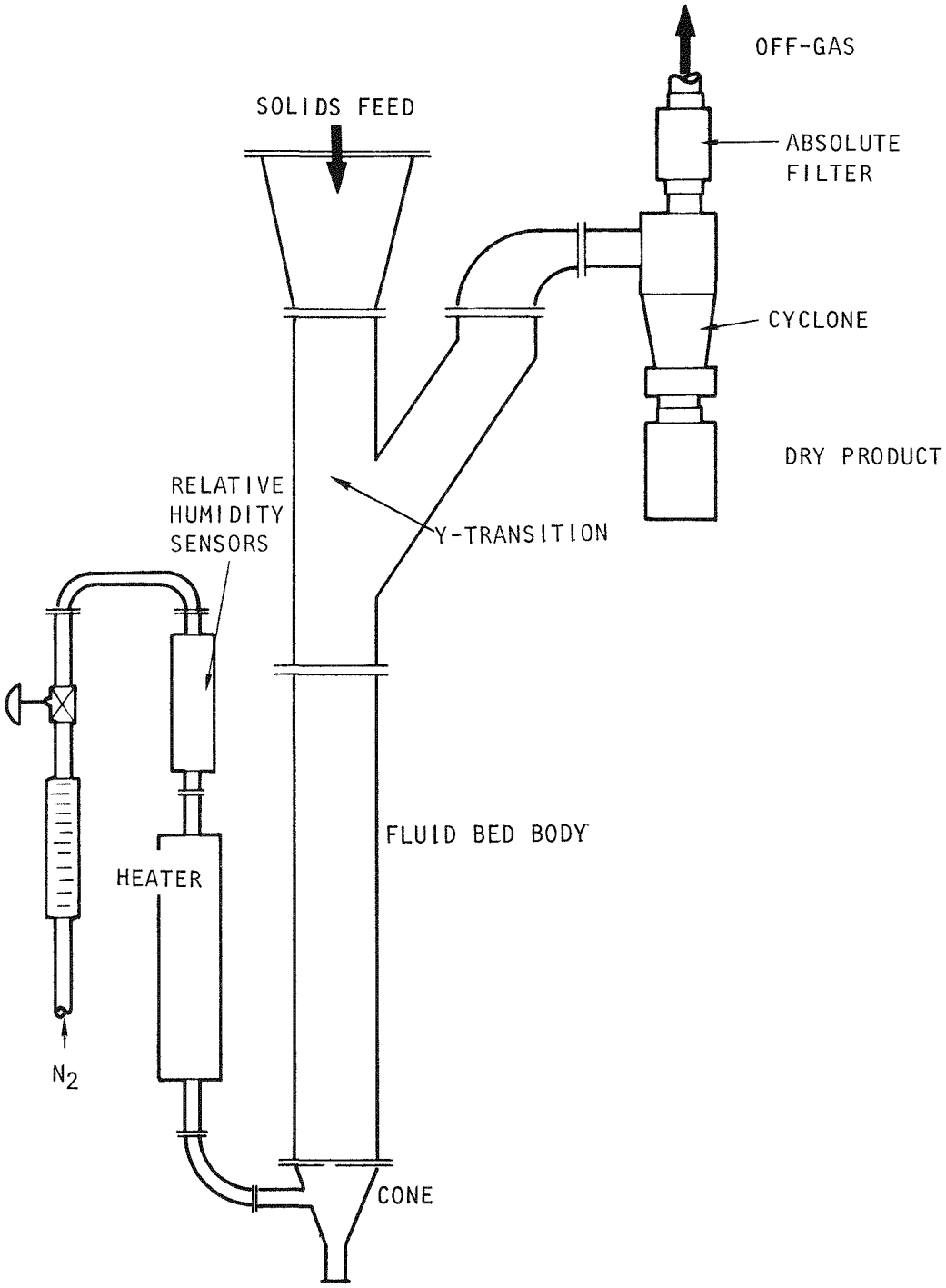

Fig. 5-11. General flow diagram for insols dryer

TABLE 5-10
OPERATING DATA FROM INSOLS DRYER RUNS 12 THROUGH 19

Drying gas	Nitrogen
Inlet gas temperature	200°C
Inlet gas mass velocity	680 lb/hr-ft^2
Dry weight of solids charge	2000 g

Run No.	Moisture Content of Solids Charge		Total Drying Time		Comments
	Wt %	g H_2O/g Dry Solids	Minutes	Minutes/kg Dry Solids	
12	5.5	0.058	23	11.5	Very smooth operation. Slug formed initially but fell shortly after start of cycle.
13	9.0	0.099	42	21.0	Same as Run 12.
14	8.0	0.087	32	16.0	Same as Run 12.
15	6.0	0.064	25	12.5	Same as Run 12.
16	30.7	0.443	128	64.0	Unusually smooth. The solids were completely saturated initially. The bed bubbled liquid at onset and splashed solids on vessel wall. No slugs formed. Carry-through of fines into cone distributor caused higher inlet pressure of nitrogen.
17	17.8	0.216	73	36.5	A very smooth run considering the high moisture content. Good mixing action once initial slug broke loose.

TABLE 5-10 (Continued)

Run No.	Moisture Content of Solids Charge		Total Drying Time		Comments
	Wt %	g H_2O/g Dry Solids	Minutes	Minutes/kg Dry Solids	
18	17.2	0.208	102	51.0	Large slug formed at onset about 3/4 of the way up vessel. Resulted in sporadic drying as seen by relative humidity of exit gas in Fig. 5-12.
19	16.4	0.196	74	37.0	Very smooth run with well defined constant and falling drying rates, as indicated in Fig. 5-13.

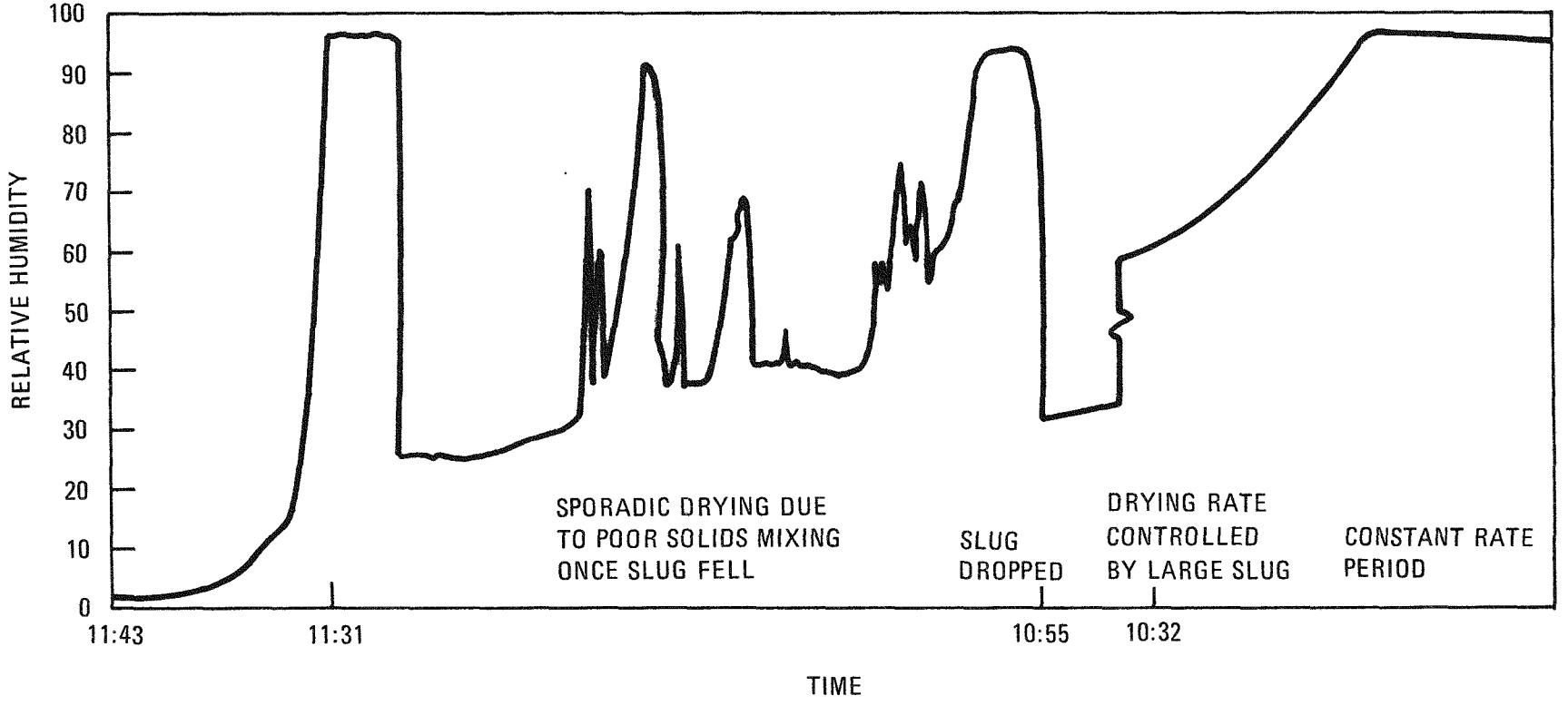

Fig. 5-12. Insols dryer exit gas relative humidity versus time, Run 18

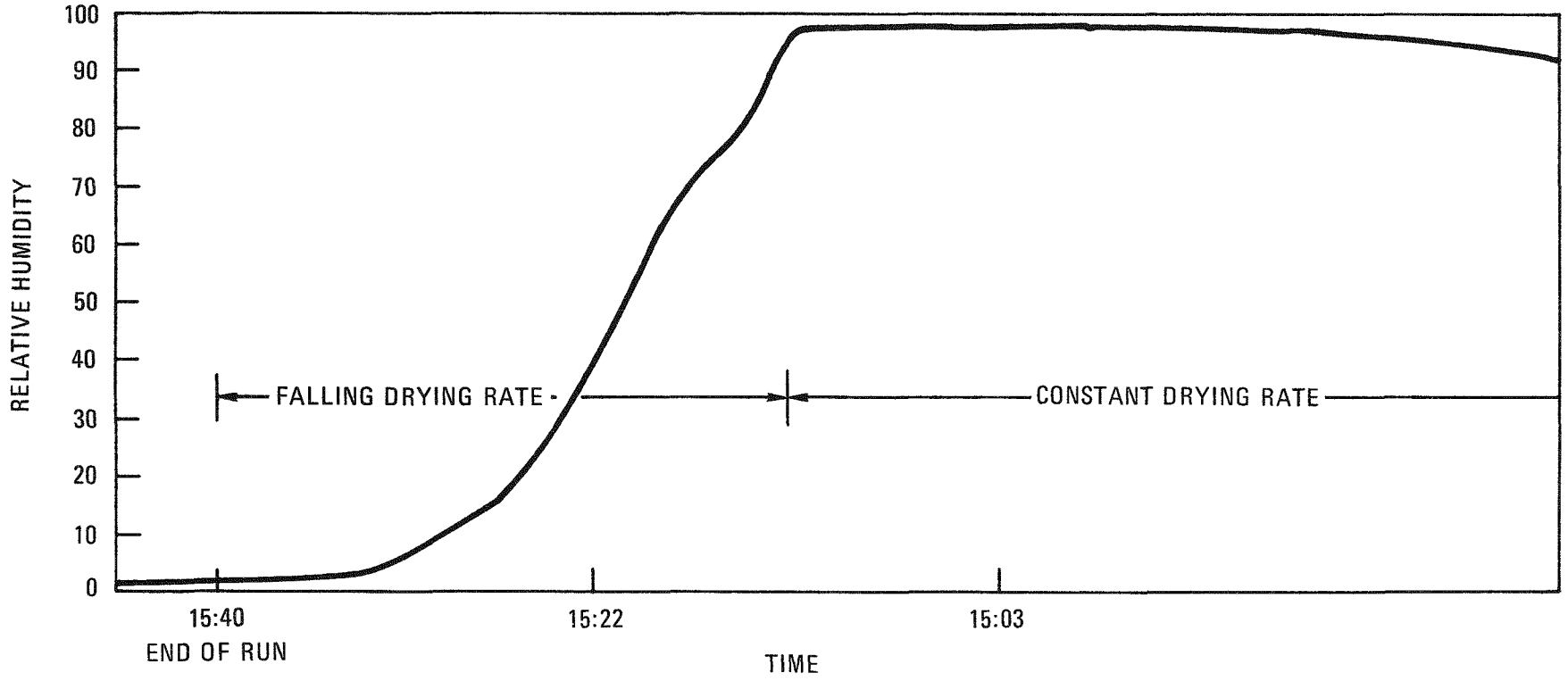

Fig. 5-13. Insols dryer exit gas relative humidity versus time, Run 19

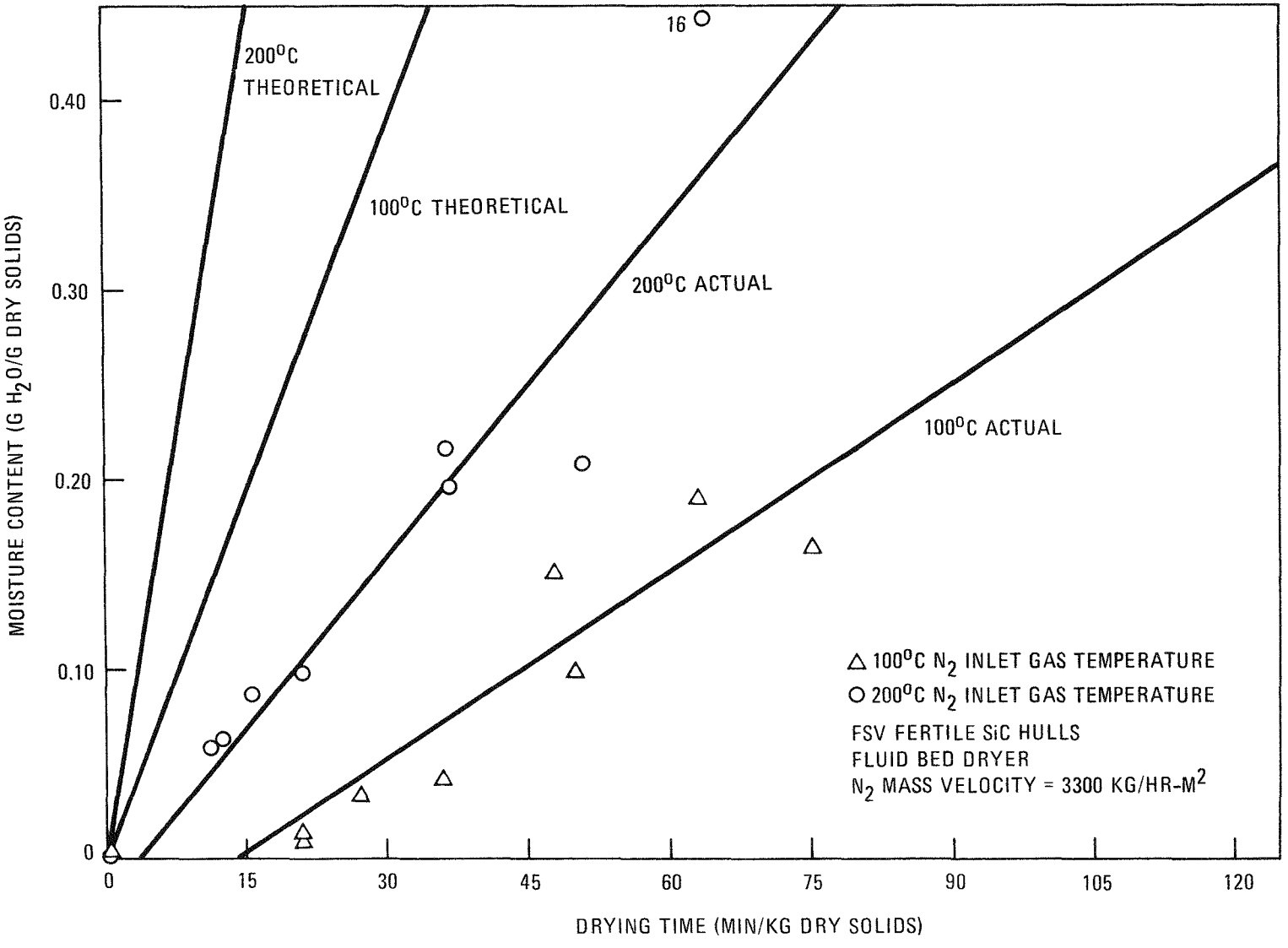

Fig. 5-14. Drying time versus feed moisture content

Comparison of experimental data to theoretical drying times indicates actual drying times for this particular system to be about five times higher. Theoretical drying times are indicated in Fig. 5-14 and are based on psychrometry assuming adiabatic cooling and constant rate drying. No attempt was made to factor into the theoretical drying times the effect of gas expansion and heat leakage from the insols dryer system. Verification of heat losses is planned via experimentation and will be reported when results are available.

Plugging of the gas distributor, a Dynapore wire mesh laminate, is believed to have resulted from a combination of conditions including static loading operations and heat degradation of a rubber-type insulation and gasket material within the electrical resistance gas heater. To alleviate additional plugging problems, a flat plate distributor has been installed with additional free area for flow, the gasket material and insulated wire have been changed, and loading operations will be carried out with a small purge through the distributor.

5.4. FEED ADJUSTMENT

Four runs were conducted on the feed adjustment system during the past quarter. Analysis of the data is incomplete, and the results will be reported next quarter.

5.5. SOLID-BOWL BATCH CENTRIFUGE TESTS

The separation of silicon carbide (SiC) hulls and SiC coated fuel particles from leachate solution is required in the reprocessing of HTGR fuel. Historically, centrifugation has been used successfully for solid-liquid separations in nuclear fuel reprocessing. Centrifugation is considered better than filtration or sedimentation because it is more readily

adaptable to the remote operation and the maintenance requirements characteristic of a reprocessing facility. Either batch or continuous centrifuge can be used.

In comparing a continuous centrifuge with a batch centrifuge, the continuous centrifuge is smaller and consequently has an advantage from the viewpoint of nuclear criticality safety. Considering the application to HTGR fuel reprocessing, a continuous centrifuge is preferred since the solid output is a damp cake suitable for direct feeding to a fluid bed dryer. By contrast, the batch centrifuges used in reprocessing plants use slurry transport to remove the solids. Such a slurry would not be suitable for direct feeding to a fluid bed dryer. However, continuous solid-bowl centrifuges have not been used in remotely operated facilities. Experiments to determine various operating parameters of a continuous solid-bowl centrifuge are being done by Allied Chemical Company at the Idaho ERDA facility. Experiments to determine various operating parameters of a batch solid-bowl centrifuge on HTGR-type solids have been done by GA, as reported in this section.

5.5.1. Separation Efficiency

Nine runs were made with SiC hulls and seven runs were made with glass beads to determine separation efficiencies as a function of g-force and feed rate in a 12-in., solid-bowl DeLaval batch centrifuge. The flow rates ranged between 1-1/2 and 13 liters/min. The g-force was either 200 or 1500 (1100 or 3000 rpm). About 50 liters of $NaNO_3$ solution (specific gravity approximately 1.3) containing 5 wt % SiC hulls or glass beads was used in each run. The glass beads (diameter of 400 to 600 μm and density of approximately 2.5 g/cm^3) were used to simulate the behavior of fertile or fissile fuel particles.

Figure 5-15 illustrates the apparatus used during the centrifugation runs. The slurry was fed to the centrifuge using a steam jet. The liquid

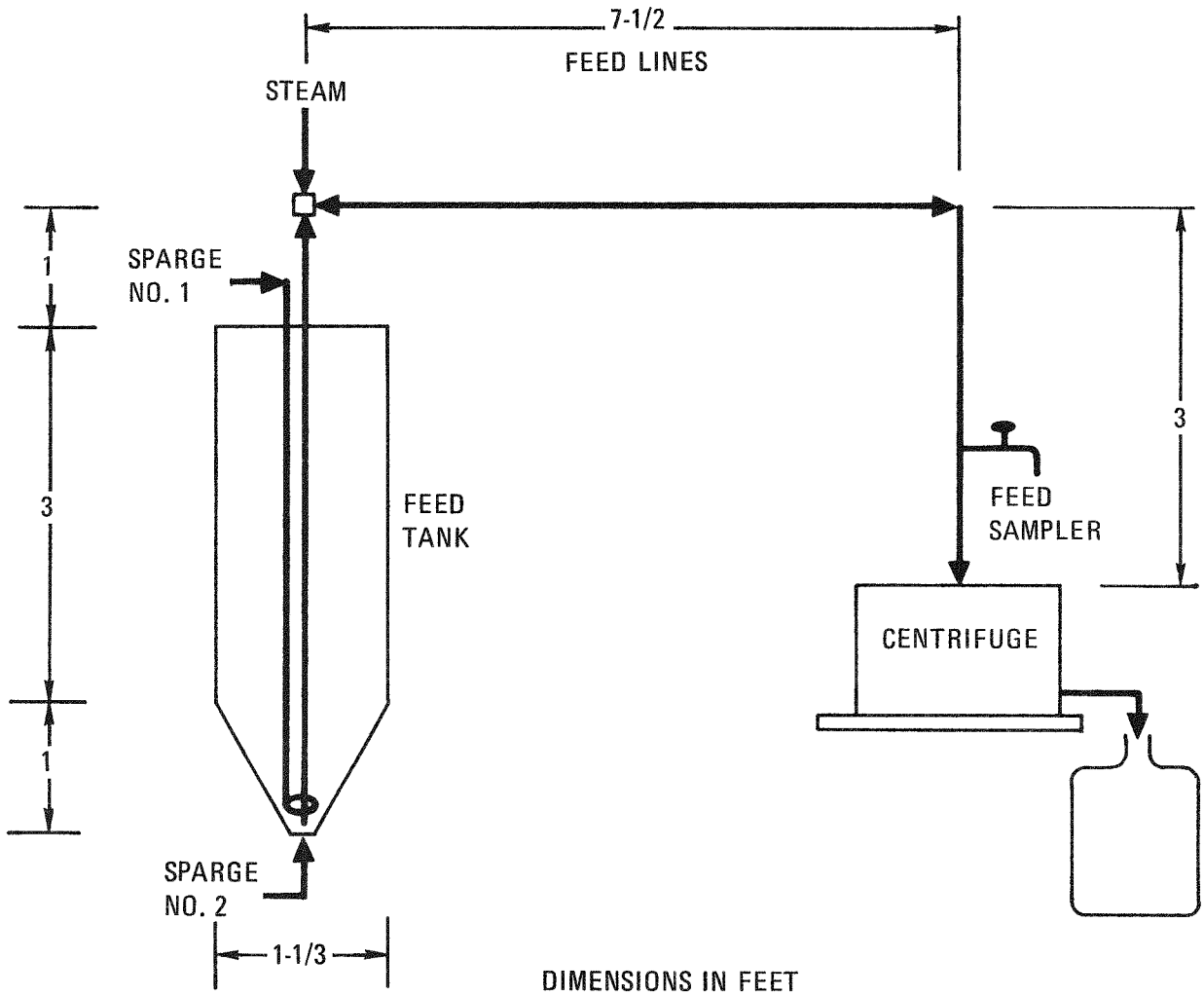

Fig. 5-15. Apparatus used in centrifugation experiments

and nonretained solids from the centrifugation operation were gravity discharged to a collection vessel, while most of the solids remained in the bowl of the centrifuge. Different feed rates were obtained by changing the sparge rates in the two spargers shown and/or changing the steam pressure to the transfer jet. The feed rate to the centrifuge was determined by measuring the feed tank dropout rate.

The concentration of hulls in the feed to the centrifuge was not uniform in composition; a major fraction of the solids was contained in the first centrifuge bowl volume of slurry. However, this is true of all slurry transfers from batch operations, and therefore the separation efficiencies are typical of those anticipated in actual application.

In Fig. 5-16, the separation efficiency for glass beads is plotted as a function of the feed rate. These data incidate a very rapid decrease in separation efficiency as the feed rate is increased, but does not indicate a significant difference in separation efficiencies at the two different g-forces. For the range of operating conditions shown in Fig. 5-16 (feed rates between 3 and 9 liters/min, g-forces of 200 and 1500), theory (Ref. 5-6) predicts that all particles with diameters greater than 4 μm would remain in the centrifuge. Since the particles used were between 400 and 600 μm in diameter, a 100% separation efficiency would be expected if theory adequately modeled the system that was used. It is possible that the vertical baffles in the centrifuge are knocking the particles out of the bowl with a "batting"-type action. It is significant to note that whatever is causing these lower-than-predicted separation efficiencies, the efficiency is much more affected by changes in feed rate than by changes in rpm.

The separation efficiency for SiC hulls as a function of feed rates is plotted in Fig. 5-17. The general trends indicate that the separation efficiency decreases with increased flow rate and decreases with decreased g-forces. These trends are also observed in Fig. 5-18, where separation efficiency is plotted as a function of g-forces.

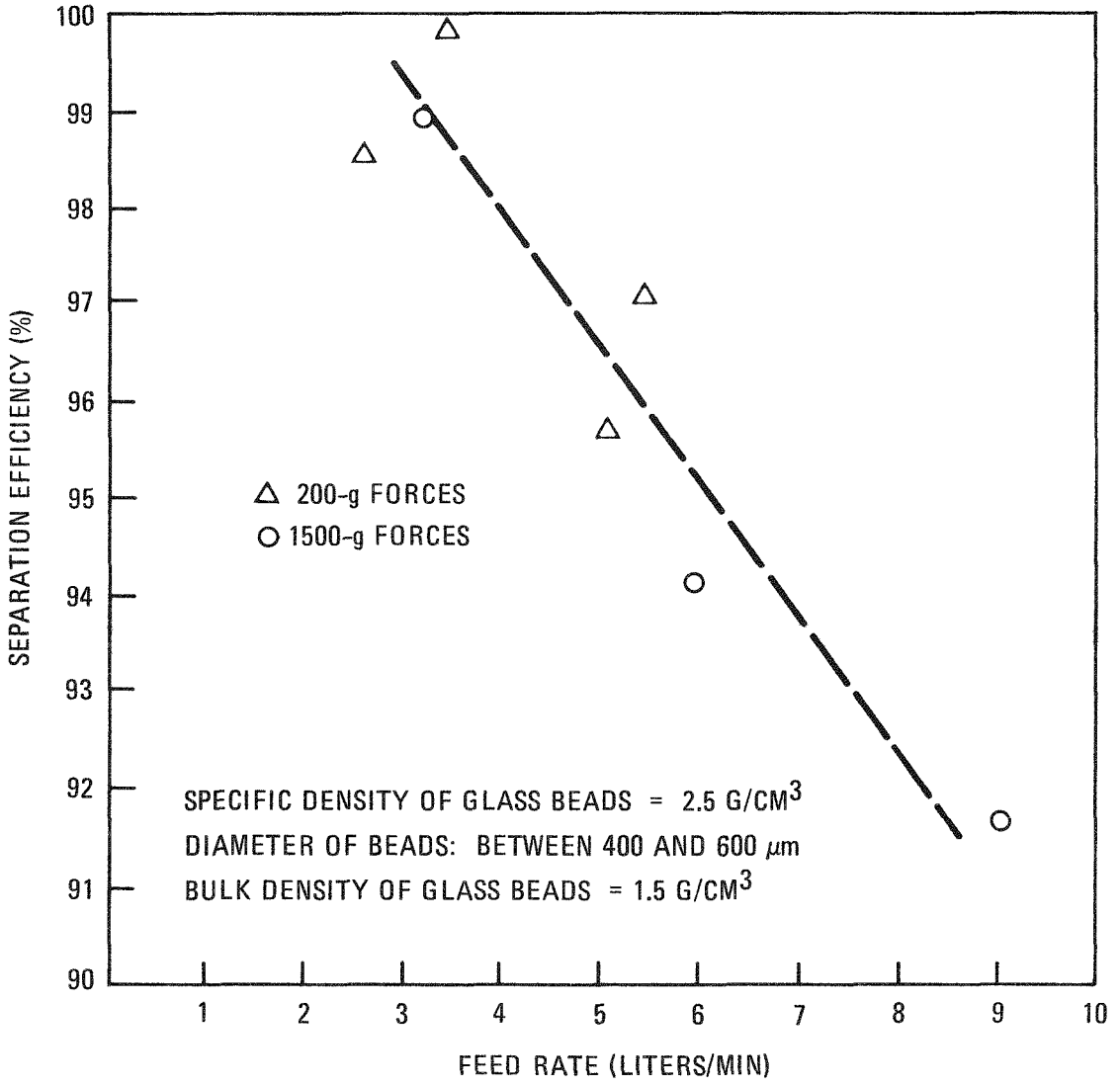

Fig. 5-16. Separation efficiency as a function of feed rate for glass beads

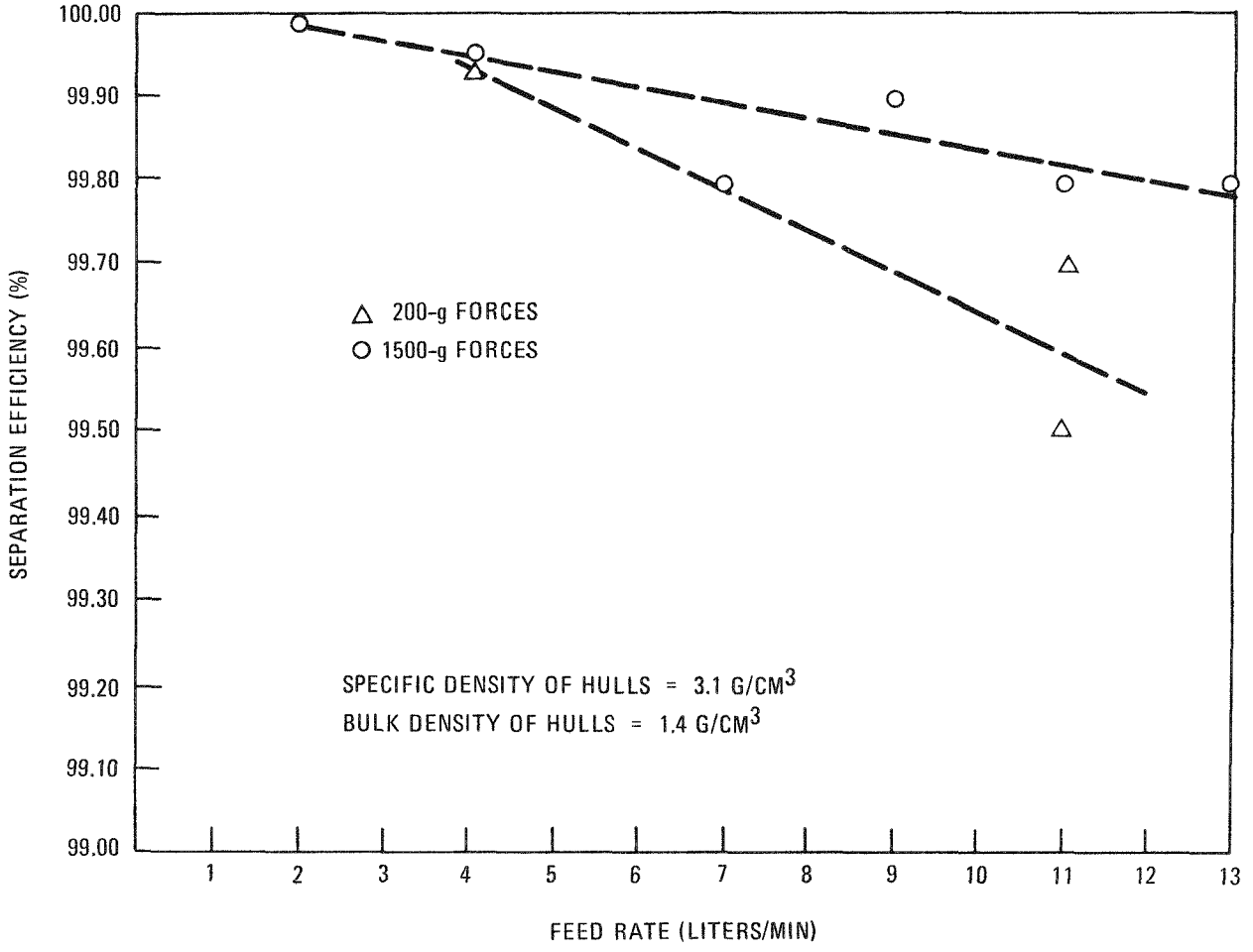

Fig. 5-17. Separation efficiency as a function of feed rate for SiC hulls

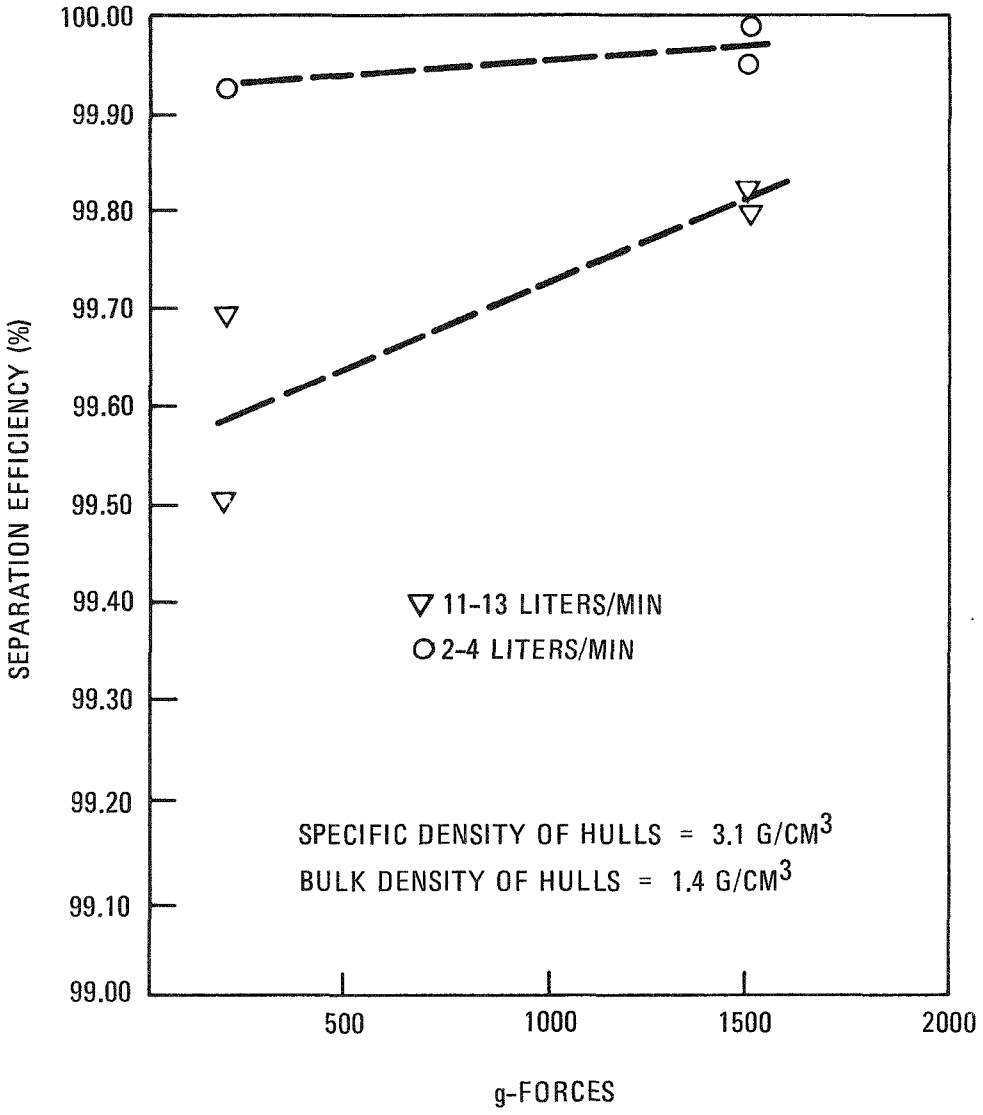

Fig. 5-18. Separation efficiency as a function of g-forces for SiC hulls

For the range of operating conditions shown in Fig. 5-17, (feed rates between 2 and 13 liters/min, g-forces of 200 and 1500), theory predicts that particles with diameters greater than 4 μm would remain in the centrifuge. This prediction, however, is based on using solid spherical particles, not multishaped hulls.

The fractional oversize graph (Fig. 5-19) does not present enough data to predict separation efficiencies when the predicted particle diameter is much less than 40 μm. The separation efficiency data are therefore analyzed empirically.

The nonretained solids that left the centrifuge in the liquid were very small. These solids readily passed through a 5-μm filter bag and took almost 2 days to settle to the bottom of the collection bottle. After each run, the solids obtained from the bottom of the collection bottle were dried, weighed, and then discarded. The SiC hulls were, therefore, continually being depleted of this very fine particulate material. In these experiments it was assumed that in the handling of the insols between runs, more of this fine particulate material would be generated to replace that lost to sampling. The measured particle sizes (Fig. 5-19) tend to support this assumption.

The variation in the weight percent of very fine particulate material (less than 5 μm in largest dimension) between the runs is probably the main source of uncertainty in the data shown in Figs. 5-17 and 5-18. Another source of uncertainty is the variation between different runs in the solid concentration in the feed versus time.

A comparison of the separation efficiencies of the SiC hulls with those of the glass beads shows that the beads have much lower separation efficiencies. For example, at a feed rate of 9 liters/min and a g-force of 1500, the hulls have a 99.9% separation efficiency whereas the beads have a 91.7% separation efficiency. The glass beads differ from the SiC hulls in

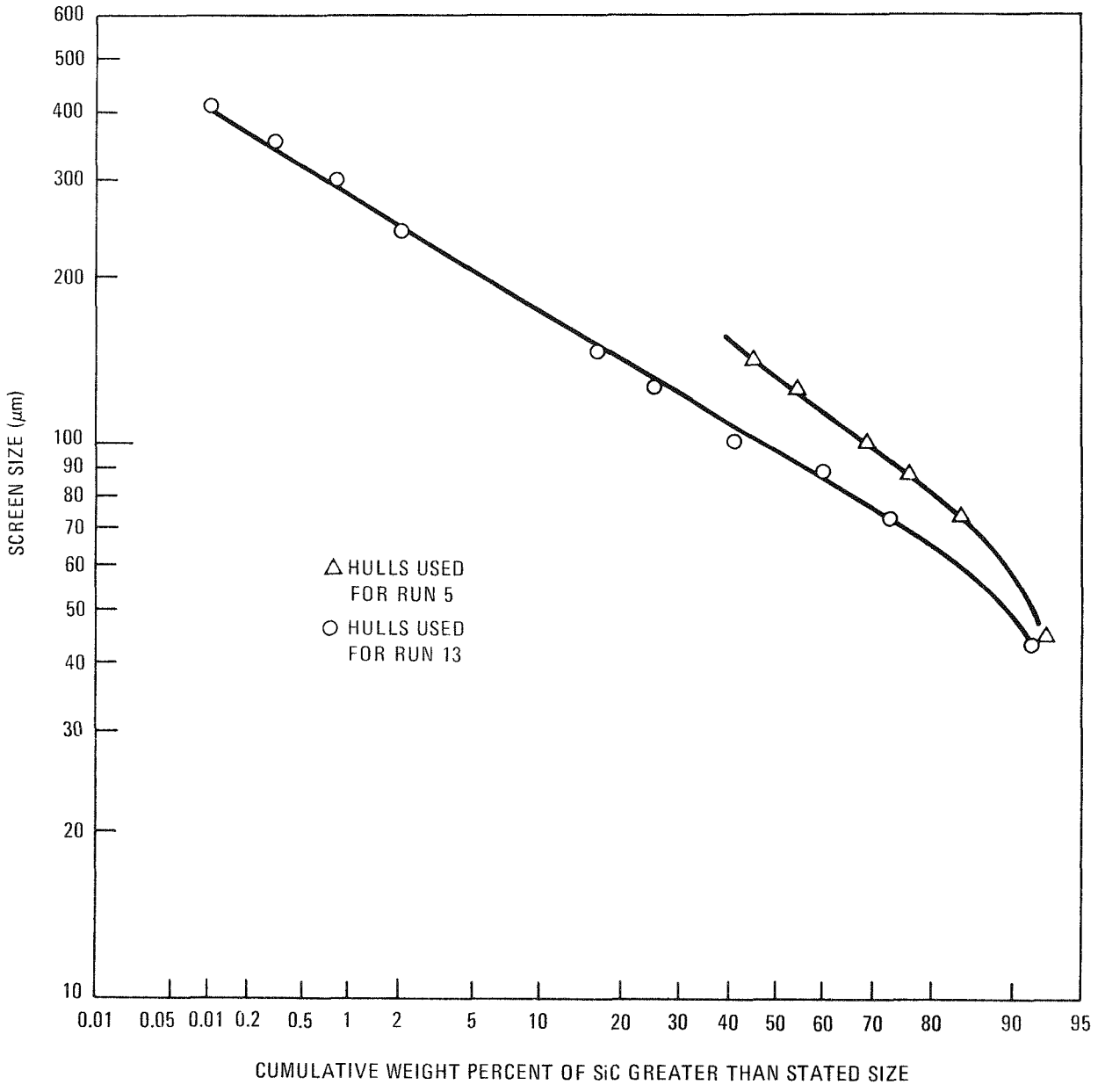

Fig. 5-19. Screen analysis of hull sizes

size, shape, and density. In addition, there is a fundamental dynamic difference in the maximum momentum that the individual particles or hulls can attain by the time they reach the baffles. The mass of a 500-μm glass bead is six times greater than the mass of the largest possible SiC hull from a 500-μm particle (assumes SiC coating is 25 μm thick). The larger momenta attained by the glass beads could account for their ability to be "knocked" out of the centrifuge bowl.

5.5.2. Washing Efficiency

A maximum content of uranium in the solids has been specified in System Design Description ACC-SDD-1.1 as 10 nCi/g or 0.163 μg/g. The above uranium residue concentration corresponds to obtaining a value of 10^5 for the decontamination factor, assuming (1) complete dissolution of uranium and (2) a saturated cake of solids at the beginning and end of the series of washes. The calculated solids washing requirements were given in Ref. 5-1 (p. 5-12).

From Fig. 5-20, the optimum tradeoff for minimizing the number of washes (N) and V_t* [when the decontamination factor (D) is equal to 10^5] is estimated to be when N is between 8 and 10. This corresponds to a value of between 2.2 and 3.2 for V_a/V_r. This range for the V_a/V_r values is quite realistic for washing operations done within the batch centrifuge.

Two preliminary scoping-type washing experiments were done with the solid-bowl batch centrifuge to determine the feasibility of using the centrifuge for washing SiC hulls. In addition, three bench-scale washing experiments were done in glassware.

The washing experimental data along with the estimated ratios of V_a/V_r are shown in Fig. 5-21 where the experimentally obtained decontamination factors are plotted as a function of the number of washings for the two washing experiments done within the centrifuge bowl. Extrapolating

*See Fig. 5-20 for definition of terms V_t, V_a and V_r.

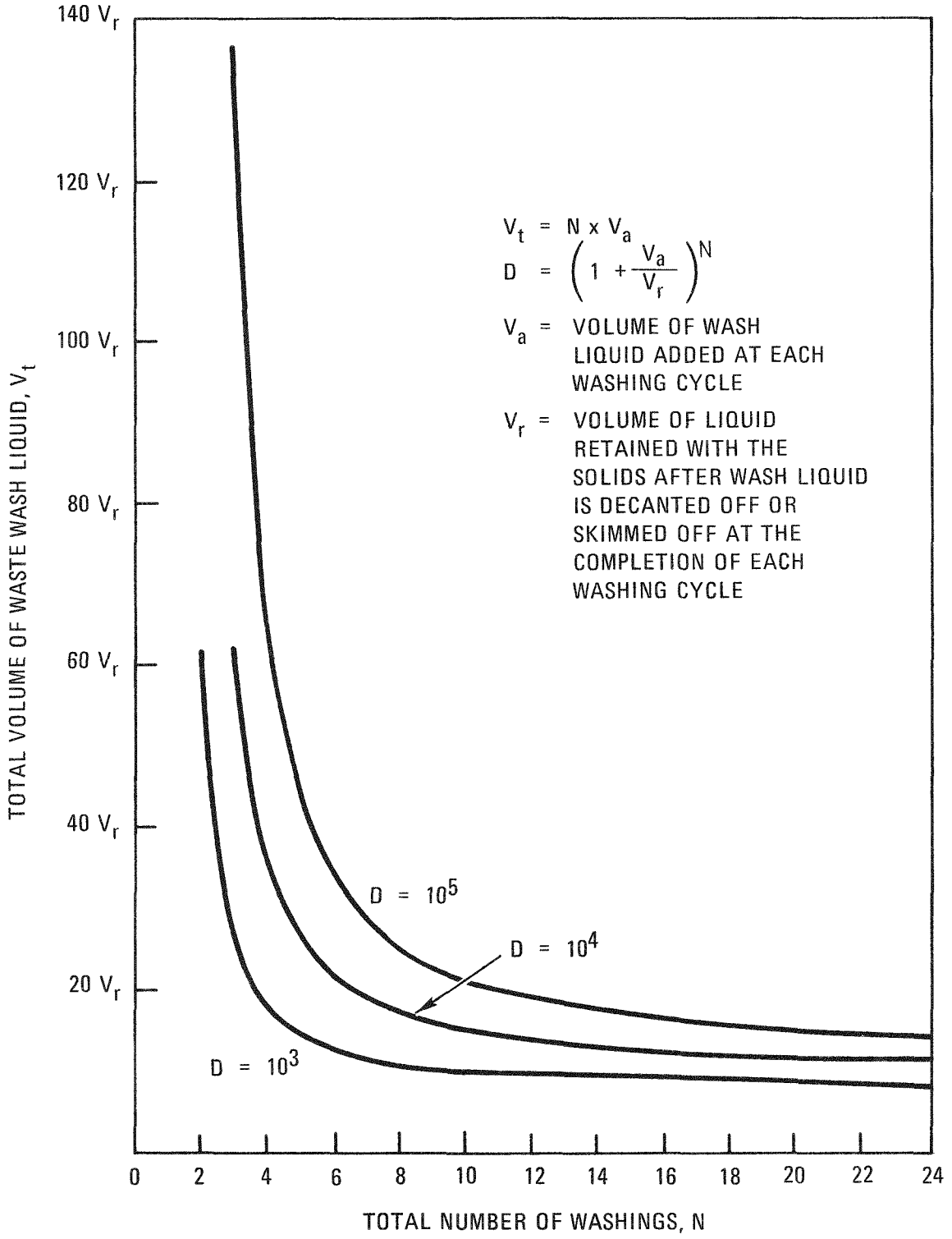

Fig. 5-20. Total volume of waste wash liquid as a function of the total number of washings for specified values of the decontamination factor (D)

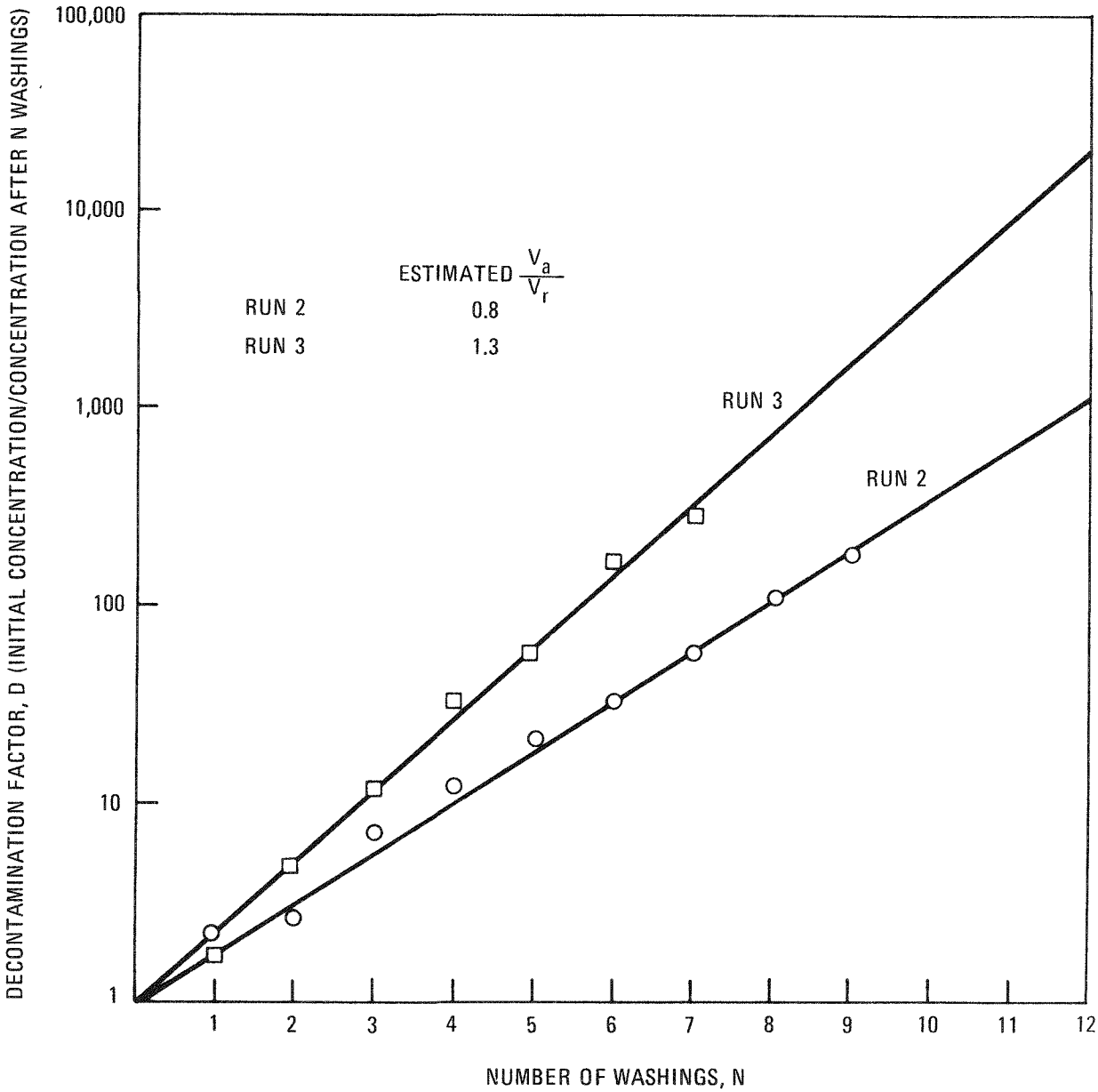

Fig. 5-21. Experimentally obtained decontamination factors from the scoping-type centrifuge tests

these results to the case where the decontamination factor is equal to 10^5 indicates that Run 2 would have required about 20 washings and Run 3 would have required about 14 washings.

It is desirable to obtain the smallest V_r value possible so that the total amount of waste wash liquid will be minimized. Further experimentation is needed to determine if the last 400 ml of liquid (not including the interstitial liquid) can be clarified.

These preliminary experiments indicate that it is feasible to wash SiC hulls within the centrifuge bowl. Further experimentation is needed to determine the most efficient method of thoroughly mixing the hulls in the wash liquid for a remotely operated centrifuge.

The three bench-scale washing experiments were done with a graduated cylinder in order to obtain better data on the validity of theory when the V_a/V_r ratio was equal to 3. Actual leachate solution was used in one of these experiments. These results should be applicable to washings done within the centrifuge providing that complete mixing of the solids in the wash liquid is obtained for each washing step.

The values for the decontamination factor as a function of the number of washings are plotted in Fig. 5-22 for the three washing experiments done within the graduated cylinder. The solid line is the value predicted by theory for a V_a/V_r ratio of 3.

The method of analyzing for thorium concentration was not sensitive enough at the low concentrations encountered beyond N = 8. The experiment with thorium shows larger than predicted values of D at larger values of N. The experiments with sodium show a smaller than predicted value of D at larger values of N; this may be due to sodium being leached from the glass. Further experimentation is needed, however, to substantiate this.

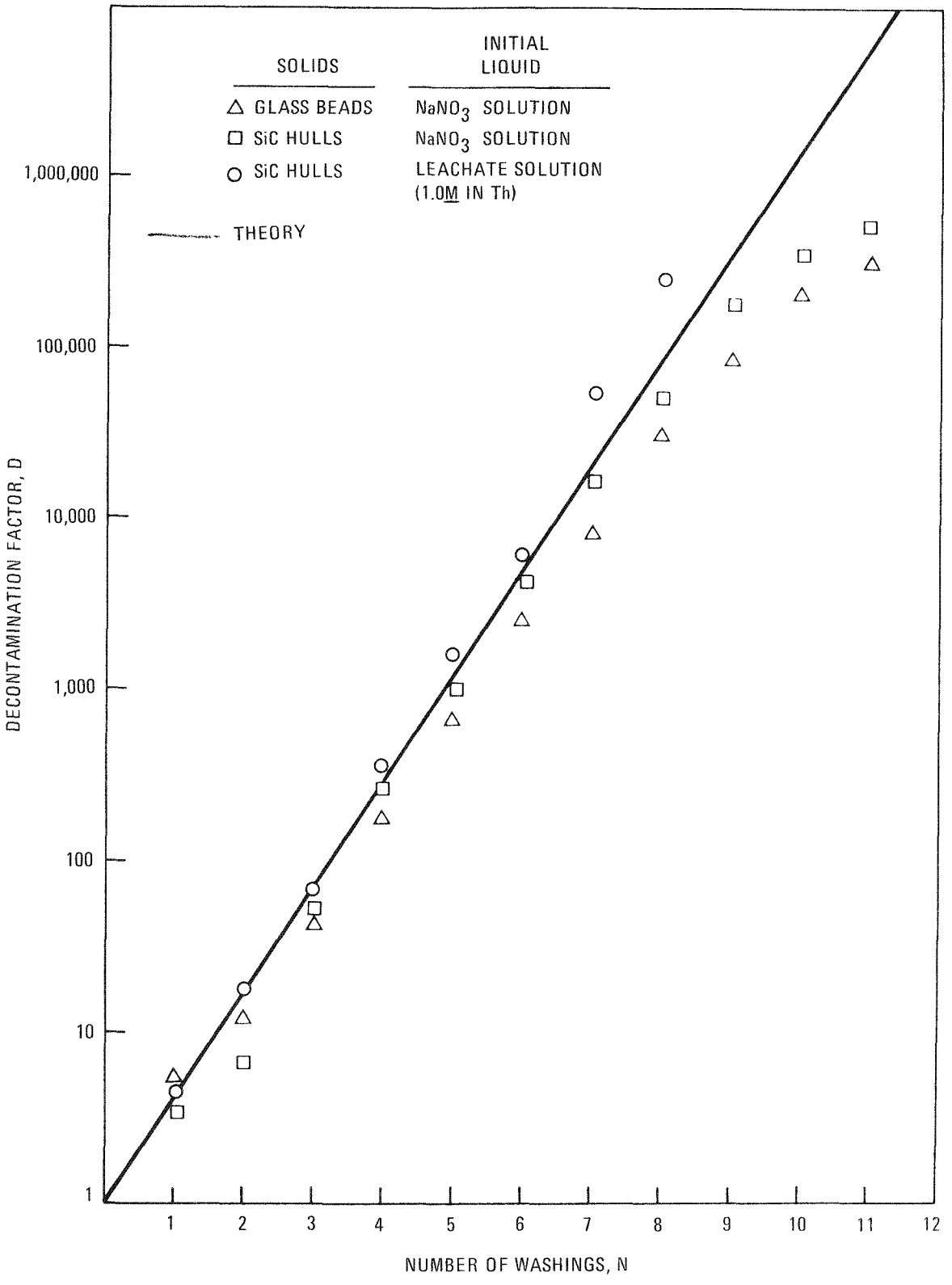

Fig. 5-22. Experimentally obtained decontamination factors as a function of N when $V_a/V_r = 3$

It is significant to note that for all three experiments where there is complete dissolution of the contaminating material, theory can predict to an accuracy of ±1 the number of washings required to obtain a specific decontamination factor for values of $D \leq 10^5$.

No additional work is scheduled on centrifuge testing during FY-76.

5.6. BENCH-SCALE INVESTIGATIONS

5.6.1. Thorium Nitrate Crystallization Studies

Bench-scale tests were conducted to determine the conditions required for thorium nitrate precipitation in mother liquors produced from Thorex dissolution of burner ash material. The present work was undertaken since it was postulated that recent leacher runs may have resulted in thorium nitrate crystal formation in the insoluble material on cooling. Of particular interest was the effect of the fluoride and aluminum present in the Thorex solution on thorium solubility.

Samples were prepared by the dissolution of weighed amounts of reagent grade thorium nitrate tetrahydrate salt in weighed quantities of simulated Thorex solution. Silicon carbide hulls were added to selected samples in an amount equal to 6% of the total sample weight. Complete dissolution was accomplished by heating to ∿70°C. Samples were allowed to equilibrate for at least 48 hr at 21°C following the appearance of crystals. Parafilm was used to cover sample containers during heating and subsequent equilibration in an effort to minimize compositional changes resulting from water losses or gains on contact with air. After equilibration, the supernatent liquids were analyzed for thorium, aluminum, and free acid content.

Samples in which no crystal growth was observed after 48 hr were treated with trace amounts of thorium nitrate tetrahydrate salt. In many cases, rapid crystal formation occurred upon thorium nitrate addition. In

most cases, sufficient quantities of thorium nitrate crystals were formed to permit visual confirmation of crystal growth, even in samples containing silicon carbide hulls. Samples in which no crystals were visually apparent were examined microscopically in polarized light to verify the absence of crystals.

Table 5-11 contains data for the experiments in which thorium nitrate was added. Analytical data obtained for thorium nitrate "seeded" sample supernatant liquids are given in Table 5-12. Figure 5-23 is a graphic presentation of data obtained for samples in which crystal growth was induced by the addition of thorium nitrate tetrahydrate. Initial and final solution composition values are indicated in Fig. 5-23.

The present work has shown that stable supersaturated thorium nitrate solution can be prepared by the addition of thorium nitrate salt to simulated Thorex solutions. Silicon carbide hulls do not serve as nucleation sites for thorium nitrate crystal growth; however, the addition of a trace of thorium nitrate salt promotes rapid crystal formation.

A region of thorium nitrate crystal formation on a ternary phase plot for the thorium-Thorex system is given in Fig. 5-23. For thorium-Thorex compositions approximating those of typical leaching run mother liquors, the phase diagram region of thorium nitrate crystallization is essentially identical to that given for the reference system (Ref. 5-7). Thus, the presence of aluminum and/or fluoride would not account for the apparent crystallization observed in the leacher runs (Section 5.2.1). Tests need to be performed with the particular burner ash to determine if extraneous materials are present which could cause unexpected thorium precipitation.

The present study has resulted in an empirical test for thorium nitrate crystallization in leaching run mother liquors. The test consists of the addition of a thorium nitrate crystal to an aliquot of a leaching run mother liquor. Supersaturation would be indicated by crystal growth

TABLE 5-11
DATA SUMMARY FOR EXPERIMENTS WITH THORIUM NITRATE ADDITION

Sample	Spontaneous Crystal Formation, 48 hr	Crystal Formation on Addition of Trace $Th(NO_3)_4$ Salt, 1 hr
18	Negative	Positive
19	Negative	Positive
20	Negative	Positive
P	Negative	Positive
Q	Negative	Positive
R	Negative	Positive
16	Negative	Negative[a]
17	Negative	Negative[b]
C	Negative	Positive

[a] Crystal dissolved in less than 1 hr.

[b] Crystal dissolved very slowly, >4 hr.

TABLE 5-12
SUMMARY OF ANALYTICAL DATA FOR EXPERIMENTS WITH THORIUM NITRATE ADDITION

Sample	$Th(NO_3)_4$ in Solution (wt %)		HNO_3 in Solution (wt %)		Crystals Present
	Initial	Final	Initial	Final	
3	57.96	35.16	14.70	29.61	Positive
11	64.90	42.87	9.40	20.16	Positive
C	52.16	37.23	17.64	27.09	Positive
J	43.47	29.70	27.89	37.80	Positive
Q	38.65	29.00	30.98	38.43	Positive
O	29.18	28.05	37.18	37.17	Negative

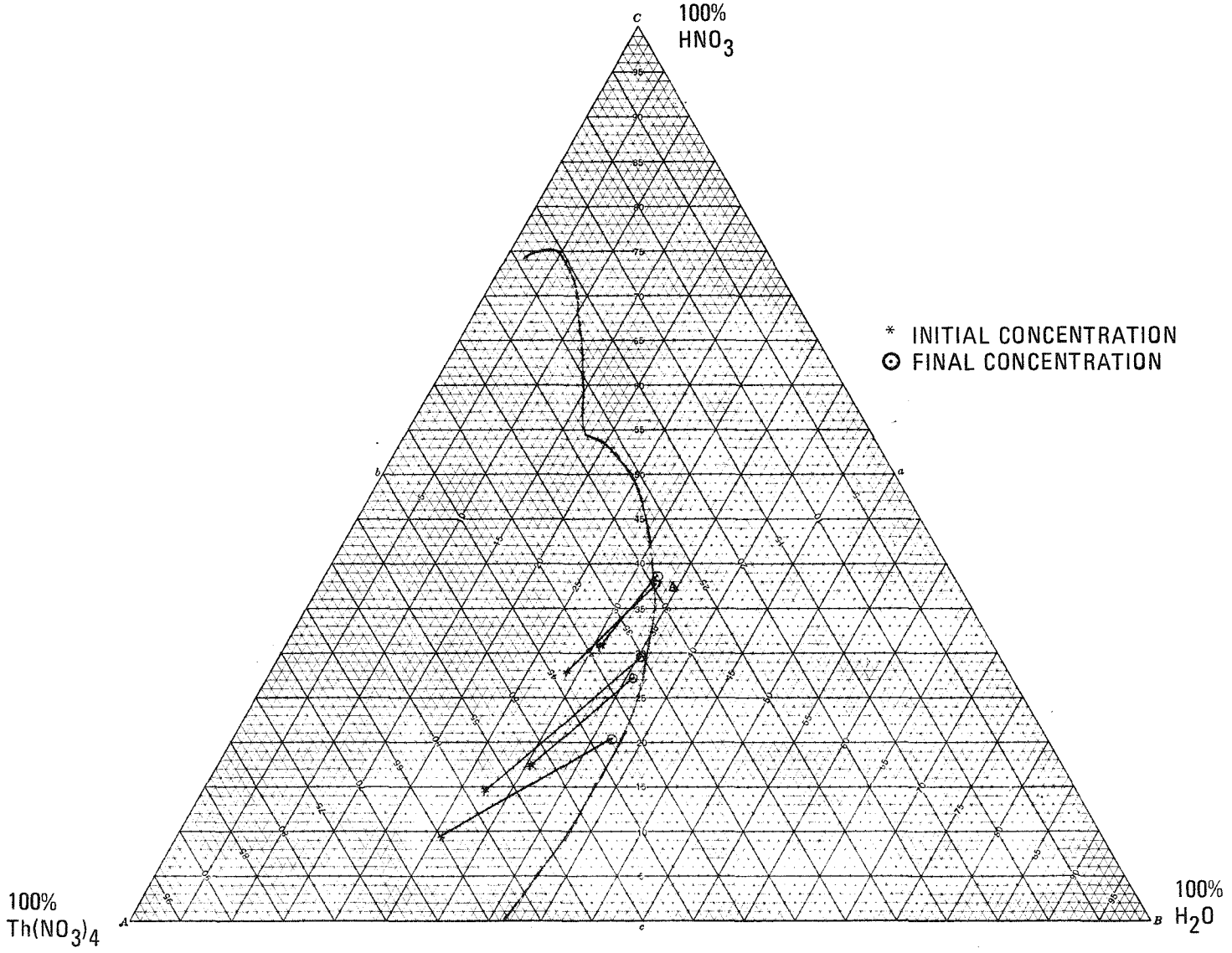

Fig. 5-23. $Th(NO_3)_4$ - HNO_3 - H_2O - Al^{+3} - HF system at 21°C

and saturation by failure of the added crystal to dissolve. Dissolution of the added crystal would constitute a negative test for thorium nitrate crystal formation in the leacher.

5.6.2. Differential Leaching of Uranium From Thorium

Experiments were completed on differential leaching of uranium from thorium. Differential leaching is based on the relative dissolution rates of U_3O_8, ThO_2, and mixed oxides in dilute nitric acid. U_3O_8 is readily soluble in dilute nitric acid, but high-fired ThO_2 is increasingly difficult to dissolve in nitric acid as a function of firing conditions. However, high-fired ThO_2 is soluble in concentrated nitric acid containing $\sim$0.05M fluoride ion (or Thorex). Mixed oxides exhibit a solubility behavior dependent on the Th/U ratio; i.e., increasing Th/U ratios yield decreasing dilute nitric acid solubility. Therefore, since bred U-233 is present in marginally soluble ThO_2-rich fertile particles and uranium from broken fissile particles is in the readily soluble U_3O_8 form, a differential leaching separation is possible.

The success of any differential leaching scheme is strongly dependent on the entire history of the material being leached. Irradiation exposure, Th/U ratio, fabrication technique, etc., are among the factors determining the ultimate success of a differential leaching approach. Experimental evidence currently available indicates that differential leaching offers a potential method of U-233/U-235 separation for the reference fuel, i.e., a mixture of uranium oxycarbide TRISO fissile particles and thorium oxide BISO fertile particles.

U_3O_8-ThO_2 sol-gel mixtures were prepared for differential leaching studies. A summary of data obtained for these mixtures is presented in Table 5-13. Table 5-14 contains data for differential leaching studies on crushed burned Fort St. Vrain fissile particles as a function of time, temperature, and acid molarity.

TABLE 5-13
SUMMARY OF DIFFERENTIAL LEACHING DATA FOR FIRED SOL-GEL ThO_2 AND FINELY DIVIDED U_3O_8

Test Conditions[a]		ThO_2 Weight (g)	U_3O_8 Weight (g)	Soluble ThO_2 Weight (g)	Soluble U_3O_8 Weight (g)	Soluble ThO_2 (%)	Soluble U_3O_8 (%)
Temp (°C)	Time (hr)						
25	2	26.1	0.276	0.0006	0.015	0.002	5.43
50	2	26.1	2.65	0.004	2.65	0.015	100.0
Reflux	2	26.4	0.330	0.003	0.330	0.011	100.0

[a] 100 ml of 2M nitric acid was used for all experiments.

TABLE 5-14
SUMMARY OF DIFFERENTIAL LEACHING DATA FOR CRUSHED-BURNED FSV FISSILE PARTICLES

Temp	Acid Molarity and Time	Sample Weight (g)	Total Uranium Sample (mg)	Total Soluble Uranium (mg)	Soluble Uranium[a] (%)	Total Thorium Sample (mg)	Total Soluble Thorium (mg)	Soluble Thorium[b] (%)
Reflux	2M 2 hr	1.2614	47.7	0.91	1.91	200.8	0.428	0.21
	2M 4 hr	1.7535	66.3	1.68	2.53	279.1	0.957	0.34
	2M 6 hr	1.5324	57.9	1.69	2.92	244.0	1.628	0.67
	4M 2 hr	1.7101	64.6	1.56	2.41	272.2	1.008	0.37
	4M 4 hr	1.5678	59.3	2.05	3.46	249.6	2.076	0.83
	4M 6 hr	1.0963	41.4	8.89	21.47	174.5	27.23	15.61
	6M 2 hr	1.5193	57.4	1.55	2.70	241.9	1.329	0.55
	6M 4 hr	1.3391	50.6	1.84	3.64	213.9	2.108	0.99
	6M 6 hr	1.4312	54.1	14.59	26.97	227.8	50.16	22.02
50°C	2M 2 hr	1.3720	51.9	1.00	1.93	218.4	0.067	0.031
	2M 4 hr	1.7482	66.1	1.52	2.30	278.3	0.124	0.045
	2M 6 hr	1.4095	53.3	1.53	2.87	224.4	0.118	0.052
	4M 2 hr	1.2853	48.6	1.24	2.55	204.6	0.085	0.041
	4M 4 hr	1.3805	52.2	1.32	2.53	219.8	0.096	0.043
	4M 6 hr	1.3007	49.2	0.83	1.69	207.1	0.119	0.058
	6M 2 hr	1.3062	49.4	1.15	2.33	207.9	0.092	0.044
	6M 4 hr	1.5692	59.3	1.49	2.51	249.8	0.150	0.060
	6M 6 hr	1.5543	58.8	1.22	2.07	247.4	0.161	0.065
Ambient	2M 2 hr	1.3901	52.6	1.23	2.34	221.3	0.015	0.007
	2M 4 hr	1.4602	55.2	1.27	2.30	232.5	0.010	0.004
	2M 6 hr	1.3824	52.3	0.86	1.64	220.0	0.013	0.006
	4M 2 hr	1.3617	51.5	0.79	1.53	216.8	0.010	0.004
	4M 4 hr	1.7306	65.4	1.52	2.32	275.5	0.037	0.013
	4M 6 hr	1.6945	64.1	1.01	1.58	269.8	0.031	0.011
	6M 2 hr	1.7654	66.7	1.24	1.86	281.1	0.050	0.018
	6M 4 hr	1.4075	53.2	1.04	1.95	224.1	0.037	0.017
	6M 6 hr	1.3258	50.1	0.69	1.38	211.1	0.031	0.015

[a] Uranium analysis by Davies-Gray titrimetry.

[b] Thorium analysis by Thorin colorimetry.

A topical report (Ref. 5-7) covering differential leaching experimentation at General Atomic has been issued. The principal conclusions contained in the report are:

1. The success of a differential leaching scheme was found to be strongly dependent on the entire history of the material being leached. Irradiation exposure, Th/U ratio, fabrication technique, etc., were among factors determining the ultimate success of a differential leaching approach.

2. Experimental data indicate that nitric acid concentrations as low as 1M were effective in separating fissile particle ash from fertile particles. Differential leaching was shown to be capable of virtually eliminating crossover of U-235 (and U-236) into the U-233 stream at the possible expense of <2% U-233 losses to the reject U-235 stream.

3. Differential leaching was found to be of no apparent benefit with Fort St. Vrain fuel. Results obtained with samples prepared to simulate the reference fuel indicate bred uranium solubilities of <0.5% would be expected for fertile particles having a Th/U ratio of 10.

REFERENCES

5-1. "Thorium Utilization Program Quarterly Progress Report for the Period Ending February 28, 1975," ERDA Report GA-A13366, General Atomic Company, May 30, 1975.

5-2. Ferraro, J. R., L. I. Katzin, and G. Gibson, "The System Thorium Nitrate - Water - Nitric Acid at 25° and the Hydrates of Thorium Nitrate," J. Am. Chem. Soc. 76, 909 (1954).

5-3. Donaldson, D. M., et al., "Reprocessing Fast Reactor Fuels at Dounreay," Trans. Met. Soc. AIME 227, 191 (1963).

5-4. Flanary, J. R., et al., "Hot-Cell Studies of Aqueous Dissolution Processes for Irradiated Carbide Reactor Fuels," USAEC Report ORNL-3660, Oak Ridge National Laboratory, September 1964.

5-5. Swanson, J. L., "Improved Zirconium Decontamination in Purex Process," USAEC Report BNWL-1573, Battelle Northwest Laboratory, May 1971.

5-6. McCabe, W. L., and J. C. Smith, Unit Operations of Chemical Engineering, McGraw-Hill Book Company, New York, 1967, Chapter 28, p. 929.

5-7. Wilbourn, R. G., "Differential Leaching Studies - HTGR Fuel Reprocessing Development," ERDA Report GA-A13552, General Atomic Company, August 1975.

6. SOLVENT EXTRACTION

6.1. SUMMARY

Five solvent extraction runs were completed during the quarter covering the first cycle and second uranium cycle of the Acid-Thorex flowsheet. Each of the runs was made using the facilities in the pilot plant five-column system. The flowsheets under investigation are related to HTGR fuel reprocessing and the Idaho HTGR fuel reprocessing pilot plant. Each of the flowsheets tested included the addition of nonradioactive zirconium to the feeds.

6.2. RUNS 33, 34, AND 35

Runs 33, 34, and 35 consisted of a demonstration of the first cycle of the partition flowsheet in Fig. 6-1. Details of these runs will be reported at a later date. Analyses of some samples from these runs have been delayed because additional analytical chemistry procedures were required due to interference of zirconium added to the feed with the uranium analyses.

6.3. RUN 36

Run 36 consisted of a demonstration of separate extraction and scrub columns for the coextraction and costrip first cycle in Fig. 6-2. The run was carried out in three columns in the pilot plant. A 30% TBP (tributyl phosphate) solvent was used to extract the uranium and thorium from the aqueous feed solution.

Table 6-1 contains the stream analyses and the flow rates for the run. Table 6-2 contains the percent loss data, flooding frequencies, and heights

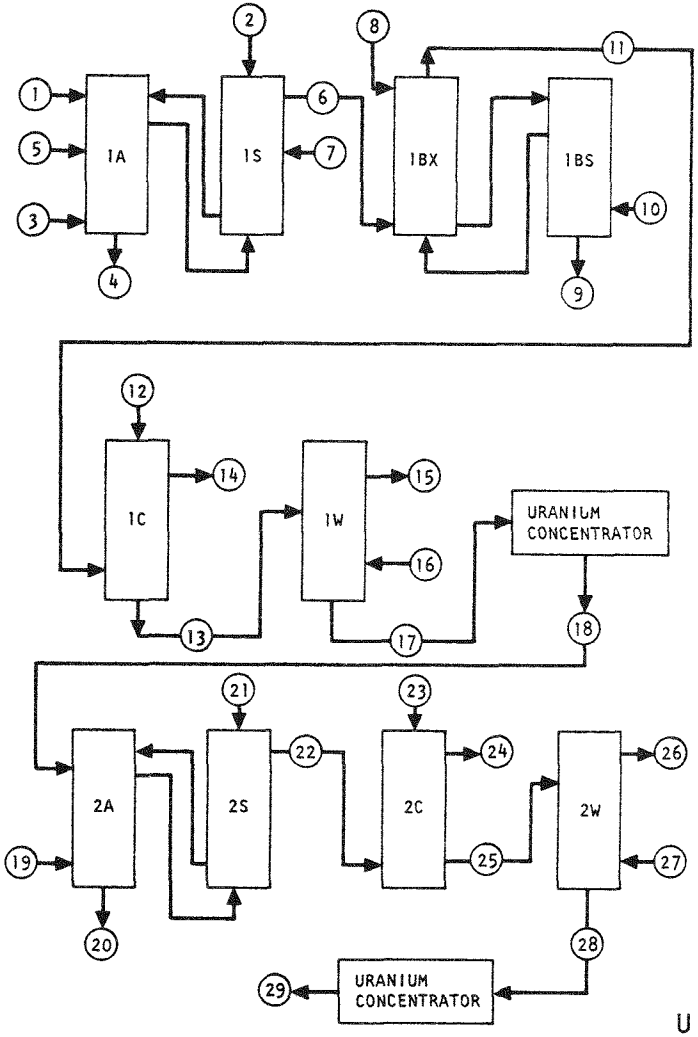

STREAM	STREAM NO.	FLOW (L/DAY)	COMPOSITION U (G/L)	Th (G/L)	HNO_3 (M)
1AF	1	725	14	348	<1.0
1AS	2	754			0.01
1AX	3	7250		(30% TBP)	
1AW	4	1903		(FISSION PRODUCTS)	
1AA	5	234			13.0
1AP	6	7250	1.4	35	
1AIS	7	190			5.0
1BX	8	4350			0.2
1BT	9	4350	Trace	102	
1BS	10	1300		(30% TBP)	
1BU	11	8550	1.19		
1CX	12	4300			0.01
1CU	13	4300	2.37		
1CW	14	8550		(30% TBP)	TO 10
1WS	15	430		(NPH)	SOLVENT WASH
1WW	16	430		(NPH)	
1WU	17	4300	2.37		
2AF	18	43.6	233		
2AX	19	858		(5% TBP)	
2AW	20	294		(WASTE)	
2AS	21	243			2.0
2AP	22	858	11.8		
2CX	23	430			0.01
2CW	24	858		(ORGANIC)	
2CU	25	430	23.6		
2WW	26	43		(NPH)	
2WS	27	43		(NPH)	
2WU	28	430	27.5		
U PRODUCT	29	43.6	233		

Fig. 6-1. Partition flowsheet

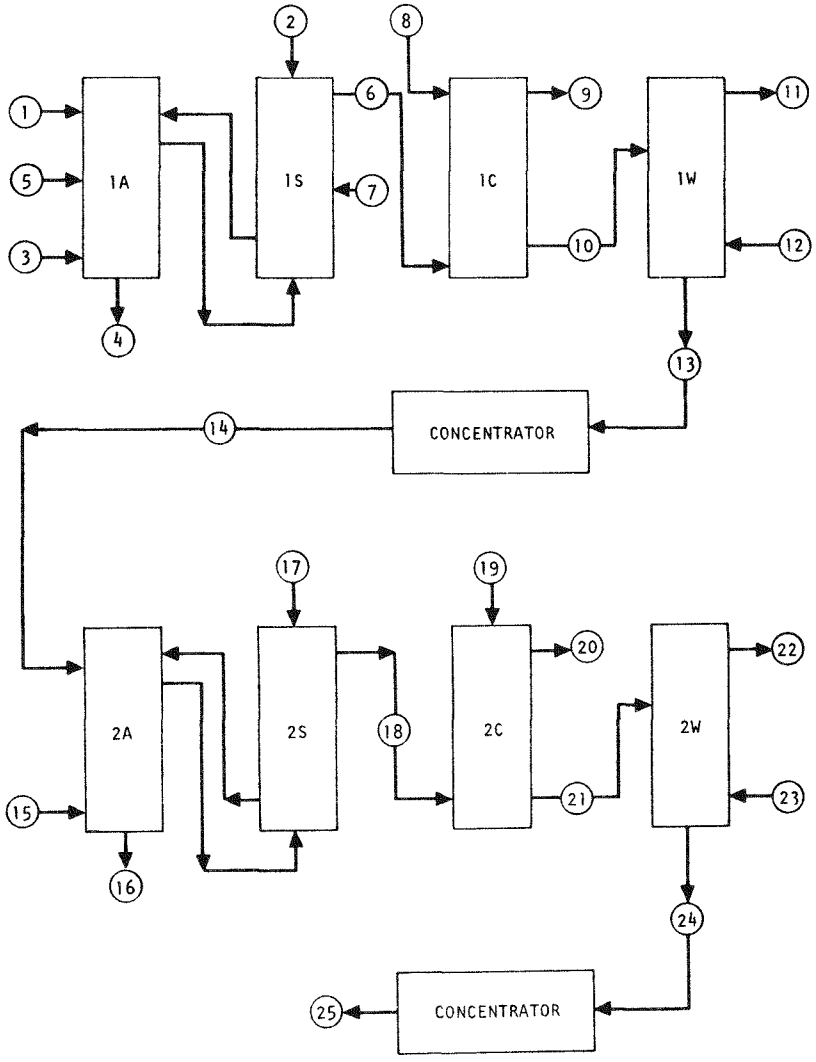

STREAM NO.	FLOW (L/DAY)	COMPOSITION U (G/L)	Th (G/L)	HNO_3 (M)
1	725	14	348	<1.0
2	754			0.01
3	7250		(30% TBP)	
4	1903		(FISSION PRODUCTS)	
5	234			13.0
6	7250	1.4	35	
7	190			5.0
8	7250			0.01
9	7250		(ORGANIC)	
10	7250	1.4	35	
11	725		(NPH)	
12	725		(NPH)	
13	7250	1.4	35	
14	725	14	348	
15	940		(5% TBP)	
16	1007		255	
17	282			2.0
18	940	10.8		
19	470			0.01
20	940		(ORGANIC)	
21	470	21.6		
22	47		(NPH)	
23	47		(NPH)	
24	470	21.6		
25	43.6	233		

Fig. 6-2. Costrip flowsheet

TABLE 6-1
ANALYTICAL DATA AND STREAM FLOW RATES FOR RUN 36

Stream	Stream No.[a]	U (g/liter)	Th (g/liter)	HNO_3 (M)	Flow (ml/min)	Relative Flow	Zr	F^- (M)
1AF	1	39.2	364.5	0.95	65	100	4.1 g/l	0.06
1AS	2	--	--	0.018	68	105	--	--
1AIS	7	--	--	4.5[b]	15	23	--	--
1AA	5	--	--	15	29	45	--	--
1AX	3	--	--	(30% TPB)	698	1074	--	--
1AW	4	8×10^{-4}	0.08	1.87	--	--	206 ppm	0.008
1AP	--	4.1[c]	42[c]	0.20	--	--	--	--
1SR	--	0.63	68.2	2.07	--	--	2125 ppm	--
1SP	6	4.09	28.12	0.13	--	--	~20 ppm	--
1CX	8	--	--	0.023	619	952	--	--
1CW	9	4.8×10^{-4}	4×10^{-3}	--	--	--	--	--
1CP	10	4.59	38.6	0.20	--	--	--	1.2×10^{-3}

[a] See Fig. 6-2.

[b] 4.5M HNO_3, 0.471M aluminum nitrate.

[c] Calculated from material balance.

TABLE 6-2
HETS, PERCENT LOSS, AND FLOODING DATA FOR RUN 36[a]

Column	Purpose	Volume Velocity (gal/hr/ft^2)	Flooding Frequency (cycles/min)	Continuous Phase	Aqueous-to-Organic Ratio	HETS (ft)		Percent Loss		Flooding Frequency (%)	Temp
						U	Th	U	Th		
1A	Extraction	629	125	Organic	0.24	--	--	0.06	0.005	71	Ambient
1S	Scrub	568	155	Organic	0.12	--	--	--	--	60	Ambient
1C	Costrip	957	∿70	Aqueous	0.89	1.9	5	0.02	0.01	∿90	125°F

[a] Cartridge descriptions:

1A - Extraction: 2-in. diameter, nozzle plates, 1/8-in.-diameter holes, nozzles down, 23% free area, 2-in. plate spacing, 22 ft of cartridge length, 1-in. pulse amplitude.

1S - Scrub: 2-in. diameter, nozzle plates, 1/8-in.-diameter holes, nozzles down, 23% free area, 2-in. plate spacing, 18 ft of cartridge length, 1-in. pulse amplitude.

1C - Strip: 2-in. diameter, nozzle plates, 3/16-in.-diameter holes, nozzles up, 23% free area, graded plate spacing -- 8-1/2 ft of 4 in., 1-1/2 ft of 3 in., 5 ft of 2 in., 15 ft of cartridge length, 1-in. pulse amplitude.

equivalent to a theoretical stage (HETS) at the indicated percentage of flooding frequency.

The 1A column in the pilot plant was used as an extraction section with a cartridge height of 22 ft. The normal solvent wash column was used as the scrub section (1S column). The scrub section cartridge was 18 ft in height. The 1C column (15-ft cartridge) was used to strip the uranium and thorium from the organic to the aqueous phase. This mode of operation was used to obtain efficiency and capacity data for the coextraction-costrip equipment per System Design Description ACC-SDD-1.2A, dated March 1975.

In the two-column 1A-1S system, both columns were operated with the organic continuous phase (bottom interface) to allow feed solids to be discharged to the aqueous waste stream. The aqueous effluent from the bottom of the 1S column is pumped to the top of the 1A column. The organic effluent from the top of the 1A column is added to the bottom of the 1S column. This interaction between the columns adds some instability to the operation of columns due to the normal cyclical response of the interface controllers. Operation with split scrub streams (0.01M HNO_3 in 1AS and 5.0M HNO_3 in the 1A-1S stream) can also cause greater column instability than a single 1.0M HNO_3 scrub stream (1AS) when normal flow variations occur.

The two contributors to column instability discussed above plus the added column length cause the control of the scrub column to be difficult. With two interacting columns such as the split 1A-1S system, recovery from flooding is also more difficult, particularly if both columns flood simultaneously.

The main difficulty with operating the Acid-Thorex flowsheet with the separate scrub column centers around handling the third phase at the organic continuous 1S column interface. At startup, separation of the heavy organic phase above the 1S column interface results in the lighter

organic phase going through the scrub section above. The lighter organic phase has a lower thorium equilibrium distribution because of its lower TBP concentration. Therefore, the split scrub stream increases thorium reflux back to the interface area, which increases the density of the heavy organic phase until it begins to fall through the interface area. In the compound extraction-scrub column, the pulser action and sieve plates prevent the two organic phases from separating. Similar agitation must be provided to use the separate scrub column with the flowsheet tested. As an alternate, a dilute flowsheet could be used so as to preclude third phase formation.

Only low losses of less than 0.1% occurred via the aqueous waste stream (1AW) from the 1A column. The thorium losses were typically less than those obtained in previous runs at the same inlet stream conditions. The significant factor influencing loss reduction was the extension of the extraction section length from the normal 13 ft to 22 ft. Uranium losses of about 0.01% via the 1AW stream were very similar to those in previous runs with comparable inlet stream conditions.

The calculated HETS values for uranium and thorium in the 1C column were about 2 and 5 ft, respectively. Similar values were obtained in previous costripping operations. The HETS is an average number for the length of column used; additional column length will change the HETS value. All HETS values will be re-evaluated with the Thorex SEPHIS code supplied by ORNL when it becomes fully operational.

Nonradioactive zirconium was added to the 1AF (feed) stream. A decontamination factor for zirconium of about 15 was obtained across the 1A and 1S columns. However, the confidence of the zirconium analysis is low based on previous analytical results. Selected solvent extraction runs will subsequently include radioactive Zr-95 tracer to resolve the effectiveness of the flowsheet for zirconium decontamination.

6.4. RUN 37

Run 37 consisted of a demonstration of the flowsheet for the second uranium cycle of the partition flowsheet (see Fig. 6-1). The run was carried out in three columns in the pilot plant. A 5% TBP solvent was used to extract uranium from the aqueous feed stream containing uranium and dilute thorium. The uranium was subsequently stripped from the solvent.

Table 6-3 contains the stream analyses and flow rates for each run. Table 6-4 contains the percent loss data, flooding frequency, and heights equivalent to a theoretical stage (HETS) at the indicated percentage of flooding frequency. The cartridge and column details are also included in Table 6-4.

Two columns were used as the 2A-2S system. The 2A column had a cartridge 22 ft in length. The 2S cartridge was 18 ft in length. Both columns were operated with the organic phase continuous.

The aqueous effluent from the bottom of the 2S column was returned to the top of the 2A column. The organic effluent from the top of the 2A column was added at the bottom of the 2S column. Cyclical response due to this double interaction between the columns adds instability to the operation of the columns.

The most significant difficulty in the operation of the columns occurred near the flooding point and after flooding occurred. Flooding can be caused by a reduction in the pulse frequency. This occurs at a point on the flooding curve that would ordinarily be within the stable region. Recovery from flooding is very difficult with the 5% TBP solvent and an organic continuous operation. The required recovery method will be to empty the flooded column and then go through the startup procedure.

TABLE 6-3
ANALYTICAL DATA AND STREAM FLOW RATES FOR RUN 37[a]

Stream	Stream No.[b]	U (g/liter)	Th (g/liter)	HNO_3 (M)	Flow (ml/min)	Relative Flow
2AF	18	235.2	1.0	2.33	54 (43)	100 (100)
2AS	21	--	--	2.42	282 (207)	522 (481)
2AX	19	--	--	(5.6% TBP)	1010 (672)	1870 (1563)
2CX	23	--	--	0.01	513 (342)	950 (795)
2AW	20	0.006 (0.156)	0.16[c] (0.17)[c]	2.14 (2.18)	--	--
2AP	--	16.4 (12.2)	0.22[c] (0.029)	0.21 (0.049)	--	--
2SR	--	23.8 (10.2)	1.4 (0.15)	2.12 (2.45)	--	--
2SP	22	8.9 (8.52)	0.004 (0.004)	0.05 (0.055)	--	--
2CW	--	0.030 (0.059)	<0.0001 (0.001)	<0.01 (<0.005)	--	--
2CU	--	17.4 (16.3)	0.026 (0.013)	0.11 (0.14)	--	--

[a] The values in parentheses correspond to a second set of operating conditions.

[b] See Fig. 6-1.

[c] Obtained from material balance calculations.

TABLE 6-4
HETS, PERCENT LOSS, AND FLOODING DATA FOR RUN 37[a,b]

Column	Purpose	Volume Velocity (gal/hr/ft^2)	Flooding Frequency (cycles/min)	Continuous Phase	Aqueous-to-Organic Ratio	HETS (ft)	Percent Loss		Flooding Frequency (%)	Temp
							U	Th		
2A	Extraction	979 (670)	123 (125)	Organic	0.33 (0.37)	4 (U)	0.015 (0.39)	-- --	70 75	Ambient
2S	Scrub	939 (639)	115 (125)	Organic	0.28 (0.31)	9 (Th)	-- --	7.3 (6.3)	75 75	Ambient
2C	Strip	1107 (737)	-- (95)	Aqueous	0.51 (0.51)	-- --	-- --	-- --	-- 87	-- 126°F

[a] The values in parentheses correspond to a second set of operating conditions.

[b] Cartridge Descriptions:

2A - Extraction: 2-in. diameter, nozzle plates, 1/8-in.-diameter holes, nozzles down, 23% free area, 2-in. plate spacing, 22 ft of cartridge length, 1-in. pulse ampltiude.

2S - Scrub: 2-in. diameter, nozzle plates, 1/8-in.-diameter holes, nozzles down, 23% free area, 2-in. plate spacing, 18 ft of cartridge length, 1-in. pulse amplitude.

2C - Strip: 2-in. diameter, nozzle plates, 3/16-in.-diameter holes, nozzles up, 23% free area, graded plate spacing -- 8-1/2 ft of 4 in., 1-1/2 ft of 3 in., 5 ft of 2 in., 15 ft of cartridge length, 1-in. pulse amplitude.

The nitric acid concentration in the aqueous phase in the 2A and 2S columns was above 2.0M to maintain good extraction characteristics for uranium, which kept losses low. Uranium losses of less than 0.02% were achieved. However, the decontamination factor for thorium across the system was only about 3. The thorium concentration in the 2CU uranium product stream was about 1500 parts of thorium per million parts of uranium. This high level of thorium is probably the result of column contamination from the previous codecontamination run. Earlier runs using 5% TBP solvent and high thorium-to-uranium ratio feeds resulted in uranium product having only 125 parts thorium per million parts uranium. The decontamination of thorium from uranium at low thorium concentrations will be resolved in later runs.

The HETS value for uranium in the 2A extraction section was about 4 ft. The HETS value for thorium in the 1S column could only be estimated because of the question of thorium cross contamination. However, assuming a normal equilibrium distribution, the HETS value was 9 ft. The HETS calculations will be further evaluated with the ORNL-supplied SEPHIS code when it becomes fully operational.

7. SYSTEM DESIGN AND DRAFTING

7.1. PROTOTYPE SIZE REDUCTION SYSTEM

All drawings have been completed, checked, and approved for the primary crusher system, and drawings for the secondary crusher system are nearing completion. The UNIFRAME welded assembly drawings were completed and prints were issued for quotations.

All components of the UNIFRAME assembly are being designed so that a simulated remote maintenance under hot cell conditions can be demonstrated. Remote handling fixtures for the crusher system include:

1. Lift fixture for top moveable jaw assembly (primary crusher).

2. Lift fixture for bottom moveable jaw assembly (secondary crusher).

3. Life fixture for top stationary jaw (primary crusher).

4. Horizontal lift fixture for stationary jaw (primary crusher).

5. Crusher shroud shutoff valve.

Conceptual designs of these fixtures were included in the previous quarterly report (Ref. 7-1, Figs. 7-1 through 7-5).

Remote fixture design is under way. An assembly layout of the removal fixture for the top moveable jaw assembly was completed and final design is under way. The conceptual design of a similar lift fixture for the bottom moveable jaw assembly was completed and a layout is being prepared.

7.2. PROTOTYPE PRIMARY BURNER

Approximately 95% of the primary burner assembly drawings have been completed and fabrication is under way. The few remaining drawings were recently reviewed for structural adequacy and the review comments are being incorporated in the design.

The commitment made to ACC-ICPP to establish a method for removal of the entire primary burner assembly was completed and transmitted to ACC. Initial installation procedures were completed. Operations and maintenance procedures were prepared, reviewed, and revised and are presently in the final review cycle.

All components of the primary burner assembly are being designed so that a simulated remote maintenance under hot cell conditions can be demonstrated. Remote handling fixtures for the primary burner include:

1. Lift fixtures.

2. Semiremote removal assembly.

3. Trunnion fixture with basket.

4. Susceptor and ceramic removal fixture.

5. Susceptor and ceramic trunnion and holding fixtures.

Conceptual designs of these fixtures were included in the previous quarterly report (Ref. 7-1, Figs. 7-6 through 7-10).

The lift fixture drawings for the primary burner were completed. The bottom spool handling cart assembly drawings were completed and are currently being reviewed. Layouts were prepared for the trunnion and holding

fixture for the primary burner; this fixture will be designed to also accommodate the secondary burner. Layouts of the susceptor and ceramic removal fixture and holding fixtures are currently being developed.

Development work was initiated to design a remote disconnect for the induction coil. Present conceptual plans are for this system to be implemented by modifying a commercially available connector. Vendor inquiries are being made.

7.3. PROTOTYPE SECONDARY BURNER

Approximately 30% of the secondary burner assembly drawings have been completed and 100% of the primary burner drawings were sent out for vendor quotation. The remaining 70% of the secondary burner drawings are scheduled for completion and release for fabrication by mid-September.

Initial installation procedures for the secondary burner assembly were prepared and are presently in draft review. Operations and maintenance procedures were also prepared and are currently being reviewed.

All components of the secondary burner assembly are being designed to permit demonstration of simulated remote maintenance operations under hot cell conditions. Remote handling fixtures for the secondary burner include:

1. Semiremote removal assembly.
2. Trunnion fixture with baskets.
3. Lift fixtures.
4. Susceptor and ceramic trunnion and holding fixture.

Conceptual designs of these were included in the previous quarterly report (Ref. 7-1, Figs. 7-6, 7-7, 7-11, and 7-12).

A detailed assembly drawing for the secondary burner lift fixture was completed. Structural analyses for this component are under way. Layout

and detail drawings of a trunnion and holding fixture were completed. The bottom spool handling cart detailed design drawings were completed and are currently being checked. Layout and detail drawings were completed for the design of a trunnion and holding fixture for the susceptor and ceramic liner.

7.4. PROTOTYPE PLANT SYSTEMS, GENERAL

Product transport design drawings are nearing completion. This system utilizes pneumatics to effect the solids transport. Seven of ten systems have been completed, with the remainder scheduled for completion by September 5, 1975.

Construction of the prototype line control room is complete and this facility is ready for installation of the instrument consoles (Ref. 7-1, Fig. 7-13, photograph 75FR1870).

The foundation for the crusher is formed and ready for pouring concrete. The UNIFRAME anchor bolt locations and structural details have been evaluated.

All ventilation systems for the prototype line have been installed.

Design of an automatic-stop control system for the 20-ton crane was completed. This control system was implemented to preclude an operator error that could result in damage to the facilities or personnel areas. The control system is now in effect.

REFERENCE

7-1. "Thorium Utilization Program Quarterly Progress Report for the Period Ending May 31, 1975," ERDA Report GA-A13510, General Atomic Company, August 15, 1975.

8. ALTERNATIVE HEAD-END REPROCESSING

Scoping work previously under way in this activity has been suspended due to an ERDA directive eliminating this item from the work scope.

9. FUEL RECYCLE SYSTEMS ANALYSIS

9.1. TECHNICAL EXCHANGE MEETING

On August 13 and 14, members from Allied Chemical Corporation (ACC), R. M. Parsons Company (RMP), Oak Ridge National Laboratory (ORNL), ERDA, and General Atomic (GA) met at GA for a technical exchange of HTGR fuel reprocessing and refabrication information. Philosophies covering the design for remote shielded recycle facilities were discussed and facility conceptual designs of an HTGR Recycle Demonstration Facility (HRDF) type were presented and discussed by the attending members. The GA HRDF pre-conceptual design and estimate summary report (Ref. 9-1) was presented and discussed, along with the initial ORNL layout concepts and a brief rundown on the ACC-RMP preliminary estimate effort.

9.2. COMPARISON OF ACC AND GA COST ESTIMATES FOR THE HRDF

At the request of ERDA, representatives of ERDA-ID, ACC, GA, ORNL, and RMP met at RMP to develop a comparison and explanation of the differences between ACC and GA HRDF estimates. As an action item following this meeting, GA submitted to ERDA-ID revised summary tables for the HRDF cost comparisons, reflecting adjusted building cost allocation and including a GA estimate prepared on an Idaho labor rate basis, productivity factors, and indirect cost percentages.

9.3. BURNER CYCLICAL OPERATIONS IN A COMMERCIAL HTGR REPROCESSING FACILITY

9.3.1. Introduction and Summary

Cyclical thermal operation of high-temperature crushed fuel element burners will have a major influence on maintenance, repair, and replacement

requirements. Therefore, the norml burner operating mode should provide as large a duration between thermal cycles as practical. Major thermal cycles occur during sweepdown of the head-end system for accountability, and minor fluctuations occur at the end of each 24-hr operating cycle when hot product ash is removed. A semicontinuous operating cycle with batch removal of the product ash is presently required to obtain a sufficiently low carbon content to preclude undesirable reactions in the leacher and operational difficulties in the solvent extraction system. A heel is retained in the burner to minimize transient effects between daily batches. Heel requirements do not affect customer accountability; however, there are criticality implications.

The work reported here is intended to provide guidance to the reprocessing development effort regarding burner cyclical opeations anticipated in a commercial-size facility and in the HRDF and to resolve questions concerning the heel operating mode and accountability requirements (GA/ACC Agreement/Commitment No. 7).

Customer accountability requirements in an HTGR commercial reprocessing facility are satisfied by campaign processing of a customer's fuel elements, daily sampling of head-end accountability tanks, and a final sweepdown of the head-end system at the end of each spent fuel lot. Customer accountability lots are assumed to be reactor half-segments of I,M fuel elements during initial operation and the I,M; 23R; and 25R fractions during recycle.

1. Duration of accountability cycles for a 10,000 spent FE/yr Phase I HRDF varies from 6 to 12 days; the total number of cycles annually for each of two primary 24-in. burners is 22.

2. Cycle durations are approximately the same when the plant capacity is doubled in Phase II, based on processing of segregated lots in each head-end line.

3. It is anticipated that the sweepdown accountability procedure may require up to 24 hr and will result in a significant thermal cycle of the primary burner.

4. Primary burner operation is semicontinuous with batch removal of product ash at the end of each 24-hr operating cycle. A heel, having a height of one or more bed diameters, is retained to reduce startup time and fines generation and to minimize temperature fluctuations between batches.

5. Batchwise inventory requirements for criticality control during processing of a customer lot require further assessment, but initial evaluations do not show these requirements to be limiting in commercial-size primary burners.

9.3.2. Discussion

Fluidized bed burners are used to burn graphite in crushed HTGR fuel elements and the outer carbon coatings on fuel particles in the head-end reprocessing system of a spent fuel recycle facility. Fuel elements are processed in customer lots, and it is anticipated that the head-end system will require complete sweepdown (during a period not to exceed 24 hr) at the end of each lot to satisfy expected customer accountability requirements. As a maximumm each lot may consist of a full reactor segment if it is comprised only of I,M elements, or the lot may be a partial segment comprising that fraction of I,M; 23R; and 25R elements present. Table 9-1 summarizes the average number of elements in HTGR refueling segments, and Table 9-2 shows the number of recycle elements expected in an equilibrium-mode 1160-MW(e) LHTGR.

Preliminary optimization of the recycle plant operating mode suggests that reprocessing of half-segment customer lots may be necessary to reduce fuel element storage requirements and to satisfy refabrication turnaround

TABLE 9-1
SPENT FUEL ELEMENTS IN HTGR REFUELING SEGMENTS[a]

	Fort St. Vrain	770 MW(e)	1160 MW(e)	1540 MW(e)
Number of elements	1,482	2,744	3,944	5,384
Refueling cycle (yr)	1	1	1	1
Fraction of core replaced each cycle	1/6	1/4	1/4	1/4
Average number of fuel elements per segment	247	686	986	1,346

[a] From Ref. 9-2.

TABLE 9-2
RECYCLE FUEL ELEMENTS IN EQUILIBRIUM-MODE
1160-MW(e) LHTGR SPENT FUEL SEGMENT

	Number of Fuel Elements
I,M	559
23R	394
25R	33
Total number in spent fuel segment	986

schedules. Accordingly, I,M customer lots will be reprocessed in half-segment quantities. Equilibrium segments will be reprocessed in I,M and 23R lots since the number of I,M and 23R elements is approximately a half-segment; the small number of 25R elements will also be processed separately. Consequently, cyclical operation of the primary burner is dependent on customer accountability requirements and is therefore a function of the number of customers, type of reactor, fuel cycle characteristics, and burner processing capacity.

9.3.2.1. Target Recycle Plant (TRP) Design Basis

The HTGR TRP conceptual design (Ref. 9-3) is based on a commercial-size facility capable of reprocessing 50,000 spent HTGR fuel elements annually. The head-end processing system has three 36-in. crushed fuel element primary burners installed in each of two head-end lines. These six burners provide a total plant processing capacity of 236 spent fuel elements per operating day (39.3 per burner and 118 per line). If each head-end line is separately used to process a customer's spent fuel lot, the accountability cycle will be about 4 days for the LHTGR (half-segment basis), with 51 cycles per year based on an average of 51 customers.

Operation is started by loading each burner with three crushed fuel elements. The crushed fuel is heated to a combustion temperature of about 850°C. Loading and heating operations require a total of appoxmately 2 hr. During the burning cycle, crushed fuel elements are fed to the burner at an average rate of 1.85 FE/hr. After a 21-hr burning cycle, feeding is discontinued and induction heating is continued with reduced oxygen flow during a bake cycle required to reduce the carbon content to 1 wt % of the ash. The ash is removed from the burner once every 24 hr and a new burner operating cycle is started while the burner is held at high temperature to minimize severe thermal cycles.

9.3.2.2. HTGR Recycle Demonstration Facility (HRDF) Design Basis

It is assumed that the ERDA HRDF is planned for a reprocessing capacity of 10,000 spent elements annually in Phase I (initial operation in mid-1984) and a total of 20,000 with a Phase II addition, which is planned to be operational in mid-1989. The GA conceptual design for Phase I specifies a head-end processing system comprising two 24-in. crushed fuel element primary burners in a single head-end line. The burners provide a total processing capacity of 43 fuel elements per operating day (21.5 per burner). The Phase II addition will double the capacity and consist of an identical head-end system.

The HRDF is sized to process spent fuel elements from Fort St. Vrain, two 770-MW(e) reactors, and 8.5 1160-MW(e) reactors by the end of Phase I. No spent recycle fuel elements will be available for reprocessing during Phase I. The Phase II capacity will accommodate an additional ten 1160-MW(e) reactors. A summary of head-end customer accountability cycles is given in Table 9-3, based on the half-segment recycle operating mode previously described except for the FSV HTGR, which will be processed in segment/full-segment segment lots. Accountability cycle durations range from approximately 12 days for 1160-MW(e) reactors to 6 days for a Fort St. Vrain full segment during Phase I.

For Phase II operation the separate, twin head-end lines allow simultaneous processing of different material lots; i.e., 23R in one line and I,M in the other, from the same customer or from different customers. Therefore the accountability cycle durations are approximately the same for Phase I and Phase II. Operation of at least one head-end line with I,M fuel elements will assure a continuous feed of uranium-235 to the Purex solvent extraction columns. Additional burner cycles are required to process 25R elements.

It is anticipated that the 25R fuel elements may be accumulated from several customers and processed through head-end as a material lot. The

TABLE 9-3
HRDF HEAD-END CUSTOMER ACCOUNTABILITY CYCLES

	Phase I (I,M Elements)		Phase II[a] (I,M Elements)		Phase II (Equilibrium Cycle)[a]					
					I,M		23R		25R[b]	
	No. of Cycles	Cycle Duration (days)	No. of Cycles	Cycle[a] Duration (days)	No. of Cycles	Cycle Duration (days)	No. of Cycles	Cycle Duration (days)	No. of Cycles	Cycle Duration (days)
Fort St. Vrain	1[c]	6	1	6	1	6	--	--	--	--
770 MW	4	8.0	4	8.0	2	9.0	2	6.4	--	--
1160 MW	17	11.5	37	11.5	19	13.0	19	9.2	--	--
									(Cumulative) 1	11.0
HRDF annual capacity	10,000		20,000		----------20,000----------					
Daily operating capacity	43		86		43		43		43	
Number of burners	2		4		2[d]		2[d]		2[d]	
Number of customers	11.5		21.5		21.5		20.5		20.5	
Total accountability cycles per year	22		42		22		21		1	

[a] Utilizing the twin head-end lines for processing segregated lots in each line.

[b] 25R spent fuel elements are accumulated and processed as a single lot.

[c] Fort St. Vrain processed as full-segment lot.

[d] Single head-end line (two burners).

25R elements will not require reprocessing at the HRDF until Phase II operation, about 1989. Procedures for fuel accountability, material safeguards, techniques for fuel management, etc., should be developed to a state of the art to justify processing of the 25R elements as accumulated lots, using in-line sampling for customer accountability.

HRDF burner operation is similar to the 24-hr semicontinuous TRP cycle described in Section 9.3.2.1. A batch of several crushed fuel elements will be charged during startup from a new customer lot, and additional crushed material will be fed to each burner at an average rate of 1 FE/hr during the burn cycle. A final bake cycle is specified to reduce the carbon content to 1 wt % of the ash. Spent fuel is principally LHTGR elements and is comprised of TRISO fissile and BISO fertile particles. These particles are classified after burning, and the fertile particles are dissolved in 13M HNO_3 Thorex solution. The fissile particles are crushed (after leaching and drying) and fired in a secondary burner to expose the fissile kernel and convert the uranium carbide to oxide in preparation for dissolution in 3.5M nitric acid solution.

The final bake operation in the primary burner operating cycle before product discharge reduces the carbon content of TRISO/BISO ash and converts broken fissile particles to the oxide form before leaching the classified fractions. Reaction of Thorex acid solution with carbides and carbon is expected to produce some organic products such as mellitic acid, which may adversely affect operation of the solvent extraction system. Carbon fines will be difficult to separate by centrifuge from the leachate and may result in reduced extraction column capacity and decontamination factors. A low carbon content of 1 wt % of the burner ash has been tentatively specified until further resolution of its effect on leaching and solvent extraction processes. Information is also needed on the effect of carbon content on waste solidification. Carbon content of the primary burner product is not restrictive for TRISO/TRISO elements (Fort St. Vrain) since an additional crushed particle burn operation is performed before leaching.

It is highly desirable to retain a heel in the crushed fuel burner after product removal at the end of the 24-hour burner cycle. The heel reduces fines generation during the crushed fuel burn step, reduces startup time, and minimizes cylical temperature variations. A heel height of one or more bed diameters is required. The heel is swept down at the end of each customer lot to satisfy accountability requirements. Burner feed and product weigh hoppers are used to maintain a batchwise material balance within an accuracy of 2% for burner process and criticality control; however, segregation within the fluidized bed will prevent an accurate accounting of the heel composition. Consequently, a criticality assessment is necessary to verify that fissile particle buildup in the 24-in. burner heel and batchwise weighing accuracy within a customer lot are acceptable. Preliminary criticality analyses indicate that semicontinuous burner operation (with heels) throughout a customer accountability lot is permissible in the HRDF 24-in. burners.

9.3.3. Conclusions

Semicontinuous operation of the primary burners with a bake-out step for each batch at the end of the burn cycle is presently specified to obtain a low ash carbon content when processing TRISO/BISO commercial HTGR fuel elements. Additional experimental data are required to identify allowable carbon (graphite and carbide) content in leacher, solvent extraction, and waste management processes. Relaxation of the present 1 wt % carbon specification may be less restrictive to the burner operating mode and may result in a reduction in the number or extent of thermal cycles experienced within a customer accountability lot. Retention of a burner heel during batch product removal is presently employed to reduce thermal transients. Semicontinuous product removal would provide additional benefits in minimizing cyclical thermal effects but would present process equipment complications. Further assessment of criticality conditions accounting for batch segregation, weighing accuracy, etc., is required to determine whether criticality control will require additional constraints

with regard to the allowable amount of heel between burner batches. Preliminary estimates indicate that criticality will not be limiting in the HRDF 24-in. burner.

9.4. U-235 RECYCLE ANALYSIS

The cost of recycling U-235 in a large commercial plant is being determined using TRP (50,000 FE/yr) capital and operating cost data. An interim report on the results will be issued early in October.

9.5. DEVELOPMENT FLOWSHEET REVIEW FOR PRODUCTION REFABRICATION REQUIREMENTS

A critical review of the requirements for production-level HTGR fuel refabrication is being performed. The review will provide baseline input for HRDF design criteria and will classify and assess the development needs for meeting the demonstration objectives of the ERDA program. An appraisal of design issues and product and process requirements will be included.

9.6. DECONTAMINATION AND DECOMMISSIONING CONFERENCE

A conference on decontamination and decommissioning of ERDA facilities, sponsored by ERDA and the Aerojet Nuclear Company, was attended on August 19-21, 1975 at Idaho Falls, Idaho.

REFERENCES

9-1. "Preconceptual Design and Estimate Summary for HTGR Recycle Demonstration Facility (HRDF)," General Atomic Report GA-A13502, to be published.

9-2. Dahlberg, R. C., R. F. Turner, and W. V. Goeddel, "HTGR Fuel and Fuel Cycle Summary Description," General Atomic Report GA-A12801, January 21, 1974.

9-3. "Conceptual Design Summary and Design Qualifications for HTGR Target Recycle Plant," General Atomic Report GA-A13365, April 30, 1975.

APPENDIX A

PROJECT REPORTS PUBLISHED DURING THE QUARTER

deLesdernier, D., "Pneumatic Classification of Fort St. Vrain Fuel Particles," ERDA Report GA-A13135, General Atomic Company, June 30, 1975.

"Conceptual Design Summary and Design Qualifications for HTGR Target Recycle Plant," General Atomic Report GA-A13365, April 30, 1975.

APPENDIX B

DISTRIBUTION LIST

J. BROIDO	E-132	R. F. TURNER	L-507
L. BROOKS	SV-111	J. J. SHEFCIK	E-244
R. C. DAHLBERG	L-503	J. F. WATSON	L-640
D. E. DAVIS	TO-ANX-2	D. HANSON	TO-356
G. B. ENGLE	L-364	B. BAXTER	E-177
W. V. GOEDDEL	SV-101	E. O. WINKLER	L-231
A. J. GOODJOHN	E-147	A. E. HUTTON	E-170
T. D. GULDEN	L-444	R. D. ZIMMERMAN	E-179
D. P. HARMON	L-436	R. W. KEE	E-164
J. JAYNE	S-137	R. BUTLER	E-167
S. LANGER	LA-161	W. HUDRITSCH	L-358
C. S. LUBY	L-608	W. R. JOHNSON	L-362
D. R. MATHEWS	TO-406	C. WALLROTH	L-514
G. B. MELESE d'HOSPITAL	L-150	R. H. HANSEN	EA2-208
D. A. NEHRIG	TO-ANX-2	M. H. MERRILL	L-510
D. JACKSON	E-086	J. HOLZGRAF	L-424
C. A. HEATH	E-170	A. MEHNER	L-523
S. BRESNICK	L-104	S. T. ALMODOVAR	EA2-202
C. L. RICKARD	L-205	G. E. BENEDICT	E-249
C. L. SMITH	L-434	R. K. KIBBE	E-170
O. STANSFIELD	L-440	J. W. ALLEN	E-169
H. B. STEWART	L-602	H. REESER	E-172
G. L. STIEHL	TO-250		

LEGAL

WASHINGTON

15 DOCUMENT CENTER

161 TIC

1 V. A. Magliano, Director, Contract Services Division
U.S. ERDA
San Francisco Operations Office
1333 Broadway
Oakland, Ca. 94612

1 J. B. Radcliffe
PMIC-SD

1 Assistant Director, Commercial Fuel Cycle Division of Nuclear Fuel Cycle and Productions
U.S. ERDA
Washington, D. C. 20545

2 Chief, HTGR Fuel Recycle Branch
Division of Nuclear Fuel Cycle and Productions
U.S. ERDA
Washington, D.C. 20545

1 Project Manager, HTGR Fuel Reprocessing Development
Allied Chemical Corp.
P. O. Box 2204
Idaho Falls, Idaho 83401

1 Director, Research and Technical Support Division
Oak Ridge Operations Office
U.S. ERDA
P. O. Box E
Oak Ridge, Tennessee 37830

1 Director, Advanced Gas-Cooled Reactor Programs
Attention: P. R. Kasten
Oak Ridge National Laboratory
P. O. Box X
Oak Ridge, Tennessee 37830

1 Office of the Manager
Idaho Operations Office
U.S. ERDA
Idaho Falls, Idaho 83401

1 G. W. Hogg
1 J. A. Rindfleisch
1 W. B. Palmer
Allied Chemical Corp.
550 Second St.
Idaho Falls, Idaho 83401

1 V.C.A. Vaughen
Chemical Technology Division
Union Carbide Co.
P. O. Box X
Oak Ridge, Tennessee 37830

1 E. E. Fischer
R. M. Parsons Co.
Pasadena, Ca. 91124

1 J. C. Scarborough
Nuclear Utility Servies
Rockville, Maryland 20850

1 W. G. Price
Vice President - Generation
Delmarva Power and Light
800 King St.
Wilmington, Deleware 19899

1 J. D. Hornbuckle
So. Calif. Edison
P. O. Box 351
Los Angeles, Ca.

1 G. F. Daebeler
Branch Head, Safety and Licensing
1 R. F. Manty
Branch Head, Fuel Management
1 H. D. Honan
Philadelphia Electric
2301 Market St.
Philadelphia, Penn. 19101

1 P. U. Fischer
1 R. Finkbeiner
General Atomic Europe
Weinbergstrasse 109
8006 Zurich
Switzerland

1 K. Paulovich
General Atomic International
c/o Pacific Gulf Oil, Ltd.
P. O. Box 43
Akasaka, Tokyo
Japan 107

1 J. Ganley
GAC Fuels Group
France
(via M. H. Merrill)

1 Mr. Claude Moreau
Commissariat a l'Energie Atomique
Centre d'Etudes Nucleaires de Saclay
BP No. 2
91190 Gif-sur-Yvette
France

1 Dr. K. Hackstein
HOBEG
6450 Hanau/Main
Postfach 787
Germany

1 Dr. D. Stoelzl
Hochtemperatur Reaktorbau Gmbh
Gottlieb-Daimler-Strasse 8
D-68 Mannheim - 1
Postfach 5360
Germany